NASA
Technical
Paper
2268

January 1984



# Hot-Flow Tests of a Series of 10-Percent-Scale Turbofan Forced Mixing Nozzles

Verlon L. Head,
Louis A. Povinelli,
and William H. Gerstenmaier



NASA

NASA
Technical
Paper
2268

1984

# Hot-Flow Tests of a Series of 10-Percent-Scale Turbofan Forced Mixing Nozzles

Verlon L. Head,
Louis A. Povinelli,
and William H. Gerstenmaier

*Lewis Research Center*
*Cleveland, Ohio*

NASA
National Aeronautics
and Space Administration

**Scientific and Technical**
**Information Office**

1984

## Summary

An approximately 1/10-scale model of a mixed-flow exhaust system was tested in a static facility with fully simulated hot-flow cruise and takeoff conditions. Nine mixer geometries with 12 to 24 lobes were tested. The areas of the core and fan stream were held constant to maintain a bypass ratio of approximately 5. The research results presented in this report were obtained as part of a program directed toward developing an improved mixer design methodology by using a combined analytical and experimental approach. The effects of lobe spacing, lobe penetration, lobe-to-centerbody gap, lobe contour, and scalloping of the radial side walls were investigated. Test measurements included total pressure and temperature surveys, flow angularity surveys, and wall and centerbody surface static pressure measurements. Contour plots at various stations in the mixing region are presented to show the mixing effectiveness for the various lobe geometries.


## Introduction

The National Aeronautics and Space Administration's Energy Efficient Engine ($E^3$) project was conducted to develop, evaluate, and demonstrate engine technology for achieving reduced installed fuel consumption and lower operating cost for future commercial transport aircraft. One of the propulsion system components investigated was the mixed-flow exhaust nozzle. The goal of the research was to demonstrate overall mixed-flow exhaust system performance gains equivalent to a reduction of 3.3 percent in thrust-specific fuel consumption. An optimized separate-flow-exhaust engine configuration was used as the reference configuration for comparison with the mixed-flow case.

The work described in this report was conducted as part of a program directed toward developing an improved mixer design methodology by using a combined analytical and experimental approach. The analytical part of the program (refs. 1 and 2) employed a calculational procedure based on the approach developed by Briley, McDonald, and Kreskovsky (ref. 3) and is designated PEPSIM.

Initial tests of the mixer configurations of this report were conducted in the Lewis Research Center's CE–22 test facility (refs. 1, 4, and 5). The testing in CE–22 was limited to temperature ratios of 1.35 ($T_{T,c}/T_{T,f}$). The data presented in this report were obtained in the coaxial hot-jet test facility, which could simulate the proper design test conditions. The design conditions were defined as $P_{T,f}/P_{T,c}=1.0$, $P_{T,f}/P_0=2.4$, and $T_{T,c}/T_{T,f}=2.5$. The takeoff conditions were $P_{T,f}/P_{T,c}=1.0$, $P_{T,f}/P_0=1.6$, and $T_{T,c}/T_{T,f}=2.5$. Temperature, pressure, and flow angularity measurements were obtained in the mixing region downstream of the mixer. Data from the CE–22 and coaxial hot-jet test facilities are presented in reference 6. No attempt was made to apply the substitution principle of Munk and Prim (ref. 7), which relates the velocities and the stagnation temperatures in hot and warm testing. Patterson has demonstrated the applicability of the principle in hot and cold mixer flows (ref. 8).

## Apparatus and Procedure

The coaxial hot-jet test facility with the mixer model assembly installed is shown in figure 1. A closeup view of the model assembly is shown in figure 2 and a cross-sectional view, in figure 3. The test apparatus consisted of two basic parts: a fixed upstream model section and a rotatable shroud (fig. 3). Heated air was supplied to the core passage and flowed through the lobe section. Unheated air was supplied to the fan passage and flowed around the interchangeable lobe section. A jet breaker plate, a choke plate, and screens were installed in the upstream sections to eliminate any swirl in the flow approaching the mixer.

An experimental test matrix of the mixer lobe geometries tested in the CE–22 facility is shown in figure 4. Also shown in figure 4 are the A, B, and C lobe contour cross sections. All of these geometries except the 18- and 20-lobe mixers were tested in the coaxial hot-jet facility. Figure 5 lists the mixer configurations and design variables investigated in the coaxial hot-jet test facility and illustrates a typical mixer lobe assembly.

The basic mixer lobe geometries were the first six listed in the configuration table of figure 5. These mixers are designated by a number from 12 to 24 (number of radial lobes) followed by a letter from A to C (lobe contour). Keeping the core areas constant and varying the number of lobes produced spacing ratios from 0.5 to 1.36 and penetration values from 0.721 to 0.822 for the basic mixers. Most of the tests were conducted on the 12-lobe mixers, and pressure and temperature survey data were taken only for these configurations.

The last three configurations listed in the table of figure 5 (1E, 2E, and 3E) were modifications of the basic configurations. The 1E mixer was designed to be used in investigating the effect of gap height on mixing. It was a 12-lobe mixer geometry with a B contour and had a larger gap between the centerbody and the bottom of the mixer lobe than the basic 12-lobe mixer. Increasing the gap while keeping the core flow area constant resulted in lobe penetration decreasing from 0.822 (12B) to 0.744 (1E).

The 2E mixer was designed for optimum core area distribution. This was accomplished by varying the width of the lobes as a function of axial position (fig. 6(e)). This gave the mixer lobes a shape similar to an aerodynamic strut and resulted in a modified B lobe contour but with greater penetration (to a value of 0.901).

The 3E mixer was a convoluted radial wall mixer with A-contoured lobes. The convolutions were added to the radial walls of each lobe to improve the azimuthal thermal mixing. (See the mixer geometry in fig. 6(f)). Both the 2E and 3E mixers were constructed with a zero degree cutback angle. The 2E mixer was later cut back to 15°41′ like the basic mixers. This cutback also allowed flow angularity to be measured.

Details and dimensions of all of the mixer geometries tested are shown in figure 6. Four of the mixers were tested with scalloped cuts made in their radial walls. The dimensions and details are shown in figure 7. The four scalloped mixers were the 12B, 2E (cutback), 1E, and 12C. The mixers were scalloped in an attempt to improve their mixing effectiveness.

Three centerbodies were tested with the mixer geometries and were designated 2AC, 3B, and reference (REF). Centerbody 2AC, when tested with mixers of contour A or C, maintained an approximately constant area through the mixer core passage. Likewise, centerbody 3B, when tested with mixers of contour B, also gave an approximately constant area distribution. All centerbodies had the same contour after the mixer lobe exit. The details and contour coordinates are given in figure 8. The reference centerbody simulated an early version of a full-scale engine.

Instrumentation for the centerbodies is shown in figure 9. All three centerbodies were instrumented the same, with two rows of surface static pressure taps starting just upstream of the core stream exit plane. The rotatable shroud contour coordinates and the static pressure instrumentation are shown in figure 10. Two rows of pressure taps were located 15° apart down the length of the inside surface.

Pressure and temperature survey rakes were mounted to the rotatable shroud for probing the mixer flow field as shown in figure 11. Total temperature rakes were located at five axial stations in the mixing region. The first station was at the lobe exit plane (station 2), the second was halfway down the plug (station 2A), the third was at the end of the plug (station 2B), the fourth was midway between the plug tip and the nozzle exit (station 2C), and the fifth was at the nozzle exit plane (station 3). The pressure and temperature rakes as well as the rotatable mechanism are shown in figure 2. Total pressures were measured at the lobe exit (station 2) and the nozzle exit station (station 3).

The 2E and 3E mixers with zero degree cutback angle had a different total pressure rake at the nozzle exit, as shown in figure 11(a). Total temperature and flow angularity were not measured for these two mixer configurations. The tube spacing dimensions and the number of probes for all of the total pressure and temperature rakes are given in figure 11(b).

The temperature and pressure contour plots were obtained by rotating the shroud and taking data at 3° increments for a total of 18 circumferential positions (54° total). A computer-generated plot was made by interpolating the measured data to obtain values of constant pressure and temperature ratioed to the conditions at station 1 (conditions upstream of the mixer/centerbody).

The flow angularity rakes located at the lobe exit plane are shown in figure 12. Each rake had six probes and each probe had three tubes. The center tube was a chamfered total pressure probe, and the two side (or upper and lower) tubes had a 45° sweepback. The pressure difference between the two side probes and the indicated total pressure from the center tube were used with a calibration curve to obtain flow directions (radial and azimuthal). Details of the probe design technique and calibration procedure are given in reference 9.

Flow angle measurements were obtained by replacing the station 2 pressure rake, which was attached to the rotatable shroud, with a flow angularity rake (either the radial or azimuthal angle rake) and taking data at discrete angular positions behind the lobes. These positions were the centerline of the fan lobe, 1° to 2° into the fan stream from the lobe wall (depending on the lobe configuration), 1° to 2° into the core stream from the lobe wall, and the centerline of the core lobe. This pattern was repeated, thus obtaining measurements for one complete lobe pattern for each flow stream. This procedure was repeated for the other flow angle rake to obtain both flow component angles. These measurements were used along with a static pressure measurement at the wall surface to compute the velocity vectors for the initial input conditions to the PEPSIM analytical program described in reference 6.

For figures 13 to 21 the mixer configurations are designated by a numerical code that describes the lobe geometry, the centerbody type, and the cutback (2E configuration only). An example of this code would be 2E/3B–CB.

## Results and Discussion

Figure 13 shows the computer-generated contour plots of total pressure and temperature ratios. These plots were generated from the pressure and temperature survey data taken at the design condition ($P_{T,f}/P_0 = P_{T,c}/P_0 = 2.4$, $T_{T,c}/T_{T,f} = 2.5$). Each plot of temperature and pressure is shown at its true circumferential position, which was determined by using the angular position location on the rotatable shroud (fig. 11). For some of the configurations only the contour plots at the lobe and shroud exits are shown although data were taken for the three total temperature measurement stations in between. Computer-generated contour plots were also obtained for a limited number of configurations at the takeoff condition ($P_{T,f}/P_0 = P_{T,c}/P_0 = 1.6$, $T_{T,c}/T_{T,f} = 2.5$). The results are shown in figure 14 for the 12B and the three $E^3$ configurations.

Static pressures measured at two rows down the plug centerbody and two on the inside of the rotatable shroud were ratioed to the fan total pressure at station 1. These data are presented in figure 15 for the design condition. Because the variation in pressures as the shroud was rotated is insignificant, only data at one shroud position are shown. Figure 16 shows the same pressure distribution at the takeoff test conditions, but only for the 12B and three $E^3$ configurations.

Measured flow angles at the mixer lobe exit plane for four of the lobe geometries (12B/3B, 12C/REF, 1E/2AC, and 2E/3B-CB), both scalloped and unscalloped, are listed in table I for the cruise test condition. Although other positions were measured, only the flow angles at the fan and core lobe centerlines are presented. The data show only small changes in measured flow angles between scalloped and unscalloped lobe geometries.

The flow angle changes due to scalloping presented in table I resulted in small changes in the nozzle exit temperature contour patterns shown in figure 17. The 12B/3B and 2E/3B-CB configurations showed small improvements in mixing effectiveness due to the smaller size of the hotter zones. The 1E/2AC configuration showed a slight decrease in mixing effectiveness due to scalloping. No attempt was made to quantify these results.

The largest change in the total temperature distribution apparently occurred with lobe contour C (fig. 18(b)). It was postulated (ref. 10) that the contour, which has basically parallel core and fan flow at the lobe exit plane, benefits from scalloping due to vortex flow formation at the scallop leading edges as well as from longer mixing time. With contours A and B, scalloping did not produce significant changes because of the large radial components of the fan and core flows at the lobe exit plane, which dominate the mixing process.

Comparing the 12B and 2E scalloped configurations in figure 17 shows little difference in the mixing effectiveness although the temperature distribution patterns are different. The 2E mixer shows the hotter regions shoved out against the shroud wall. This scrubbing of the shroud wall was caused by the greater penetration and larger outward flow angle of the 2E core mixer lobe. Thus, the 2E mixer had more pressure drop than the 12B mixer, as evidenced by the exit pressure contours (station 3) shown in figures 13(b) and (p).

Figure 18 shows the effect of pressure ratio on the mixer exit temperature contour at a temperature ratio of 2.5. The temperature contour plots show an insignificant effect of nozzle pressure ratio on temperature distribution. The example shown is the 12B/3B mixer configuration and the same result holds true for the other configurations.

The general effect, not quantitative, of mixer lobe penetration on temperature ratio distribution at the mixer exit is shown in figure 19. As lobe penetration decreased, less radial mixing occurred, as can be seen in the three temperature contour plots. Since the spacing ratio increased as lobe penetration decreased, the degree of mixing from penetration alone cannot be determined from these data.

The effect of centerbody gap height (the radial distance between the centerbody and the bottom of the lobes as shown in fig. 5) on temperature distribution is shown in figure 20 by the temperature contour plots of the 12B and 1E lobe configurations. The 12B had a nominal gap height of 0.190 cm (0.075 in.) and the 1E had a nominal gap height of 0.825 cm (0.325 in.). The contour plots of temperature ratio show that a core of hot air formed as a result of the greater gap height for the 1E mixer than for the 12B mixer, where the core is relatively cool.

The 3E mixer was essentially a 12A mixer with modified lobe side walls that resulted in the change in exit temperature distribution shown in figure 21. The contour plots show that the 3E mixer was more effective with the convolutions in the radial walls. One would reasonably expect the mixer pressure drop to increase with the greater wetted perimeter. Comparing the station 3 pressure contour in figure 13(q) with those in figure 13(f) (12A/2AC) shows that there was indeed a significant increase in pressure drop for the 3E configuration. If this same technique were applied to a more effective mixer, such as the 12B mixer, there might be some optimum design where the trade-off between mixing effectiveness and mixer pressure drop would result in a more efficient mixer.

## Summary of Results

To develop a better mixer design methodology, an experimental program was conducted at the Lewis Research Center that used a hot-jet test facility to fully simulate the hot-flow design temperature ratio ($T_{T,c}/T_{T,f} = 2.5$). Earlier tests in the CE-22 facility at Lewis could only obtain results at a temperature ratio of 1.35. Most of the configurations that were tested in CE-22, along with the three new configurations, were tested in the coaxial hot-jet test facility, and the results are presented in this report.

The effect of scalloping the lobe radial side walls of four configurations and the effect of varying lobe-to-centerbody gap height were also investigated in this test

TABLE I. – MEASURED FLOW ANGLES AT MIXER LOBE EXIT PLANE FOR FOUR SCALLOPED AND UNSCALLOPED 12-LOBE GEOMETRIES (CRUISE CONDITION)

(a) 12B/3B mixer configuration

| Radial, distance, $R/R_{max}$ | Unscalloped | | | | Scalloped | | | |
|---|---|---|---|---|---|---|---|---|
| | Fan centerline | | Core centerline | | Fan centerline | | Core centerline | |
| | Flow angle, deg | | | | | | | |
| | $\alpha$ | $\beta$ | $\alpha$ | $\beta$ | $\alpha$ | $\beta$ | $\alpha$ | $\beta$ |
| 0.447 | 18.68 | −1.00 | 11.39 | 6.95 | 24.70 | −0.06 | 13.25 | 8.54 |
| .525 | 29.48 | −1.61 | 8.40 | .34 | 24.71 | −1.79 | 8.85 | .26 |
| .603 | 25.81 | −1.48 | 7.43 | −1.06 | 24.09 | −1.47 | 8.79 | 1.68 |
| .681 | 22.55 | −.64 | 9.39 | .91 | 25.81 | .07 | 6.05 | −2.52 |
| .759 | 25.72 | .69 | 9.39 | .91 | 29.94 | .76 | 9.01 | 1.46 |
| .842 | 25.29 | 1.15 | 18.60 | −3.32 | 20.68 | .56 | 19.32 | −2.37 |

(b) 12C/REF mixer configuration

| | | | | | | | | |
|---|---|---|---|---|---|---|---|---|
| 0.447 | 17.68 | −1.0 | 18.32 | 0.94 | 28.62 | 0 | 13.99 | −2.17 |
| .525 | 24.68 | .57 | 11.13 | −.93 | 32.25 | −1.06 | 9.35 | 1.83 |
| .603 | 24.08 | .52 | 8.90 | −1.91 | 23.57 | −2.12 | 10.16 | −.96 |
| .681 | 17.89 | −.09 | 5.81 | .79 | 16.81 | −2.85 | 9.94 | 0 |
| .759 | 20.53 | −.15 | 20.84 | .19 | 21.10 | −2.30 | 21.40 | .19 |
| .842 | 23.71 | −.15 | 22.93 | .17 | 22.87 | .49 | 22.65 | −.37 |

(c) 1E/2AC mixer configuration

| | | | | | | | | |
|---|---|---|---|---|---|---|---|---|
| 0.447 | 19.60 | −2.48 | 15.15 | −0.18 | 19.92 | −1.18 | 14.91 | −0.39 |
| .525 | 23.69 | −1.02 | 9.39 | .19 | 25.97 | −.97 | 8.228 | −.54 |
| .603 | 25.35 | 1.44 | 6.89 | −.84 | 25.98 | −.47 | 7.232 | −1.22 |
| .681 | 20.65 | −.35 | 4.30 | −1.91 | 20.72 | −.96 | 4.39 | .18 |
| .759 | 22.50 | −.13 | 13.24 | −1.23 | 21.38 | −1.18 | 15.02 | .84 |
| .842 | 23.20 | −.05 | 21.25 | .02 | 23.12 | −.27 | 21.43 | 0 |

(d) 2E/3B-CB mixer configuration

| | | | | | | | | |
|---|---|---|---|---|---|---|---|---|
| 0.447 | 29.95 | −1.0 | 12.32 | 3.0 | 28.87 | −1.03 | 12.68 | 7.52 |
| .525 | 27.27 | −2.53 | 7.35 | 2.30 | 29.06 | −1.0 | 7.26 | 1.23 |
| .603 | 25.23 | −2.51 | 7.99 | 2.31 | 25.56 | −.81 | 8.75 | 3.90 |
| .681 | 24.10 | −1.85 | 7.97 | 2.39 | 25.62 | −3.69 | 7.58 | −1.34 |
| .759 | 28.78 | −.90 | 7.67 | −2.52 | 28.75 | −2.96 | 7.43 | −1.0 |
| .842 | 29.22 | −.53 | 9.61 | −2.0 | 28.76 | −2.94 | 8.13 | −2.0 |

program. Test measurements included total pressure and temperature surveys, flow angularity surveys, and wall-plus-centerbody-surface static pressure measurements. Contour plots at various stations in the mixing region are presented to show the mixing effectiveness for the various lobe geometries for two flow conditions, cruise and takeoff.

Some general results, which can be determined from the test data, are summarized as follows:

1. The effect of scalloping on mixing effectiveness was only minimal as evidenced by the small flow angle changes and the small changes in the mixer exit temperature contour plots. Some weight savings could at least be accomplished.

2. Varying the nozzle pressure ratio at constant temperature ratio had essentially no effect on nozzle exit temperature profiles and therefore no effect on mixing effectiveness.

3. Increasing lobe penetration increased the radial mixing and thus gave higher mixing effectiveness.

4. Increasing the gap height between the lobe and the centerbody caused a core of hot flow to remain at the exhaust nozzle centerline and decreased the mixing effectiveness.

5. Modifying the radial walls of the mixer lobes by making them convoluted increased the mixing effectiveness at the expense of higher pressure losses. Used with the optimum lobe geometry, this could possibly be an effective method for improving mixing effectiveness.

National Aeronautics and Space Administration
Lewis Research Center
Cleveland, Ohio, July 13, 1983

# Appendix – Symbols

A,B,C letter following lobe numbers designating a specific lobe contour

CB cutback to 15°41′ deg

$L_m$ length of mixing zone, 16.713 cm (6.58 in.)

$P$ surface static pressure, $N/m^2$ ($lb/in^2$)

$P_T$ total (stagnation) pressure, $N/m^2$ ($lb/in^2$)

$P_0$ ambient pressure, $N/m^2$ ($lb/in^2$)

$R$ radial distance for locating pressure and temperature rake tubes, cm (in.)

$R_{max}$ shroud radius at mixer lobe exit plane, 11.278 cm (4.44 in.)

$T_T$ total temperature (stagnation), °C (°R)

$X$ axial distance from a reference location for describing test hardware geometry, cm (in.)

$X_s$ shroud reference length, 34.608 cm (13.625 in.)

$Y$ radial dimension for describing test mixer lobe geometry, cm (in.)

$Y_r$ radial dimension for describing shroud and centerbody geometry, cm (in.)

$\alpha$ radial flow angle relative to nozzle axis, deg

$\beta$ circumferential flow angle relative to nozzle axis, deg

$\theta$ angular position, deg

$\theta_c$ angular width of core lobe, deg

$\theta_f$ angular width of fan lobe, deg

$\varphi$ cutback angle of lobe exit plane relative to radial direction, deg

Subscripts:

$c$ core stream

$f$ fan stream

$o$ outer lip of mixer lobe at mixer exit

$i$ inner lip of mixer lobe at mixer exit

1 charging station upstream of mixer

2 mixer lobe exit station

2A,2B,2C intermediate measurement stations between stations 2 and 3

3 nozzle exit station

1–12 for mixer lobe geometry coordinates (e.g., $H_1$, $R_1$, $X_1$, $Y_1$, etc., fig. 6)

# References

1. Povinelli, L. A.; Anderson, B. H., and Gerstenmaier, W.: Computation of Three-Dimensional Flow in Turbofan Mixers and Comparison with Experimental Data. AIAA Paper 80-0227, Jan. 1980.
2. Bowditch, D. N.; et al.: Computational Fluid Mechanics of Internal Flow. Aeropropulsion 1979, NASA CP-2092, 1979, pp. 187–230.
3. Briley, W. R.; and McDonald, H.: Analysis and Computation of Viscous Subsonic Primary and Secondary Flows. Computational Fluid Dynamics Conference, AIAA, 1979, pp. 74–88.
4. Kozlowski, H.; and Kraft, J.: Experimental Evaluation of Exhaust Mixers for an Energy Efficient Engine. AIAA Paper 80-1088, June 1980.
5. Anderson, B. H.; Povinelli, L. A.; and Gerstenmaier, W. G.: Influence of Pressure Driven Secondary Flows on the Behavior of Turbofan Forced Mixers. AIAA Paper 80-1198, July 1980.
6. Anderson, B. H.; and Povinelli, L. A.: Factors Which Influence the Behavior of Turbofan Forced Mixer Nozzles. NASA TM-81668, 1981.
7. Munk, M.; and Prim, R. C.: On the Multiplicity of Steady Gas Flows Having the Same Streamline Pattern. Proc. Nat. Acad Sci., U.S., vol. 33, no. 5, 1947, pp. 137–141.
8. Patterson, R. W.: Turbofan Forced Mixer-Nozzle Internal Flowfield. I—A Benchmark Experimental Study. NASA CR-3492, Apr. 1982.
9. Dudzinski, T. J.; and Krause, L. N.: Flow-Direction Measurement with Fixed-Position Probes. NASA TM X-1904, 1969.
10. Povinelli, L. A.; Anderson, B. H.; and Head, V. L.: Scalloping Effects on Temperature Distribution in Turbofan Forced Mixers. AIAA Paper 82–0131, Jan. 1982.

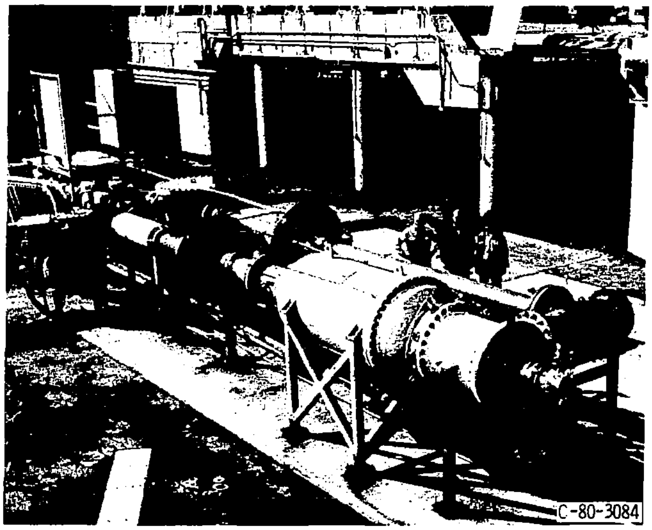


Figure 1. – Lewis Research Center's coaxial hot-jet test facility with the mixer nozzle assembly installed.

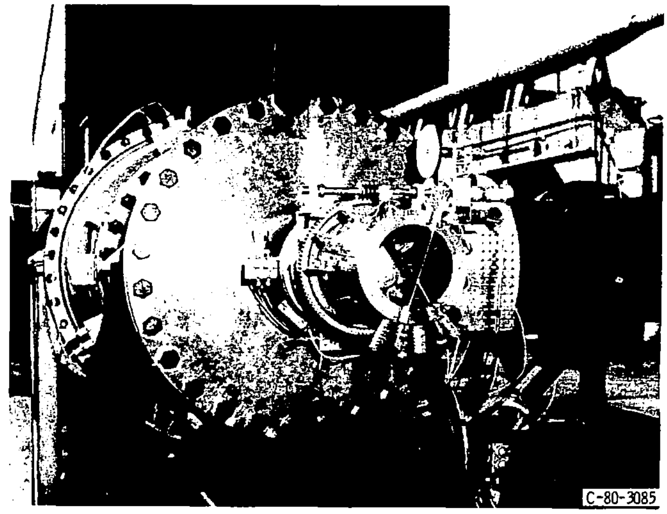


Figure 2. – Closeup view of mixer nozzle installation.

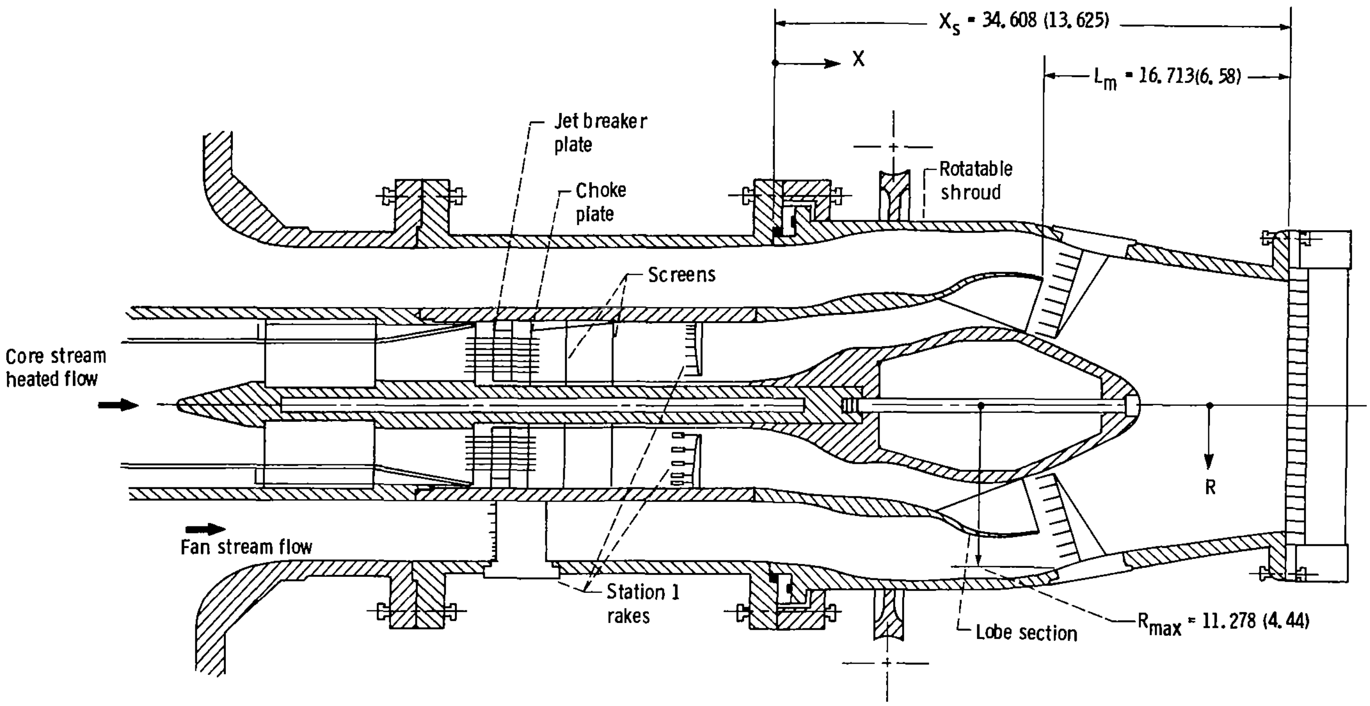


Figure 3. – Mixer nozzle model cross section. (Dimensions are in centimeters (in.).)

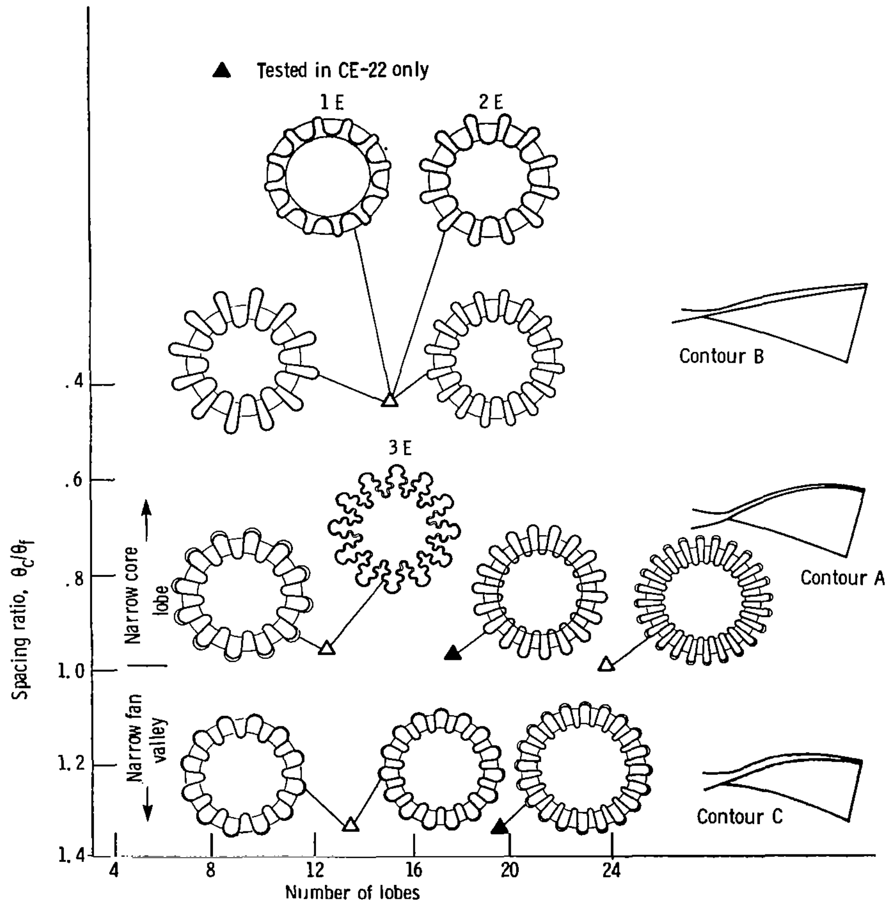


Figure 4. – Experimental test matrix, constant flow area.

| Mixer configuration | Number of lobes | Spacing ratio, $\theta_c/\theta_f$ | Penetration, $R/R_{max}$ | Centerbody gap | | Radial flow relative to nozzle axis, deg | | $L_m/2R_{max}$ | Cutback angle, $\varphi$ |
|---|---|---|---|---|---|---|---|---|---|
| | | | | cm | in. | Outer lip, $\alpha_o$ | Inner lip, $\alpha_i$ | | |
| 12A | 12 | 1.0 | 0.776 | 0.152 - 0.229 | 0.060 - 0.090 | 11.13 | 24.43 | 0.71 | 15°41' |
| 12B | 12 | .5 | .822 | ↓ | ↓ | -2.51 | 24.23 | ↓ | ↓ |
| 12C | 12 | 1.36 | .721 | | | 11.31 | 23.50 | | |
| 15C | 15 | 1.36 | .721 | | | 11.31 | 23.50 | | |
| 16B | 16 | .5 | .822 | | | -2.51 | 24.23 | | |
| 24A | 24 | 1.0 | .776 | | | 11.31 | 24.43 | | |
| 1E | 12 | .5 | .744 | .787 - .864 | .310 - .340 | -2.51 | 25.91 | | |
| 2E | 12 | [a] .5 | .901 | .152 - .229 | .060 - .090 | -10.96 | 23.63 | | 0° and 15°41' |
| 3E | 12 | [b] 1.0 | .776 | .152 - .229 | .060 - .090 | 12.34 | 24.82 | | 0° |

[a] At mixer exit plane.
[b] Average.

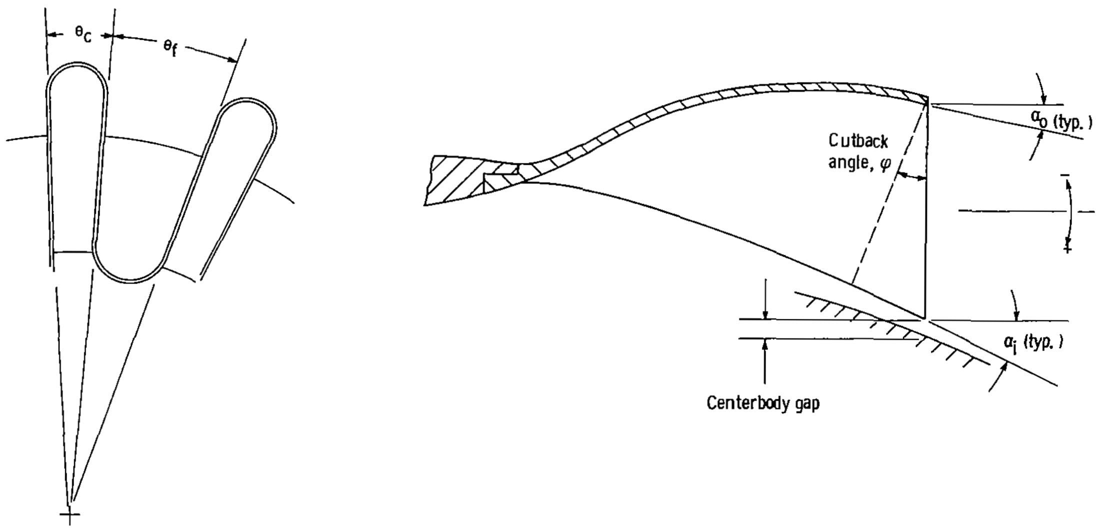


(a)

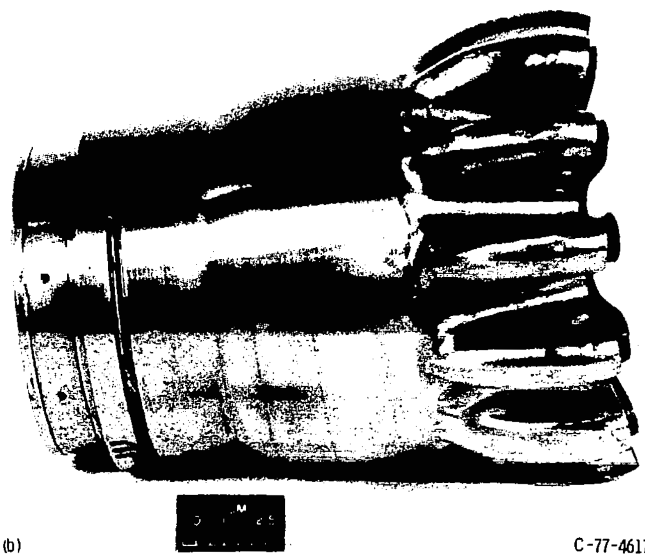

(b)

C-77-4617

(a) Configuration table and variables.
(b) Typical mixer lobe assembly.

Figure 5. – Mixer configurations and design variables.

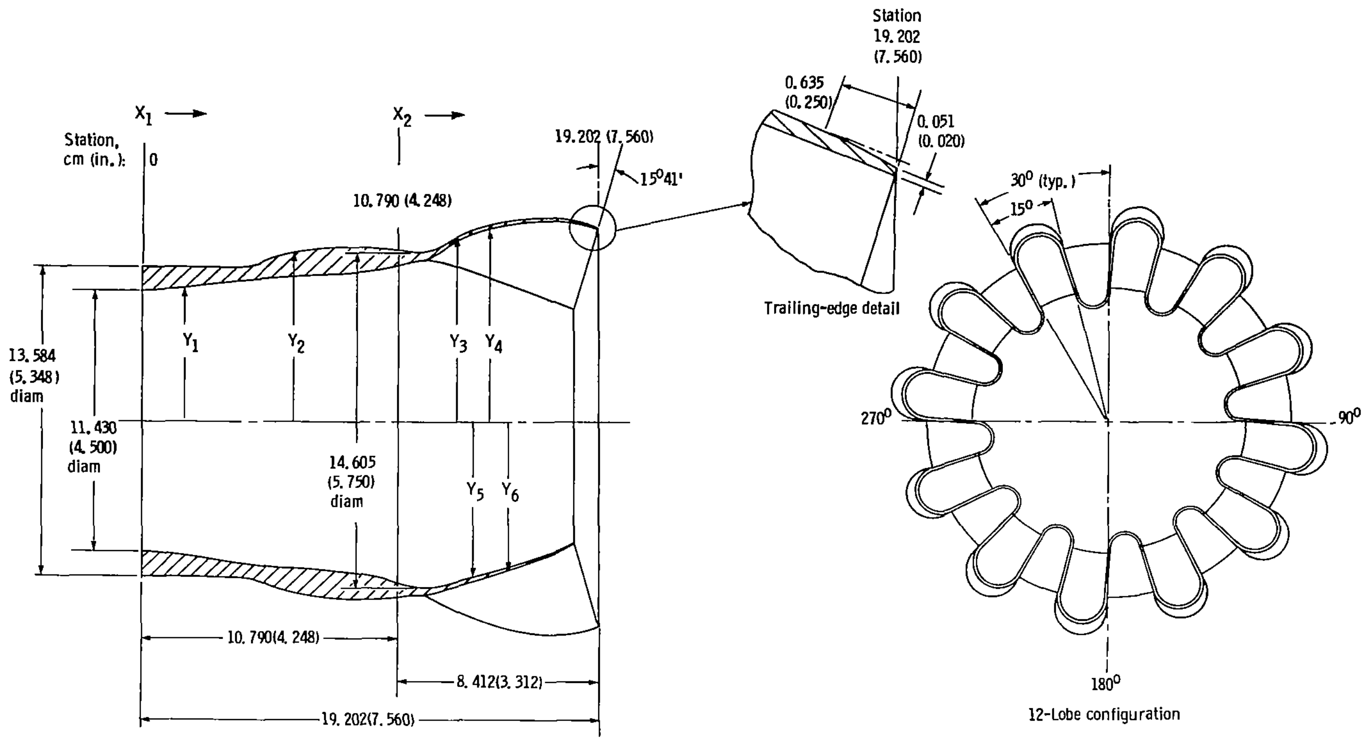


| $X_1 \pm 0.010$, cm | $X_1 \pm 0.010$, in. | Internal contour, $Y_1 \pm 0.010$, cm | Internal contour, $Y_1 \pm 0.010$, in. | External contour, $Y_2 \pm 0.010$, cm | External contour, $Y_2 \pm 0.010$, in. |
|---|---|---|---|---|---|
| 0 | 0 | 5.715 | 2.250 | 6.795 | 2.675 |
| .508 | .200 | 5.720 | 2.252 | 6.795 | 2.675 |
| 2.032 | .800 | 5.888 | 2.318 | 6.795 | 2.675 |
| 3.480 | 1.200 | 6.020 | 2.370 | 6.797 | 2.676 |
| 4.318 | 1.700 | 6.162 | 2.426 | 6.927 | 2.727 |
| 5.334 | 2.100 | 6.274 | 2.470 | 7.115 | 2.801 |
| 6.604 | 2.600 | 6.403 | 2.521 | 7.379 | 2.903 |
| 7.366 | 2.900 | 6.464 | 2.545 | 7.513 | 2.958 |
| 8.382 | 3.300 | 6.533 | 2.572 | 7.628 | 3.003 |
| 9.398 | 3.700 | 6.622 | 2.607 | 7.673 | 3.021 |
| 10.160 | 4.000 | 6.671 | 2.662 | 7.650 | 3.012 |
| 10.668 | 4.200 | 6.896 | 2.715 | 7.607 | 2.995 |
| 10.790 | 4.248 | 6.934 | 2.730 | 7.592 | 2.989 |
| 10.922 | 4.300 | ----- | ----- | 7.579 | 2.984 |

| $X_2 \pm 0.010$, cm | $X_2 \pm 0.010$, in. | Internal contour, $Y_4 \pm 0.010$, cm | Internal contour, $Y_4 \pm 0.010$, in. | Internal contour, $Y_5 \pm 0.010$, cm | Internal contour, $Y_5 \pm 0.010$, in. | External contour, $Y_3 \pm 0.010$, cm | External contour, $Y_3 \pm 0.010$, in. | External contour, $Y_6 \pm 0.010$, cm | External contour, $Y_6 \pm 0.010$, in. |
|---|---|---|---|---|---|---|---|---|---|
| 10.790 | 4.248 | 6.934 | 2.730 | 6.934 | 2.730 | 7.592 | 2.989 | 7.592 | 2.989 |
| 11.430 | 4.500 | 7.127 | 2.806 | 7.094 | 2.793 | 7.508 | 2.956 | 7.508 | 2.956 |
| 11.938 | 4.700 | 7.315 | 2.880 | ----- | ----- | 7.554 | 2.974 | ----- | ----- |
| 12.065 | 4.750 | 7.369 | 2.901 | 7.150 | 2.815 | 7.587 | 2.987 | 7.379 | 2.905 |
| 12.700 | 5.000 | 7.696 | 3.030 | 7.041 | 2.772 | 7.877 | 3.101 | 7.221 | 2.843 |
| 13.335 | 5.250 | 8.070 | 3.177 | 6.863 | 2.703 | 8.242 | 3.245 | 7.038 | 2.771 |
| 13.970 | 5.500 | 8.397 | 3.306 | 6.688 | 2.633 | 8.542 | 3.363 | 6.833 | 2.690 |
| 14.605 | 5.750 | 8.636 | 3.400 | 6.482 | 2.552 | 8.771 | 3.453 | 6.617 | 2.605 |
| 15.240 | 6.000 | 8.799 | 3.464 | 6.256 | 2.463 | 8.933 | 3.517 | 6.391 | 2.516 |
| 15.875 | 6.250 | 8.903 | 3.505 | 6.020 | 2.370 | 9.037 | 3.558 | 6.154 | 2.423 |
| 16.510 | 6.500 | 8.959 | 3.527 | 5.773 | 2.273 | 9.093 | 3.580 | 5.999 | 2.326 |
| 17.145 | 6.750 | 8.981 | 3.536 | 5.525 | 2.175 | 9.116 | 3.589 | 5.659 | 2.228 |
| 17.780 | 7.000 | 8.976 | 3.534 | 5.260 | 2.071 | 9.111 | 3.587 | 5.395 | 2.124 |
| 18.160 | 7.150 | ----- | ----- | 5.095 | 2.006 | ----- | ----- | 5.230 | 2.039 |
| 18.415 | 7.250 | 8.905 | 3.506 | ----- | ----- | 9.040 | 3.559 | ----- | ----- |
| 19.202 | 7.560 | 8.750 | 3.445 | ----- | ----- | 8.885 | 3.498 | ----- | ----- |

(a)

(a) 12A mixer.

Figure 6. – Dimensions and details of mixer nozzle configurations. (Linear dimensions are in centimeters (in.).)

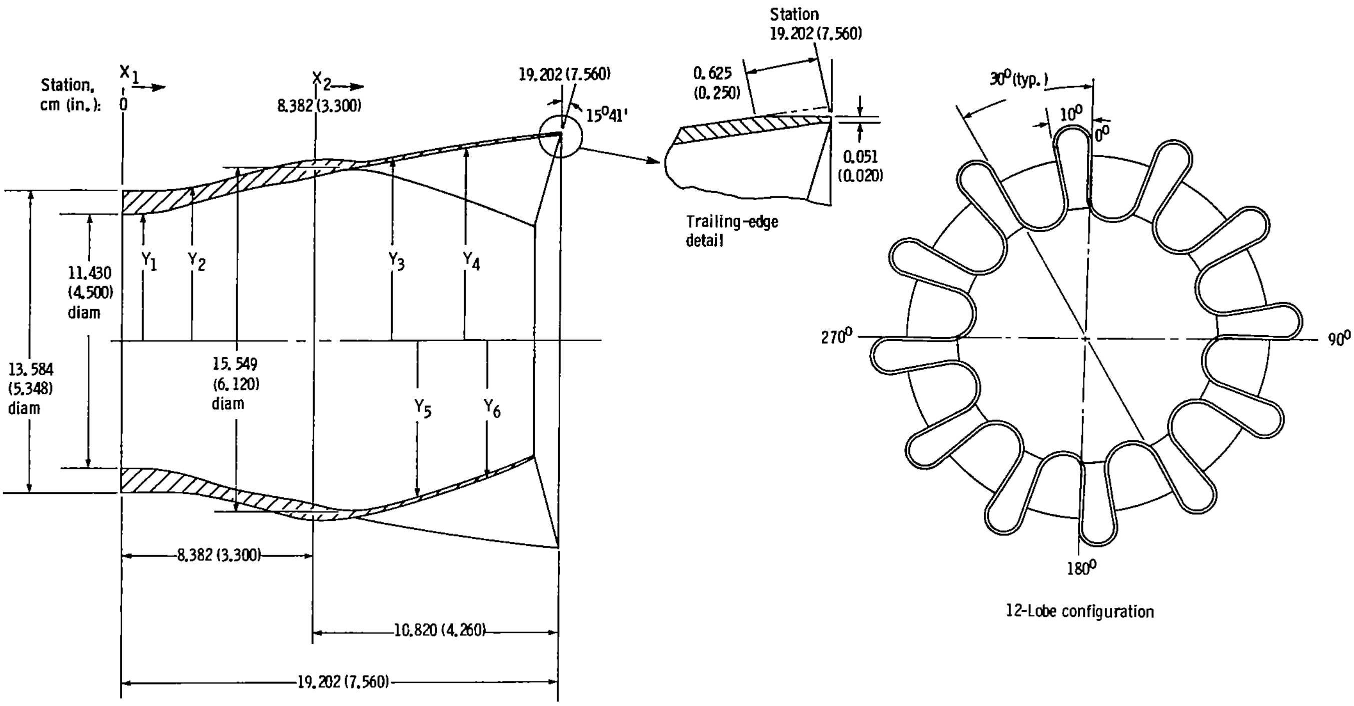


| $X_1 \pm 0.010$ | | Internal contour, $Y_1 \pm 0.010$ | | External contour, $Y_2 \pm 0.010$ | |
|---|---|---|---|---|---|
| cm | in. | cm | in. | cm | in. |
| 0 | 0 | 5.715 | 2.250 | 6.792 | 2.674 |
| .508 | .200 | 5.725 | 2.254 | ----- | ----- |
| 1.016 | .400 | 5.756 | 2.266 | ----- | ----- |
| 1.270 | .500 | ----- | ----- | 6.792 | 2.674 |
| 1.524 | .600 | 5.812 | 2.288 | 6.800 | 2.677 |
| 2.032 | .800 | 5.898 | 2.322 | 6.817 | 2.684 |
| 2.540 | 1.000 | 5.994 | 2.360 | 6.838 | 2.692 |
| 3.048 | 1.200 | 6.106 | 2.404 | 6.883 | 2.710 |
| 3.556 | 1.400 | 6.233 | 2.454 | 6.944 | 2.734 |
| 4.064 | 1.600 | 6.370 | 2.508 | 7.036 | 2.770 |
| 4.572 | 1.800 | 6.518 | 2.566 | 7.153 | 2.816 |
| 5.080 | 2.000 | 6.660 | 2.622 | 7.285 | 2.868 |
| 5.588 | 2.200 | 6.797 | 2.676 | 7.424 | 2.923 |
| 6.096 | 2.400 | 6.922 | 2.725 | 7.564 | 2.978 |
| 6.604 | 2.600 | 7.028 | 2.767 | 7.701 | 3.032 |
| 7.112 | 2.800 | 7.127 | 2.806 | 7.823 | 3.080 |
| 7.620 | 3.000 | 7.224 | 2.844 | 7.927 | 3.121 |
| 8.128 | 3.200 | 7.325 | 2.884 | 7.996 | 3.148 |
| 8.382 | 3.300 | 7.366 | 2.900 | 8.019 | 3.157 |
| 8.636 | 3.400 | ----- | ----- | 8.029 | 3.161 |

| $X_2 \pm 0.010$ | | Internal contour | | | | External contour | | | |
|---|---|---|---|---|---|---|---|---|---|
| cm | in. | $Y_4 \pm 0.010$ | | $Y_5 \pm 0.010$ | | $Y_3 \pm 0.010$ | | $Y_6 \pm 0.010$ | |
| | | cm | in. | cm | in. | cm | in. | cm | in. |
| 8.382 | 3.300 | 7.376 | 2.904 | 7.376 | 2.904 | 8.019 | 3.157 | 8.019 | 3.157 |
| 9.017 | 3.550 | ----- | ----- | ----- | ----- | 8.052 | 3.170 | 8.052 | 3.170 |
| 9.144 | 3.600 | 7.554 | 2.974 | 7.554 | 2.974 | ----- | ----- | ----- | ----- |
| 9.652 | 3.800 | 7.681 | 3.024 | 7.650 | 3.012 | 8.070 | 3.177 | 8.037 | 3.164 |
| 10.160 | 4.000 | 7.808 | 3.074 | 7.706 | 3.034 | 8.103 | 3.190 | 7.998 | 3.149 |
| 10.668 | 4.200 | 7.930 | 3.122 | 7.704 | 3.033 | 8.161 | 3.213 | 7.930 | 3.122 |
| 11.176 | 4.400 | 8.047 | 3.168 | 7.658 | 3.015 | 8.235 | 3.242 | 7.844 | 3.088 |
| 11.684 | 4.600 | 8.164 | 3.214 | 7.579 | 2.984 | 8.321 | 3.276 | 7.732 | 3.044 |
| 12.192 | 4.800 | 8.275 | 3.258 | 7.468 | 2.940 | 8.418 | 3.314 | 7.605 | 2.994 |
| 12.700 | 5.000 | 8.382 | 3.300 | 7.330 | 2.886 | 8.517 | 3.353 | 7.465 | 2.939 |
| 13.208 | 5.200 | 8.484 | 3.340 | 7.168 | 2.822 | 8.618 | 3.393 | 7.303 | 2.875 |
| 13.716 | 5.400 | 8.580 | 3.378 | 6.993 | 2.753 | 8.715 | 3.431 | 7.127 | 2.806 |
| 14.224 | 5.600 | 8.669 | 3.413 | 6.807 | 2.680 | 8.804 | 3.466 | 6.942 | 2.733 |
| 14.732 | 5.800 | 8.748 | 3.444 | 6.607 | 2.601 | 8.882 | 3.497 | 6.741 | 2.654 |
| 15.240 | 6.000 | 8.824 | 3.474 | 6.398 | 2.519 | 8.959 | 3.527 | 6.533 | 2.572 |
| 15.748 | 6.200 | 8.900 | 3.504 | 6.182 | 2.434 | 9.035 | 3.557 | 6.317 | 2.457 |
| 16.256 | 6.400 | 8.971 | 3.532 | 5.959 | 2.346 | 9.106 | 3.585 | 6.093 | 2.399 |
| 16.764 | 6.600 | 9.042 | 3.560 | 5.730 | 2.256 | 9.177 | 3.613 | 5.865 | 2.309 |
| 17.272 | 6.800 | 9.108 | 3.586 | 5.502 | 2.166 | 9.243 | 3.639 | 5.636 | 2.219 |
| 17.780 | 7.000 | 9.167 | 3.609 | 5.273 | 2.076 | 9.301 | 3.662 | 5.408 | 2.129 |
| 18.085 | 7.120 | ----- | ----- | 5.136 | 2.022 | ----- | ----- | 5.271 | 2.075 |
| 18.288 | 7.200 | 9.215 | 3.628 | ----- | ----- | 9.350 | 3.681 | ----- | ----- |
| 18.796 | 7.400 | 9.253 | 3.643 | ----- | ----- | 9.388 | 3.696 | ----- | ----- |
| 19.202 | 7.560 | 9.271 | 3.650 | ----- | ----- | 9.406 | 3.703 | ----- | ----- |

(b)

(b) 12B mixer.

Figure 6. – Continued.

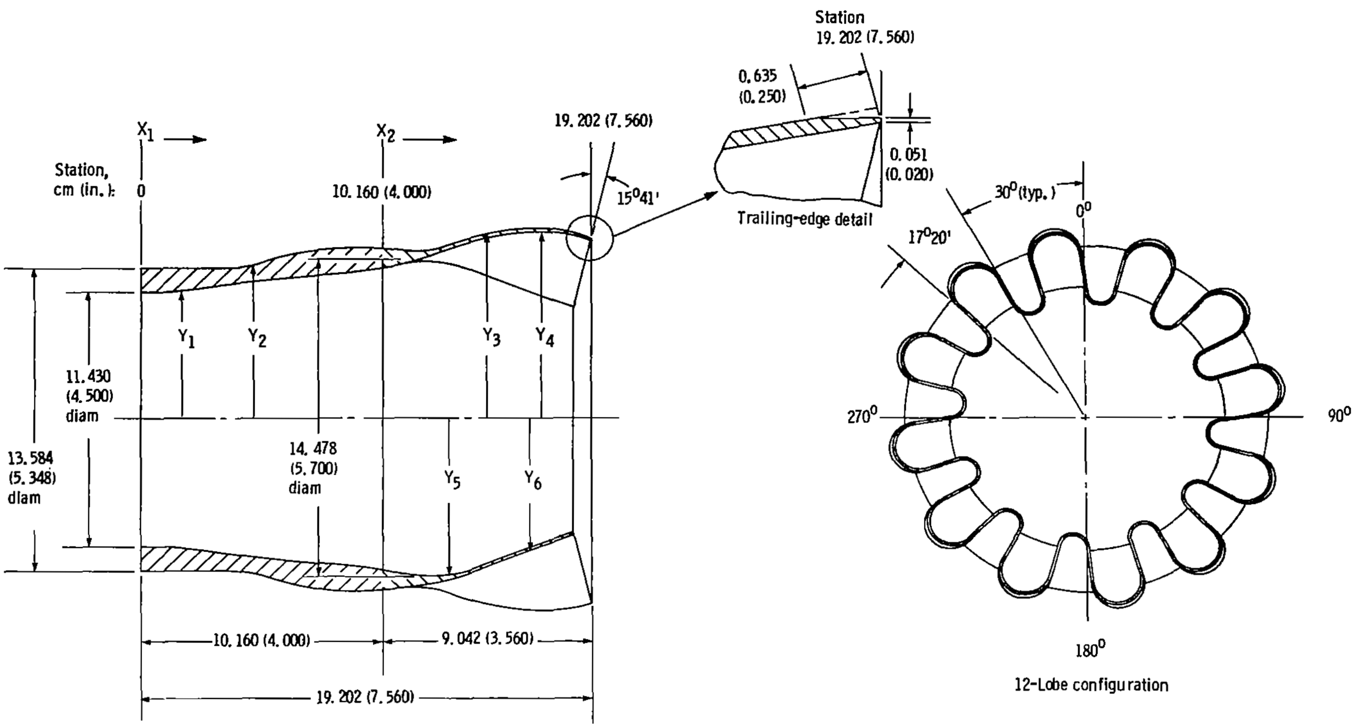


| $X_1 \pm 0.010$ cm | $X_1 \pm 0.010$ in. | Internal contour, $Y_1 \pm 0.010$ cm | Internal contour, $Y_1 \pm 0.010$ in. | External contour, $Y_2 \pm 0.010$ cm | External contour, $Y_2 \pm 0.010$ in. |
|---|---|---|---|---|---|
| ------ | ----- | 5.715 | 2.250 | 6.792 | 2.674 |
| 0.518 | 0.200 | 5.720 | 2.252 | ----- | ----- |
| 2.032 | .800 | 5.888 | 2.318 | 6.795 | 2.675 |
| 3.480 | 1.200 | 6.020 | 2.370 | 6.797 | 2.676 |
| 4.318 | 1.700 | 6.162 | 2.426 | 6.927 | 2.727 |
| 5.334 | 2.100 | 6.274 | 2.470 | 7.115 | 2.801 |
| 6.604 | 2.600 | 6.403 | 2.521 | 7.379 | 2.905 |
| 7.366 | 2.900 | 6.464 | 2.545 | 7.513 | 2.958 |
| 8.382 | 3.300 | 6.533 | 2.572 | 7.628 | 3.003 |
| 9.398 | 3.700 | 6.622 | 2.607 | 7.673 | 3.021 |
| 10.160 | 4.000 | 6.761 | 2.662 | 7.650 | 3.012 |
| 10.795 | 4.250 | ----- | ----- | 7.595 | 2.990 |

| $X_2 \pm 0.010$ cm | $X_2 \pm 0.010$ in. | Internal contour, $Y_4 \pm 0.010$ cm | Internal contour, $Y_4 \pm 0.010$ in. | Internal contour, $Y_5 \pm 0.010$ cm | Internal contour, $Y_5 \pm 0.010$ in. | External contour, $Y_3 \pm 0.010$ cm | External contour, $Y_3 \pm 0.010$ in. | External contour, $Y_6 \pm 0.010$ cm | External contour, $Y_6 \pm 0.010$ in. |
|---|---|---|---|---|---|---|---|---|---|
| 10.160 | 4.000 | 6.761 | 2.662 | 6.761 | 2.662 | 7.650 | 3.012 | 7.650 | 3.012 |
| 10.795 | 4.250 | 6.909 | 2.720 | 6.899 | 2.716 | 7.595 | 2.990 | 7.595 | 2.990 |
| 11.176 | 4.400 | 7.008 | 2.759 | 6.972 | 2.745 | 7.559 | 2.976 | 7.544 | 2.970 |
| 11.684 | 4.600 | 7.155 | 2.817 | 7.051 | 2.776 | 7.554 | 2.974 | 7.452 | 2.934 |
| 12.192 | 4.800 | 7.313 | 2.879 | 7.074 | 2.785 | 7.595 | 2.990 | 7.356 | 2.896 |
| 12.700 | 5.000 | 7.485 | 2.947 | 7.043 | 2.773 | 7.686 | 3.026 | 7.244 | 2.852 |
| 13.208 | 5.200 | 7.663 | 3.017 | 6.957 | 2.739 | 7.818 | 3.078 | 7.112 | 2.800 |
| 13.716 | 5.400 | 7.836 | 3.085 | 6.830 | 2.689 | 7.971 | 3.138 | 6.965 | 2.742 |
| 14.224 | 5.600 | 8.001 | 3.150 | 6.668 | 2.625 | 8.136 | 3.203 | 6.802 | 2.678 |
| 14.732 | 5.800 | 8.146 | 3.207 | 6.495 | 2.557 | 8.280 | 3.260 | 6.629 | 2.610 |
| 15.240 | 6.000 | 8.265 | 3.254 | 6.312 | 2.485 | 8.400 | 3.307 | 6.447 | 2.538 |
| 15.748 | 6.200 | 8.354 | 3.289 | 6.119 | 2.409 | 8.489 | 3.342 | 6.253 | 2.462 |
| 16.256 | 6.400 | 8.412 | 3.312 | 5.918 | 2.330 | 8.547 | 3.365 | 6.053 | 2.383 |
| 16.764 | 6.600 | 8.433 | 3.320 | 5.718 | 2.251 | 8.567 | 3.373 | 5.852 | 2.304 |
| 17.272 | 6.800 | 8.418 | 3.314 | 5.514 | 2.171 | 8.552 | 3.367 | 5.649 | 2.224 |
| 17.780 | 7.000 | 8.369 | 3.295 | 5.309 | 2.090 | 8.504 | 3.348 | 5.443 | 2.143 |
| 18.288 | 7.200 | 8.298 | 3.267 | 5.103 | 2.009 | 8.433 | 3.320 | 5.237 | 2.062 |
| 18.346 | 7.223 | ----- | ----- | 5.077 | 1.999 | ----- | ----- | 6.212 | 2.052 |
| 18.796 | 7.400 | 8.209 | 3.232 | ----- | ----- | 8.344 | 3.285 | ----- | ----- |
| 19.202 | 7.560 | 8.128 | 3.200 | ----- | ----- | 8.263 | 3.253 | ----- | ----- |

(c)

(c) 12C mixer.

Figure 6. – Continued.

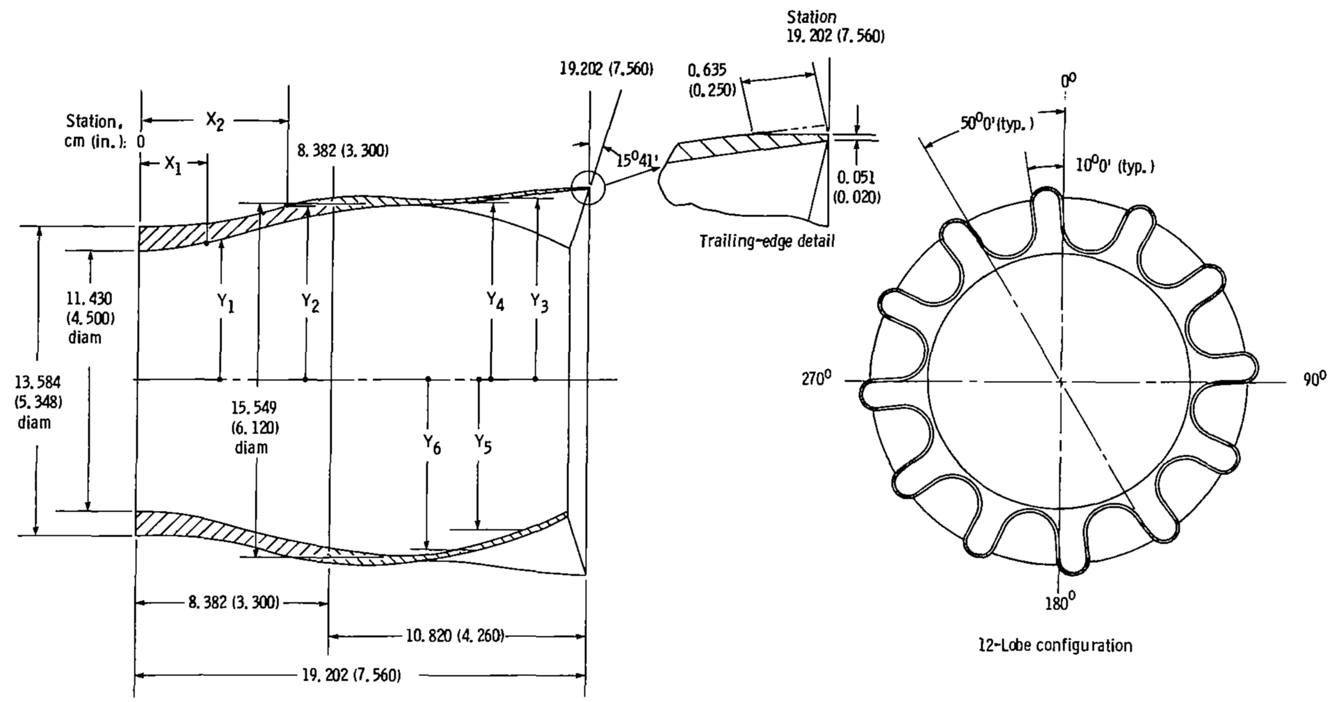


(d)

| $X_1 \pm 0.010$ | | Internal contour, $Y_1 \pm 0.010$ | | External contour, $Y_2 \pm 0.010$ | |
|---|---|---|---|---|---|
| cm | in. | cm | in. | cm | in. |
| 0 | 0 | 5.715 | 2.250 | 6.792 | 2.674 |
| .508 | .200 | 5.725 | 2.254 | 6.792 | 2.674 |
| 1.016 | .400 | 5.756 | 2.266 | 6.792 | 2.674 |
| 1.270 | .500 | ----- | ----- | 6.792 | 2.674 |
| 1.524 | .600 | 5.812 | 2.288 | 6.800 | 2.677 |
| 2.032 | .800 | 5.898 | 2.322 | 6.817 | 2.684 |
| 2.540 | 1.000 | 5.994 | 2.360 | 6.838 | 2.692 |
| 3.048 | 1.200 | 6.106 | 2.404 | 6.883 | 2.710 |
| 3.556 | 1.400 | 6.233 | 2.454 | 6.944 | 2.734 |
| 4.064 | 1.600 | 6.370 | 2.508 | 7.036 | 2.770 |
| 4.572 | 1.800 | 6.518 | 2.566 | 7.153 | 2.816 |
| 5.080 | 2.000 | 6.660 | 2.622 | 7.285 | 2.868 |
| 5.588 | 2.200 | 6.797 | 2.676 | 7.424 | 2.923 |
| 6.096 | 2.400 | 6.922 | 2.725 | 7.564 | 2.978 |
| 6.604 | 2.600 | 7.028 | 2.767 | 7.701 | 3.032 |
| 7.112 | 2.800 | 7.130 | 2.807 | 7.823 | 3.080 |
| 7.620 | 3.000 | 7.229 | 2.846 | 7.927 | 3.121 |
| 8.128 | 3.200 | 7.328 | 2.885 | 7.993 | 3.147 |
| 8.382 | 3.300 | 7.376 | 2.904 | ----- | ----- |
| 8.636 | 3.400 | ----- | ----- | 8.031 | 3.162 |
| 9.144 | 3.600 | ----- | ----- | 8.049 | 3.169 |

| $X_2 \pm 0.010$ | | Internal contour | | | | External contour | | | |
|---|---|---|---|---|---|---|---|---|---|
| cm | in. | $Y_4 \pm 0.010$ | | $Y_5 \pm 0.010$ | | $Y_3 \pm 0.010$ | | $Y_6 \pm 0.010$ | |
| | | cm | in. | cm | in. | cm | in. | cm | in. |
| 8.382 | 3.300 | 7.376 | 2.904 | 7.376 | 2.904 | 8.016 | 3.156 | 8.016 | 3.156 |
| 8.636 | 3.400 | 7.424 | 2.923 | 7.424 | 2.923 | 8.031 | 3.162 | 8.031 | 3.162 |
| 9.144 | 3.600 | 7.440 | 2.959 | 7.440 | 2.959 | 8.049 | 3.169 | 8.049 | 3.169 |
| 9.652 | 3.800 | 7.595 | 2.990 | 7.595 | 2.990 | 8.049 | 3.169 | 8.049 | 3.169 |
| 10.160 | 4.000 | 7.658 | 3.015 | 7.658 | 3.015 | 8.031 | 3.162 | 8.031 | 3.162 |
| 10.668 | 4.200 | 7.704 | 3.033 | 7.704 | 3.033 | 8.001 | 3.150 | 8.001 | 3.150 |
| 11.176 | 4.400 | 7.722 | 3.040 | 7.722 | 3.040 | 7.958 | 3.133 | 7.958 | 3.133 |
| 11.684 | 4.600 | 7.724 | 3.041 | 7.714 | 3.037 | 7.915 | 3.116 | 7.904 | 3.112 |
| 12.192 | 4.800 | 7.732 | 3.044 | 7.691 | 3.028 | 7.882 | 3.103 | 7.841 | 3.087 |
| 12.700 | 5.000 | 7.744 | 3.049 | 7.648 | 3.011 | 7.864 | 3.096 | 7.770 | 3.059 |
| 13.208 | 5.200 | 7.765 | 3.057 | 7.590 | 2.988 | 7.864 | 3.096 | 7.691 | 3.028 |
| 13.716 | 5.400 | 7.793 | 3.068 | 7.511 | 2.957 | 7.884 | 3.104 | 7.602 | 2.993 |
| 14.224 | 5.600 | 7.752 | 3.052 | 7.409 | 2.917 | 7.920 | 3.118 | 7.501 | 2.953 |
| 14.732 | 5.800 | 7.877 | 3.101 | 7.277 | 2.865 | 7.968 | 3.137 | 7.376 | 2.904 |
| 15.240 | 6.000 | 7.943 | 3.127 | 7.137 | 2.810 | 8.034 | 3.163 | 7.229 | 2.846 |
| 15.748 | 6.200 | 8.019 | 3.157 | 7.962 | 2.741 | 8.110 | 3.193 | 7.054 | 2.777 |
| 16.256 | 6.400 | 8.090 | 3.185 | 6.754 | 2.659 | 8.181 | 3.221 | 6.845 | 2.695 |
| 16.764 | 6.600 | 8.161 | 3.213 | 6.533 | 2.572 | 8.252 | 3.249 | 6.624 | 2.608 |
| 17.272 | 6.800 | 8.227 | 3.239 | 6.309 | 2.484 | 8.319 | 3.275 | 6.401 | 2.520 |
| 17.780 | 7.000 | 8.285 | 3.262 | 6.083 | 2.395 | 8.377 | 3.298 | 6.175 | 2.431 |
| 18.288 | 7.200 | 8.334 | 3.281 | 5.852 | 2.304 | 8.425 | 3.317 | 5.944 | 2.340 |
| 18.466 | 7.270 | ----- | ----- | 5.766 | 2.270 | ----- | ----- | 5.857 | 2.306 |
| 18.796 | 7.400 | 8.372 | 3.296 | ----- | ----- | 8.463 | 3.332 | ----- | ----- |
| 19.202 | 7.560 | 8.390 | 3.303 | ----- | ----- | 8.481 | 3.339 | ----- | ----- |

(d) 1E mixer.

Figure 6. – Continued.

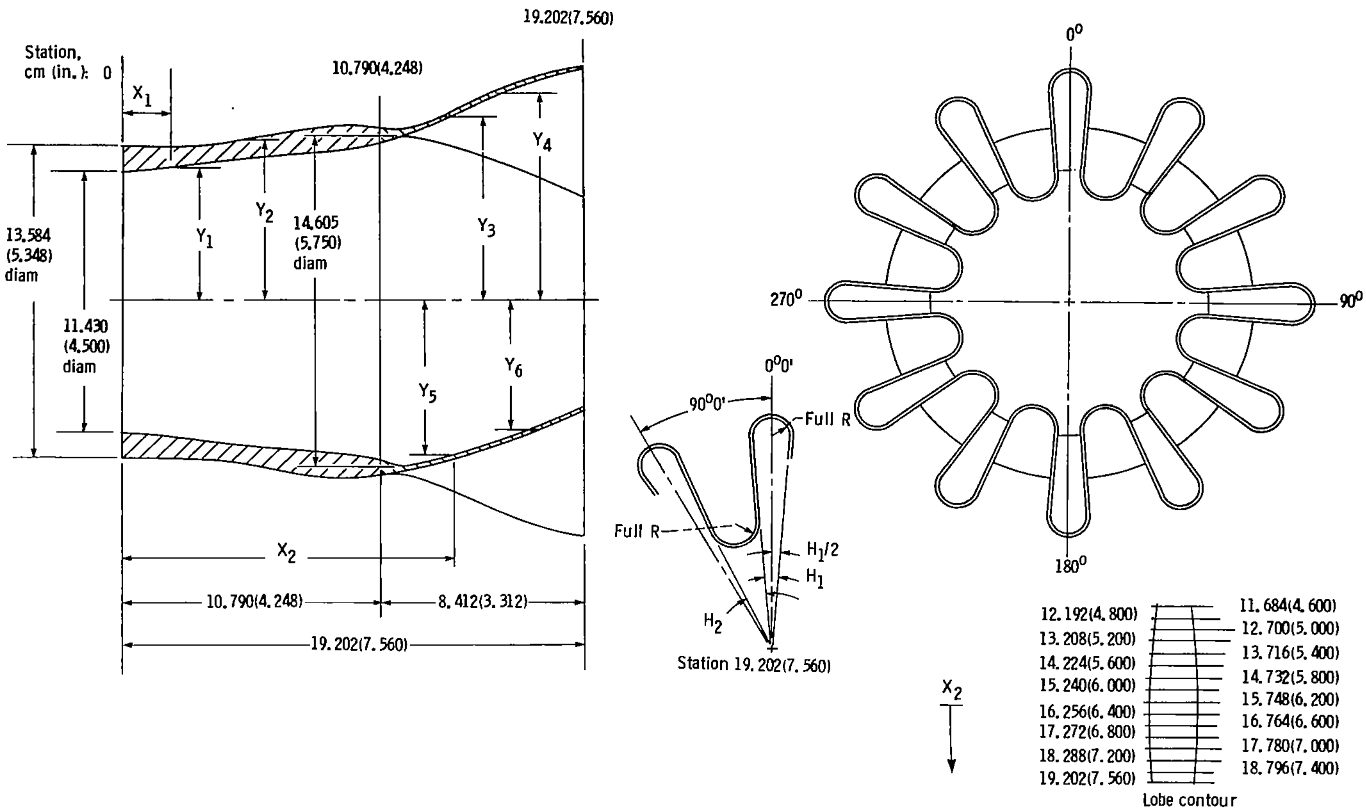


(e)

| $X_1 \pm 0.010$ | | Internal contour, $Y_1 \pm 0.010$ | | External contour, $Y_2 \pm 0.010$ | |
|---|---|---|---|---|---|
| cm | in. | cm | in. | cm | in. |
| 0 | 0 | 5.715 | 2.250 | 6.795 | 2.675 |
| .508 | .200 | 5.720 | 2.252 | 6.795 | 2.675 |
| 2.032 | .800 | 5.888 | 2.318 | 6.795 | 2.675 |
| 3.048 | 1.200 | 6.020 | 2.370 | 6.797 | 2.676 |
| 4.318 | 1.700 | 6.162 | 2.426 | 6.927 | 2.727 |
| 5.334 | 2.100 | 6.274 | 2.470 | 7.115 | 2.801 |
| 6.604 | 2.600 | 6.403 | 2.521 | 7.379 | 2.905 |
| 7.366 | 2.900 | 6.464 | 2.545 | 7.513 | 2.958 |
| 8.382 | 3.300 | 6.533 | 2.572 | 7.628 | 3.003 |
| 9.398 | 3.700 | 6.622 | 2.607 | 7.673 | 3.021 |
| 10.160 | 4.000 | 6.761 | 2.662 | 7.650 | 3.012 |
| 10.668 | 4.200 | 6.896 | 2.715 | 7.607 | 2.995 |
| 10.790 | 4.248 | 6.934 | 2.730 | 7.592 | 2.989 |
| 10.922 | 4.300 | ----- | ----- | 7.579 | 2.984 |
| 11.430 | 4.500 | ----- | ----- | 7.508 | 2.956 |

| $X_2 \pm 0.010$ | | Internal contour | | | | External contour | | | | $H_1$ | $H_2$ |
|---|---|---|---|---|---|---|---|---|---|---|---|
| cm | in. | $Y_4 \pm 0.010$ | | $Y_5 \pm 0.010$ | | $Y_3 \pm 0.010$ | | $Y_6 \pm 0.010$ | | | |
| | | cm | in. | cm | in. | cm | in. | cm | in. | | |
| 10.790 | 4.248 | 6.934 | 2.730 | 6.934 | 2.730 | 7.592 | 2.989 | 7.592 | 2.989 | ------ | ------ |
| 11.176 | 4.400 | 7.066 | 2.782 | 7.066 | 2.782 | 7.523 | 2.962 | 7.523 | 2.962 | ------ | ------ |
| 11.684 | 4.600 | 7.178 | 2.826 | 7.254 | 2.856 | 7.493 | 2.950 | 7.417 | 2.920 | 10° 34' | 19° 26' |
| 12.192 | 4.800 | 7.168 | 2.822 | 7.457 | 2.936 | 7.574 | 2.982 | 7.285 | 2.868 | 11° 34' | 18° 26' |
| 12.700 | 5.000 | 7.043 | 2.773 | 7.681 | 3.024 | 7.780 | 3.063 | 7.142 | 2.812 | 12° 8' | 17° 52' |
| 13.208 | 5.200 | 6.886 | 2.711 | 7.925 | 3.120 | 8.024 | 3.159 | 6.985 | 2.750 | 12° 42' | 17° 18' |
| 13.716 | 5.400 | 6.721 | 2.646 | 8.169 | 3.216 | 8.268 | 3.255 | 6.820 | 2.685 | 13° 18' | 16° 42' |
| 14.224 | 5.600 | 6.558 | 2.582 | 8.407 | 3.310 | 8.504 | 3.348 | 6.655 | 2.620 | 13° 52' | 16° 8' |
| 14.732 | 5.800 | 6.396 | 2.518 | 8.636 | 3.400 | 8.733 | 3.438 | 6.492 | 2.556 | 14° 26' | 15° 34' |
| 15.240 | 6.000 | 6.226 | 2.451 | 8.862 | 3.489 | 8.959 | 3.527 | 6.322 | 2.489 | 15° 0' | 15° 0' |
| 15.748 | 6.200 | 6.050 | 2.382 | 9.078 | 3.574 | 9.180 | 3.614 | 6.147 | 2.420 | 14° 22' | 15° 38' |
| 16.256 | 6.400 | 5.872 | 2.312 | 9.281 | 3.654 | 9.378 | 3.692 | 5.969 | 2.350 | 13° 44' | 16° 16' |
| 16.764 | 6.600 | 5.674 | 2.234 | 9.489 | 3.736 | 9.586 | 3.774 | 5.771 | 2.272 | 13° 6' | 16° 54' |
| 17.272 | 6.800 | 5.471 | 2.154 | 9.672 | 3.808 | 9.769 | 3.846 | 5.568 | 2.192 | 12° 26' | 17° 34' |
| 17.780 | 7.000 | 5.258 | 2.070 | 9.830 | 3.870 | 9.926 | 3.908 | 5.354 | 2.108 | 11° 48' | 17° 12' |
| 18.288 | 7.200 | 5.042 | 1.985 | 9.970 | 3.925 | 10.066 | 3.963 | 5.138 | 2.023 | 11° 10' | 18° 50' |
| 18.796 | 7.400 | 4.826 | 1.900 | 10.086 | 3.971 | 10.183 | 4.009 | 4.923 | 1.938 | 10° 32' | 19° 28' |
| 19.202 | 7.560 | 4.648 | 1.830 | 10.165 | 4.002 | 10.262 | 4.040 | 4.745 | 1.868 | 10° 0' | 20° 0' |

(e) 2E mixer.

**Figure 6. – Continued.**

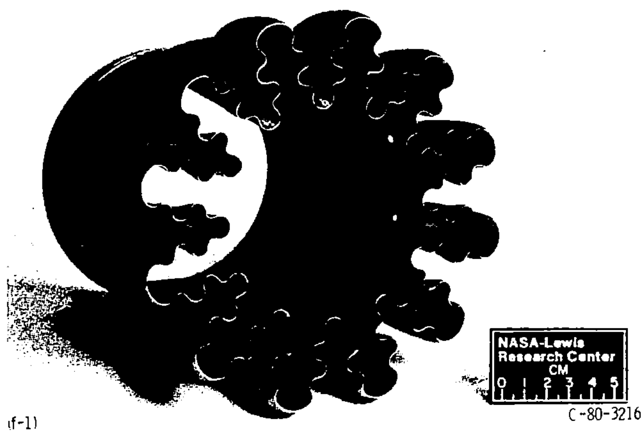


(f-1)

(f) 3E mixer.

Figure 6. – Continued.

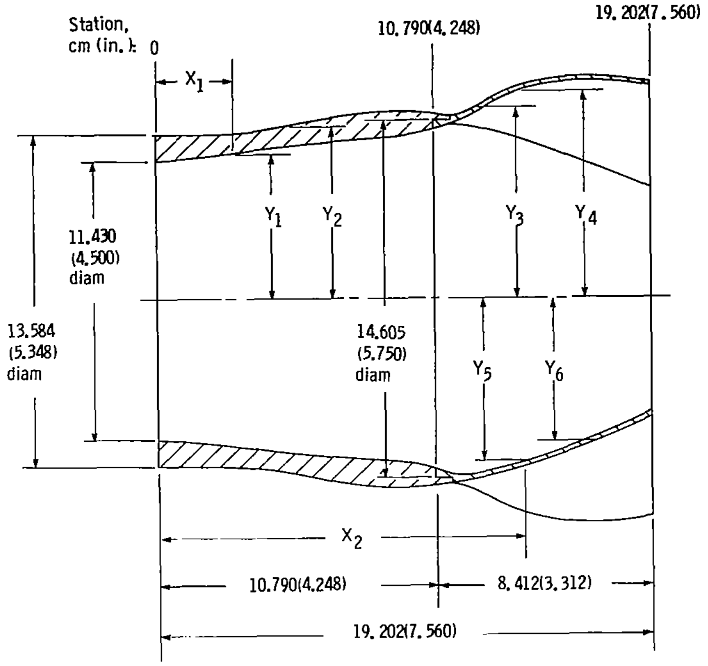


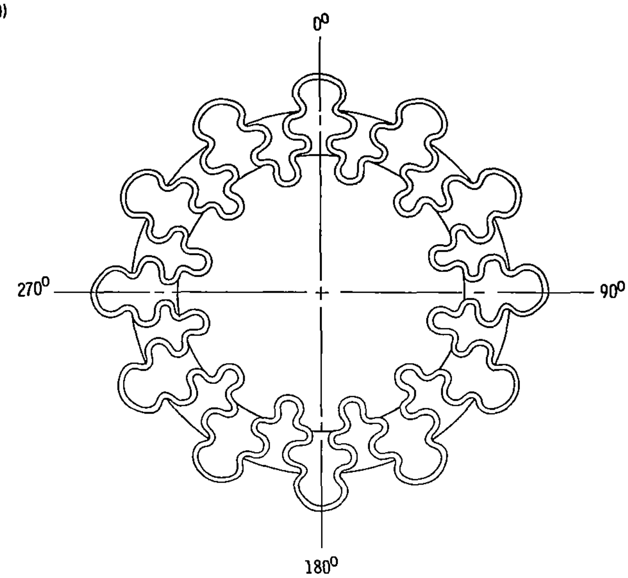


12-Lobe configuration

| $X_1 \pm 0.010$ cm | $X_1 \pm 0.010$ in. | Internal contour, $Y_1 \pm 0.010$ cm | Internal contour, $Y_1 \pm 0.010$ in. | External contour, $Y_2 \pm 0.010$ cm | External contour, $Y_2 \pm 0.010$ in. |
|---|---|---|---|---|---|
| 0 | 0 | 5.715 | 2.250 | 6.795 | 2.675 |
| .508 | .200 | 5.720 | 2.252 | 6.795 | 2.675 |
| 2.032 | .800 | 5.888 | 2.318 | 6.795 | 2.675 |
| 3.048 | 1.200 | 6.020 | 2.570 | 6.797 | 2.676 |
| 4.318 | 1.700 | 6.162 | 2.426 | 6.927 | 2.727 |
| 5.334 | 2.100 | 6.274 | 2.470 | 7.115 | 2.801 |
| 6.604 | 2.600 | 6.403 | 2.521 | 7.379 | 2.905 |
| 7.366 | 2.900 | 6.464 | 2.545 | 7.513 | 2.958 |
| 8.382 | 3.300 | 6.533 | 2.572 | 7.628 | 3.003 |
| 9.398 | 3.700 | 6.622 | 2.607 | 7.673 | 3.021 |
| 10.160 | 4.000 | 6.761 | 2.662 | 7.650 | 3.012 |
| 10.668 | 4.200 | 6.896 | 2.715 | 7.607 | 2.995 |
| 10.790 | 4.248 | 6.934 | 2.730 | 7.592 | 2.989 |
| 10.922 | 4.300 | ----- | ----- | 7.579 | 2.984 |
| 11.430 | 4.500 | ----- | ----- | 7.508 | 2.956 |

| $X_2 \pm 0.010$ cm | $X_2 \pm 0.010$ in. | Internal contour, $Y_4 \pm 0.010$ cm | Internal contour, $Y_4 \pm 0.010$ in. | Internal contour, $Y_5 \pm 0.010$ cm | Internal contour, $Y_5 \pm 0.010$ in. | External contour, $Y_3 \pm 0.010$ cm | External contour, $Y_3 \pm 0.010$ in. | External contour, $Y_6 \pm 0.010$ cm | External contour, $Y_6 \pm 0.010$ in. |
|---|---|---|---|---|---|---|---|---|---|
| 10.790 | 4.248 | 6.934 | 2.730 | 6.930 | 2.730 | 7.592 | 2.989 | 7.592 | 2.989 |
| 11.176 | 4.400 | 7.043 | 2.773 | 7.043 | 2.773 | 7.544 | 2.970 | 7.544 | 2.970 |
| 11.684 | 4.600 | 7.211 | 2.839 | 7.122 | 2.804 | 7.577 | 2.975 | 7.468 | 2.940 |
| 12.192 | 4.800 | 7.430 | 2.925 | 7.107 | 2.798 | 7.676 | 3.022 | 7.353 | 2.895 |
| 12.700 | 5.000 | 7.823 | 3.080 | 7.018 | 2.763 | 7.899 | 3.110 | 7.221 | 2.843 |
| 13.208 | 5.200 | 7.991 | 3.145 | 6.904 | 2.718 | 8.164 | 3.214 | 7.076 | 2.786 |
| 13.716 | 5.400 | 8.275 | 3.258 | 6.767 | 2.664 | 8.423 | 3.316 | 6.914 | 2.722 |
| 14.224 | 5.600 | 8.509 | 3.350 | 6.614 | 2.604 | 8.644 | 3.403 | 6.749 | 2.657 |
| 14.732 | 5.800 | 8.674 | 3.415 | 6.441 | 2.536 | 8.809 | 3.468 | 6.576 | 2.589 |
| 15.240 | 6.000 | 8.799 | 3.464 | 6.256 | 2.463 | 8.933 | 3.517 | 6.391 | 2.516 |
| 15.748 | 6.200 | 8.895 | 3.502 | 6.071 | 2.390 | 9.030 | 3.555 | 6.205 | 2.443 |
| 16.256 | 6.400 | 8.941 | 3.520 | 5.883 | 2.316 | 9.075 | 3.573 | 6.017 | 2.369 |
| 16.764 | 6.600 | 8.971 | 3.532 | 5.679 | 2.236 | 9.106 | 3.585 | 5.814 | 2.289 |
| 17.272 | 6.800 | 8.992 | 3.540 | 5.471 | 2.154 | 9.126 | 3.593 | 5.606 | 2.207 |
| 17.780 | 7.000 | 8.976 | 3.534 | 5.263 | 2.072 | 9.111 | 3.587 | 5.398 | 2.125 |
| 18.288 | 7.200 | 8.931 | 3.516 | 5.034 | 1.982 | 9.065 | 3.569 | 5.169 | 2.035 |
| 18.796 | 7.400 | 8.839 | 3.480 | 4.801 | 1.890 | 8.974 | 3.533 | 4.935 | 1.943 |
| 19.202 | 7.560 | 8.750 | 3.445 | 4.613 | 1.816 | 8.885 | 3.498 | 4.747 | 1.869 |

(f-2)

(f) Continued.

Figure 6. – Continued.

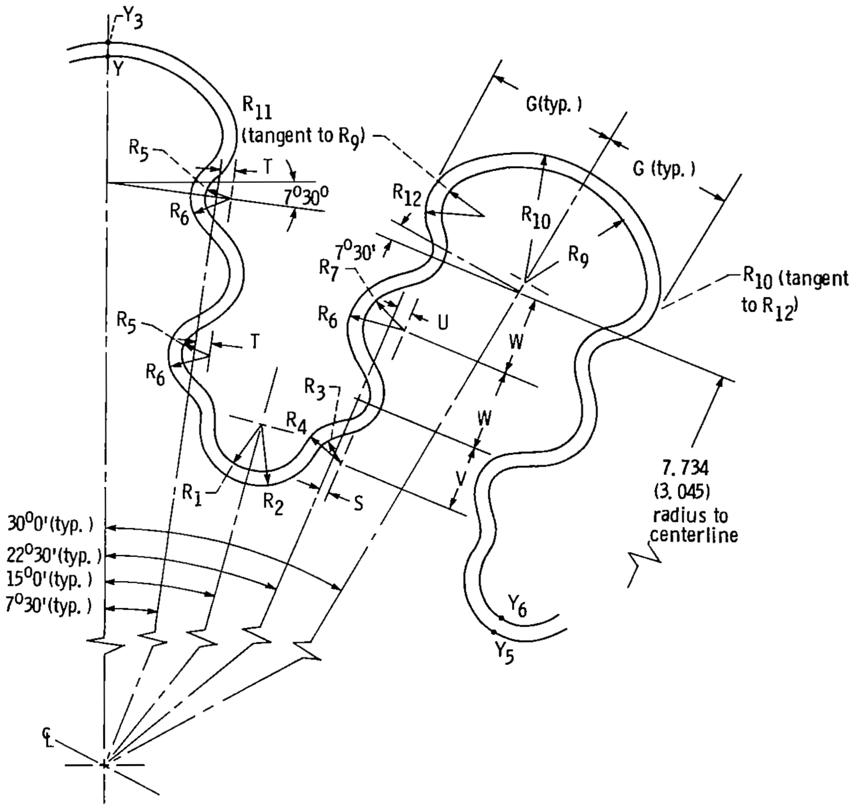


Typical cross section through lobes

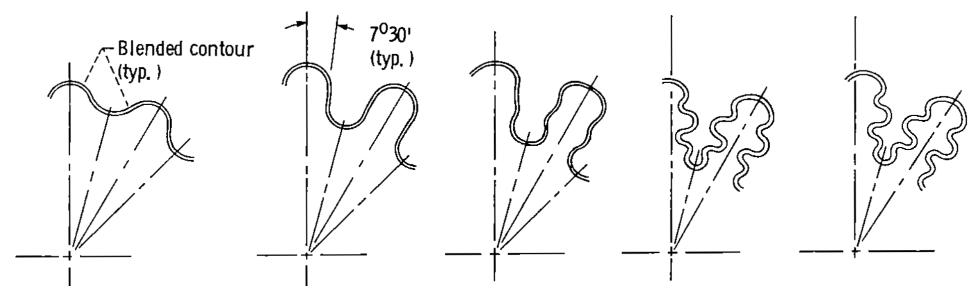


Approximate bumpy lobe contour through respective stations

(f-3)

(f) Continued.

Figure 6. – Continued.

| $X_2$ | | $R_1$ | | $R_2$ | | $R_3$ | | $R_4$ | | $R_5$ | | $R_6$, $R_7$ and $R_{11}$ | | $R_8$ and $R_{12}$ | |
|---|---|---|---|---|---|---|---|---|---|---|---|---|---|---|---|---|---|
| cm | in. | cm | in. | cm | in. | cm | in. | cm | in. | cm | in. | cm | in. | cm | in. | cm | in. |
| 12.192 | 4.80 | 4.425 | 1.742 | 4.671 | 1.839 | ----- | ----- | ----- | ----- | ----- | ----- | ----- | ----- | ----- | ----- |
| 13.208 | 5.20 | 1.080 | .425 | 1.252 | .493 | ----- | ----- | ----- | ----- | ----- | ----- | ----- | ----- | ----- | ----- |
| 14.224 | 5.60 | .859 | .338 | .993 | .391 | ----- | ----- | ----- | ----- | ----- | ----- | ----- | ----- | ----- | ----- |
| 15.240 | 6.00 | .805 | .317 | .940 | .370 | ----- | ----- | ----- | ----- | ----- | ----- | ----- | ----- | ----- | ----- |
| 16.256 | 6.40 | .749 | .295 | .884 | .348 | ----- | ----- | ----- | ----- | ----- | ----- | ----- | ----- | ----- | ----- |
| 17.272 | 6.80 | .765 | .301 | .899 | .354 | ----- | ----- | ----- | ----- | 0.246 | 0.097 | 0.381 | 0.150 | 0.516 | 0.203 |
| 17.780 | 7.00 | .686 | .270 | .820 | .323 | 0.246 | 0.097 | 0.381 | 0.150 | ↓ | ↓ | ↓ | ↓ | ↓ | ↓ |
| 18.288 | 7.20 | .457 | .180 | .592 | .233 | ↓ | ↓ | ↓ | ↓ | ↓ | ↓ | ↓ | ↓ | ↓ | ↓ |
| 18.796 | 7.40 | .381 | .150 | .516 | .203 | ↓ | ↓ | ↓ | ↓ | ↓ | ↓ | ↓ | ↓ | ↓ | ↓ |
| 19.202 | 7.56 | .381 | .150 | .516 | .203 | ↓ | ↓ | ↓ | ↓ | ↓ | ↓ | ↓ | ↓ | ↓ | ↓ |

| $X_2$ | | $R_9$ | | $R_{10}$ | | S | | T and U | | V | | W | | G | |
|---|---|---|---|---|---|---|---|---|---|---|---|---|---|---|---|
| cm | in. | cm | in. | cm | in. | cm | in. | cm | in. | cm | in. | cm | in. | cm | in. |
| 12.192 | 4.80 | 2.111 | 0.831 | 2.357 | 0.928 | ----- | ----- | ----- | ----- | ----- | ----- | ----- | ----- | ----- | ----- |
| 13.208 | 5.20 | 1.064 | .419 | 1.237 | .487 | ----- | ----- | ----- | ----- | ----- | ----- | ----- | ----- | ----- | ----- |
| 14.224 | 5.60 | .983 | .387 | 1.118 | .440 | ----- | ----- | ----- | ----- | ----- | ----- | ----- | ----- | ----- | ----- |
| 15.240 | 6.00 | 1.016 | .400 | 1.151 | .453 | ----- | ----- | ----- | ----- | ----- | ----- | ----- | ----- | ----- | ----- |
| 16.256 | 6.40 | 1.031 | .406 | 1.166 | .459 | ----- | ----- | ----- | ----- | ----- | ----- | ----- | ----- | ----- | ----- |
| 17.272 | 6.80 | 1.039 | .409 | 1.173 | .462 | 0.302 | 0.119 | 0.302 | 0.119 | 0.627 | 0.247 | 0.762 | 0.300 | 1.133 | 0.446 |
| 17.780 | 7.00 | 1.036 | .408 | 1.171 | .461 | .142 | .056 | .224 | .088 | ↓ | ↓ | ↓ | ↓ | 1.097 | .432 |
| 18.288 | 7.20 | 1.018 | .406 | 1.166 | .459 | .091 | .036 | .142 | .056 | ↓ | ↓ | ↓ | ↓ | 1.062 | .418 |
| 18.796 | 7.40 | 1.105 | .435 | 1.240 | .488 | .041 | .016 | .064 | .025 | ↓ | ↓ | ↓ | ↓ | 1.024 | .403 |
| 19.202 | 7.56 | 1.016 | .400 | 1.151 | .453 | 0 | 0 | 0 | 0 | ↓ | ↓ | ↓ | ↓ | .996 | .392 |

(f-4)

(f) Concluded.

Figure 6. – Continued.

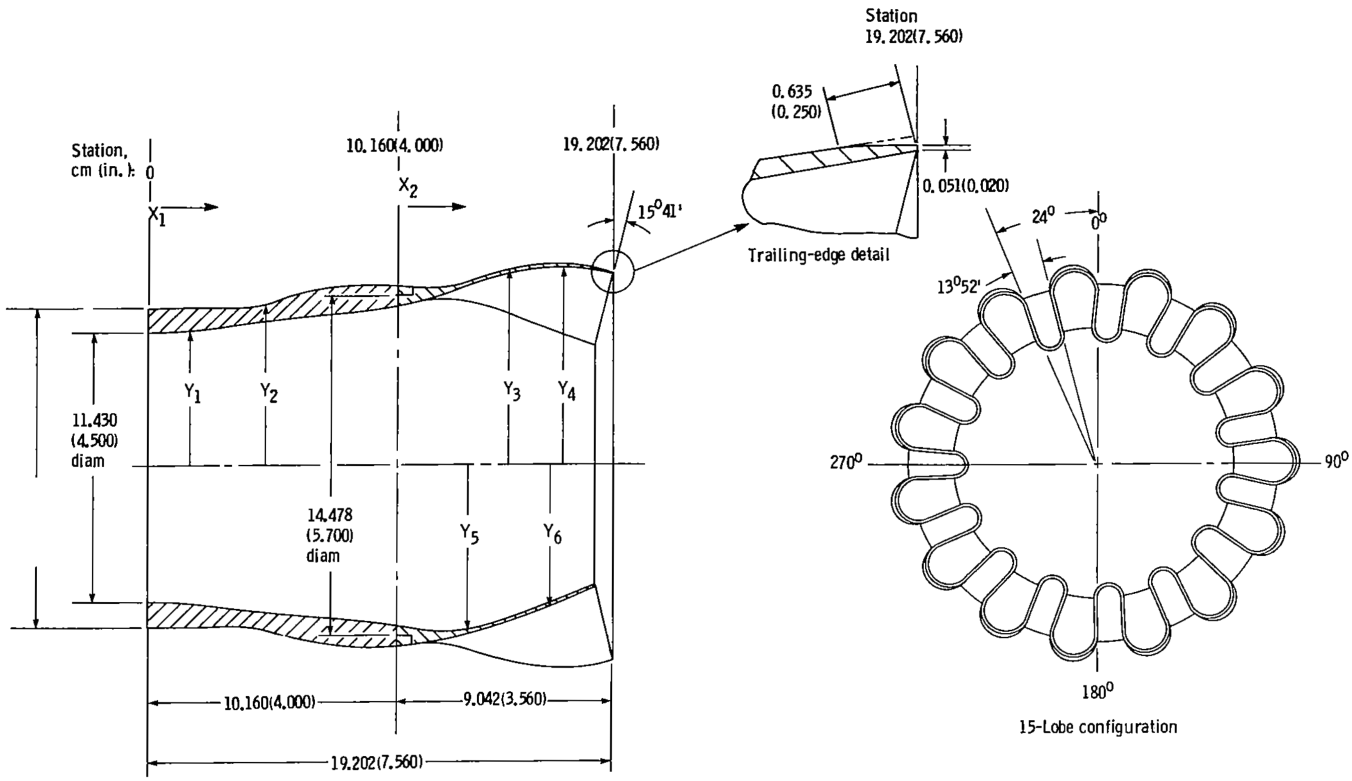


(g)

| $X_1 \pm 0.010$ cm | $X_1 \pm 0.010$ in. | Internal contour, $Y_1 \pm 0.010$ cm | Internal contour, $Y_1 \pm 0.010$ in. | External contour, $Y_2 \pm 0.010$ cm | External contour, $Y_2 \pm 0.010$ in. |
|---|---|---|---|---|---|
| 0 | 0 | 5.715 | 2.250 | 6.792 | 2.674 |
| .518 | .200 | 5.720 | 2.252 | ----- | ----- |
| 2.032 | .800 | 6.888 | 2.318 | 6.795 | 2.675 |
| 3.480 | 1.200 | 6.020 | 2.370 | 6.797 | 2.676 |
| 4.318 | 1.700 | 6.162 | 2.426 | 6.927 | 2.727 |
| 5.334 | 2.100 | 6.274 | 2.470 | 7.115 | 2.801 |
| 6.604 | 2.600 | 6.403 | 2.521 | 7.379 | 2.905 |
| 7.366 | 2.900 | 6.464 | 2.545 | 7.513 | 2.958 |
| 8.382 | 3.300 | 6.533 | 2.572 | 7.628 | 3.003 |
| 9.398 | 3.700 | 6.622 | 2.607 | 7.673 | 3.021 |
| 10.160 | 4.000 | 6.761 | 2.662 | 7.650 | 3.012 |
| 10.795 | 4.250 | ----- | ----- | 7.595 | 2.990 |

| $X_2 \pm 0.010$ | | Internal contour | | | | External contour | | | |
|---|---|---|---|---|---|---|---|---|---|
| | | $Y_4 \pm 0.010$ | | $Y_5 \pm 0.010$ | | $Y_3 \pm 0.010$ | | $Y_6 \pm 0.010$ | |
| cm | in. | cm | in. | cm | in. | cm | in. | cm | in. |
| 10.160 | 4.000 | 6.761 | 2.662 | 6.761 | 2.662 | 7.650 | 3.012 | 7.650 | 3.012 |
| 10.795 | 4.250 | 6.909 | 2.720 | 6.899 | 2.716 | 7.595 | 2.990 | 7.595 | 2.990 |
| 11.176 | 4.400 | 7.008 | 2.759 | 6.972 | 2.745 | 7.559 | 2.976 | 7.544 | 2.970 |
| 11.684 | 4.600 | 7.155 | 2.817 | 7.051 | 2.776 | 7.554 | 2.974 | 7.452 | 2.934 |
| 12.192 | 4.800 | 7.313 | 2.879 | 7.074 | 2.785 | 7.595 | 2.990 | 7.356 | 2.896 |
| 12.700 | 5.000 | 7.485 | 2.947 | 7.043 | 2.773 | 7.686 | 3.026 | 7.244 | 2.852 |
| 13.208 | 5.200 | 7.663 | 3.017 | 6.957 | 2.739 | 7.818 | 3.078 | 7.112 | 2.800 |
| 13.716 | 5.400 | 7.836 | 3.085 | 6.830 | 2.689 | 7.971 | 3.138 | 6.965 | 2.742 |
| 14.224 | 5.600 | 8.001 | 3.150 | 6.668 | 2.625 | 8.136 | 3.203 | 6.802 | 2.678 |
| 14.732 | 5.800 | 8.146 | 3.207 | 6.495 | 2.557 | 8.280 | 3.260 | 6.629 | 2.610 |
| 15.240 | 6.000 | 8.265 | 3.254 | 6.312 | 2.485 | 8.400 | 3.307 | 6.447 | 2.538 |
| 15.748 | 6.200 | 8.354 | 3.289 | 6.119 | 2.409 | 8.489 | 3.342 | 6.253 | 2.462 |
| 16.256 | 6.400 | 8.412 | 3.312 | 5.918 | 2.330 | 8.547 | 3.365 | 6.053 | 2.383 |
| 16.764 | 6.600 | 8.433 | 3.320 | 5.718 | 2.251 | 8.567 | 3.373 | 5.852 | 2.304 |
| 17.272 | 6.800 | 8.418 | 3.314 | 5.514 | 2.171 | 8.552 | 3.367 | 5.649 | 2.224 |
| 17.780 | 7.000 | 8.369 | 3.295 | 5.309 | 2.090 | 8.504 | 3.348 | 5.443 | 2.143 |
| 18.288 | 7.200 | 8.298 | 3.267 | 5.103 | 2.009 | 8.433 | 3.320 | 5.237 | 2.062 |
| 18.346 | 7.223 | ----- | ----- | 5.077 | 1.999 | ----- | ----- | 5.212 | 2.052 |
| 18.796 | 7.400 | 8.209 | 3.232 | ----- | ----- | 8.344 | 3.285 | ----- | ----- |
| 19.202 | 7.560 | 8.128 | 3.200 | ----- | ----- | 8.263 | 3.253 | ----- | ----- |

(g) 15C mixer.

Figure 6. – Continued.

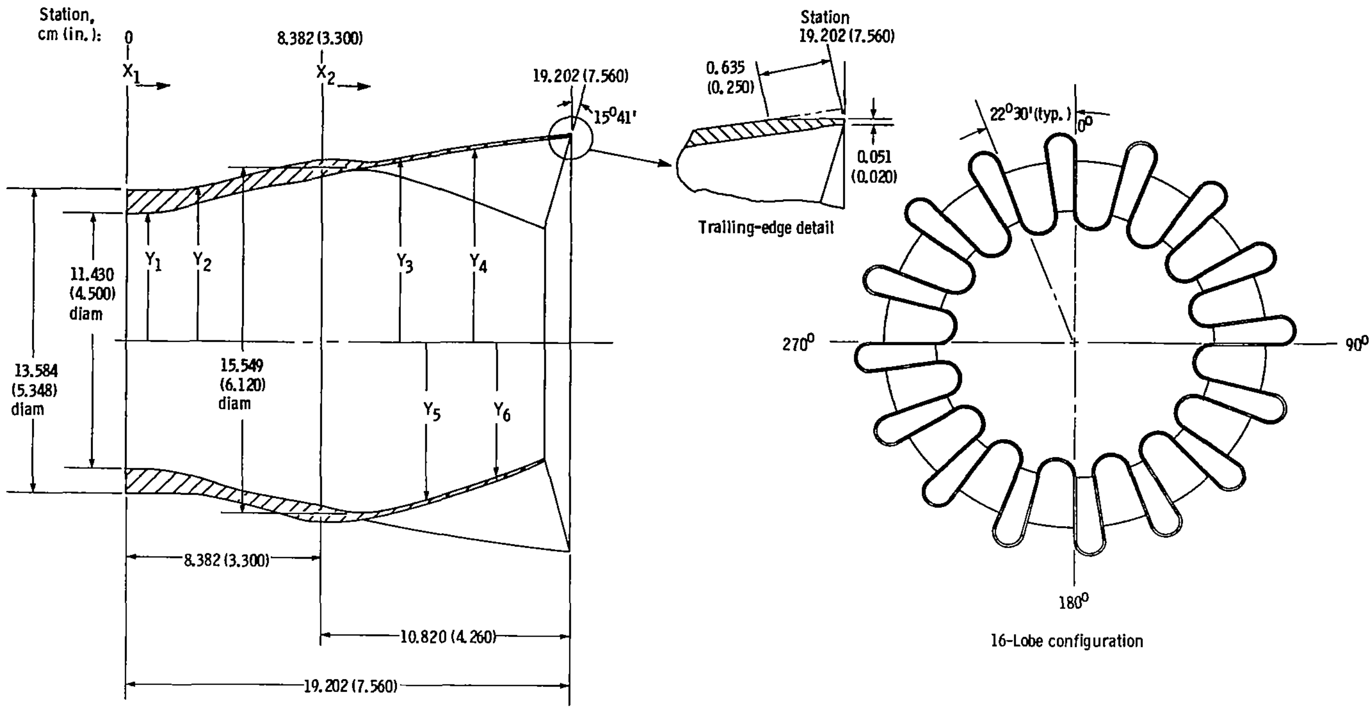


| $X_1 \pm 0.010$, cm | $X_1 \pm 0.010$, in. | Internal contour, $Y_1 \pm 0.010$, cm | Internal contour, $Y_1 \pm 0.010$, in. | External contour, $Y_2 \pm 0.010$, cm | External contour, $Y_2 \pm 0.010$, in. |
|---|---|---|---|---|---|
| 0 | 0 | 5.715 | 2.250 | 6.792 | 2.674 |
| .508 | .200 | 5.725 | 2.254 | ----- | ----- |
| 1.016 | .400 | 5.756 | 2.266 | ----- | ----- |
| 1.270 | .500 | ----- | ----- | 6.792 | 2.674 |
| 1.524 | .600 | 5.812 | 2.288 | 6.800 | 2.677 |
| 2.032 | .800 | 5.898 | 2.322 | 6.817 | 2.684 |
| 2.540 | 1.000 | 5.994 | 2.360 | 6.838 | 2.692 |
| 3.048 | 1.200 | 6.106 | 2.404 | 6.883 | 2.710 |
| 3.556 | 1.400 | 6.233 | 2.454 | 6.944 | 2.734 |
| 4.064 | 1.600 | 6.370 | 2.508 | 7.036 | 2.770 |
| 4.572 | 1.800 | 6.518 | 2.566 | 7.153 | 2.816 |
| 5.080 | 2.000 | 6.660 | 2.622 | 7.285 | 2.868 |
| 5.588 | 2.200 | 6.797 | 2.676 | 7.424 | 2.923 |
| 6.096 | 2.400 | 6.922 | 2.725 | 7.564 | 2.978 |
| 6.604 | 2.600 | 7.028 | 2.767 | 7.701 | 3.032 |
| 7.112 | 2.800 | 7.127 | 2.806 | 7.823 | 3.080 |
| 7.620 | 3.000 | 7.224 | 2.844 | 7.927 | 3.121 |
| 8.128 | 3.200 | 7.325 | 2.884 | 7.996 | 3.148 |
| 8.382 | 3.300 | 7.366 | 2.900 | 8.019 | 3.157 |
| 8.636 | 3.400 | ----- | ----- | 8.029 | 3.161 |

| $X_2 \pm 0.010$, cm | $X_2 \pm 0.010$, in. | Internal contour, $Y_4 \pm 0.010$, cm | Internal contour, $Y_4 \pm 0.010$, in. | Internal contour, $Y_5 \pm 0.010$, cm | Internal contour, $Y_5 \pm 0.010$, in. | External contour, $Y_3 \pm 0.010$, cm | External contour, $Y_3 \pm 0.010$, in. | External contour, $Y_6 \pm 0.010$, cm | External contour, $Y_6 \pm 0.010$, in. |
|---|---|---|---|---|---|---|---|---|---|
| 8.382 | 3.300 | 7.376 | 2.904 | 7.376 | 2.904 | 8.019 | 3.157 | 8.019 | 3.157 |
| 9.017 | 3.550 | ----- | ----- | ----- | ----- | 8.052 | 3.170 | 8.052 | 3.170 |
| 9.144 | 3.600 | 7.554 | 2.974 | 7.554 | 2.974 | ----- | ----- | ----- | ----- |
| 9.652 | 3.800 | 7.681 | 3.024 | 7.650 | 3.012 | 8.070 | 3.177 | 8.037 | 3.164 |
| 10.160 | 4.000 | 7.808 | 3.074 | 7.706 | 3.034 | 8.103 | 3.190 | 7.998 | 3.149 |
| 10.668 | 4.200 | 7.930 | 3.122 | 7.704 | 3.033 | 8.161 | 3.213 | 7.930 | 3.122 |
| 11.176 | 4.400 | 8.047 | 3.168 | 7.658 | 3.105 | 8.235 | 3.242 | 7.844 | 3.088 |
| 11.684 | 4.600 | 8.164 | 3.214 | 7.579 | 2.984 | 8.321 | 3.276 | 7.732 | 3.044 |
| 12.192 | 4.800 | 8.275 | 3.258 | 7.468 | 2.940 | 8.418 | 3.314 | 7.605 | 2.994 |
| 12.700 | 5.000 | 8.382 | 3.300 | 7.330 | 2.886 | 8.517 | 3.353 | 7.465 | 2.939 |
| 13.208 | 5.200 | 8.484 | 3.340 | 7.168 | 2.822 | 8.618 | 3.393 | 7.303 | 2.875 |
| 13.716 | 5.400 | 8.580 | 3.378 | 6.993 | 2.753 | 8.715 | 3.431 | 7.127 | 2.806 |
| 14.224 | 5.600 | 8.669 | 3.413 | 6.807 | 2.680 | 8.804 | 3.466 | 6.942 | 2.733 |
| 14.732 | 5.800 | 8.748 | 3.444 | 6.607 | 2.601 | 8.882 | 3.497 | 6.741 | 2.654 |
| 15.240 | 6.000 | 8.824 | 3.474 | 6.398 | 2.519 | 8.959 | 3.527 | 6.533 | 2.572 |
| 15.748 | 6.200 | 8.900 | 3.504 | 6.182 | 2.434 | 9.035 | 3.557 | 6.317 | 2.457 |
| 16.256 | 6.400 | 8.971 | 3.532 | 5.959 | 2.346 | 9.106 | 3.585 | 6.093 | 2.399 |
| 16.764 | 6.600 | 9.042 | 3.560 | 5.730 | 2.256 | 9.177 | 3.613 | 5.865 | 2.309 |
| 17.272 | 6.800 | 9.108 | 3.586 | 5.502 | 2.166 | 9.243 | 3.639 | 5.636 | 2.219 |
| 17.780 | 7.000 | 9.167 | 3.609 | 5.273 | 2.076 | 9.301 | 3.662 | 5.408 | 2.129 |
| 18.085 | 7.120 | ----- | ----- | 5.136 | 2.022 | ----- | ----- | 5.271 | 2.075 |
| 18.288 | 7.200 | 9.215 | 3.628 | ----- | ----- | 9.350 | 3.681 | ----- | ----- |
| 18.796 | 7.400 | 9.253 | 3.643 | ----- | ----- | 9.388 | 3.696 | ----- | ----- |
| 19.202 | 7.560 | 9.271 | 3.650 | ----- | ----- | 9.406 | 3.703 | ----- | ----- |

(h)

**(h) 16B mixer.**

**Figure 6. – Continued.**

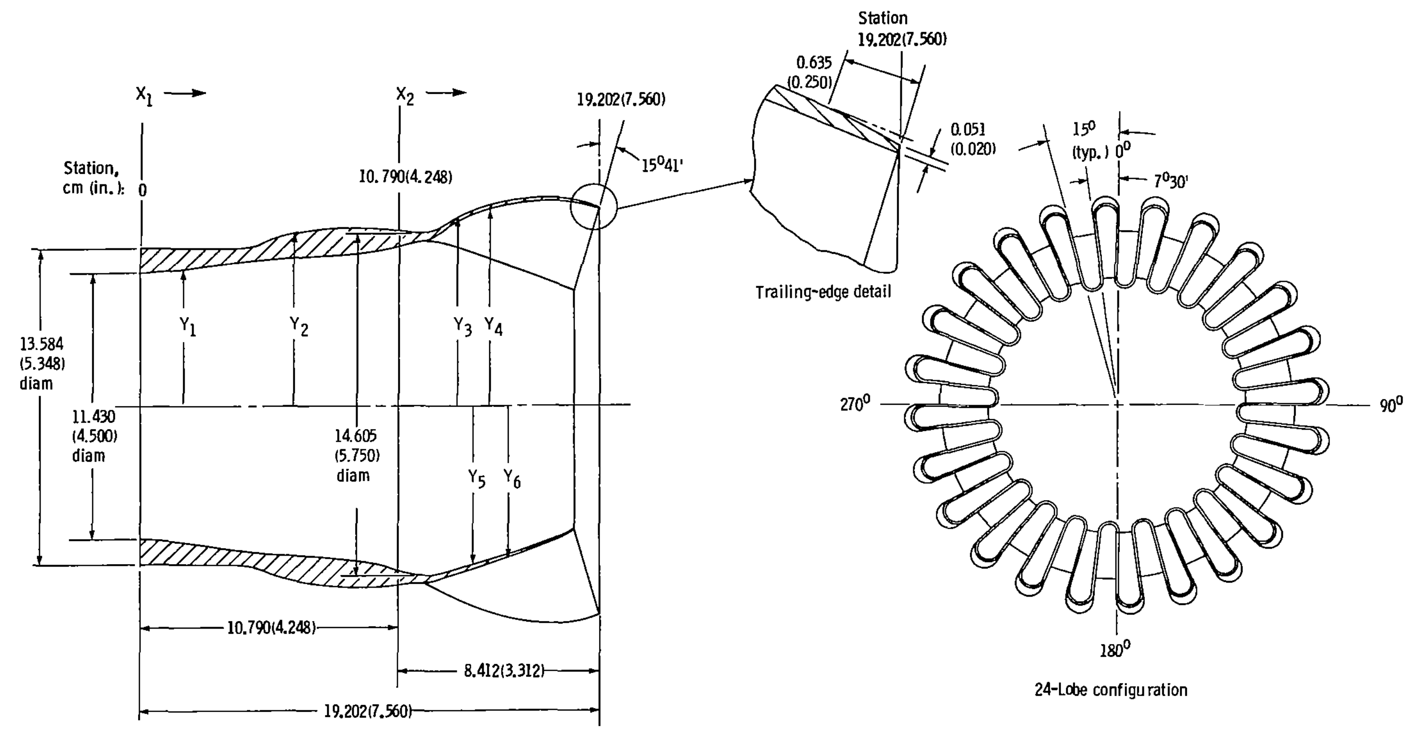


(i)

| $X_1 \pm 0.010$ | | Internal contour, $Y_1 \pm 0.010$ | | External contour, $Y_2 \pm 0.010$ | |
|---|---|---|---|---|---|
| cm | in. | cm | in. | cm | in. |
| 0 | 0 | 5.715 | 2.250 | 6.795 | 2.675 |
| .508 | .200 | 5.720 | 2.252 | 6.795 | 2.675 |
| 2.032 | .800 | 5.888 | 2.318 | 6.795 | 2.675 |
| 3.480 | 1.200 | 6.020 | 2.370 | 6.797 | 2.676 |
| 4.318 | 1.700 | 6.162 | 2.426 | 6.927 | 2.727 |
| 5.334 | 2.100 | 6.274 | 2.470 | 7.115 | 2.801 |
| 6.604 | 2.600 | 6.403 | 2.521 | 7.379 | 2.905 |
| 7.366 | 2.900 | 6.464 | 2.545 | 7.513 | 2.958 |
| 8.382 | 3.300 | 6.533 | 2.572 | 7.628 | 3.003 |
| 9.398 | 3.700 | 6.622 | 2.607 | 7.673 | 3.021 |
| 10.160 | 4.000 | 6.671 | 2.662 | 7.650 | 3.012 |
| 10.668 | 4.200 | 6.896 | 2.715 | 7.607 | 2.995 |
| 10.790 | 4.248 | 6.934 | 2.730 | 7.592 | 2.989 |
| 10.922 | 4.300 | ----- | ----- | 7.579 | 2.984 |

| $X_2 \pm 0.010$ | | Internal contour | | | | External contour | | | |
|---|---|---|---|---|---|---|---|---|---|
| | | $Y_4 \pm 0.010$ | | $Y_5 \pm 0.010$ | | $Y_3 \pm 0.010$ | | $Y_6 \pm 0.010$ | |
| cm | in. | cm | in. | cm | in. | cm | in. | cm | in. |
| 10.790 | 4.248 | 6.934 | 2.730 | 6.934 | 2.730 | 7.592 | 2.989 | 7.592 | 2.989 |
| 11.430 | 4.500 | 7.127 | 2.806 | 7.094 | 2.793 | 7.508 | 2.956 | 7.508 | 2.956 |
| 11.938 | 4.700 | 7.315 | 2.880 | ----- | ----- | 7.554 | 2.974 | ----- | ----- |
| 12.065 | 4.750 | 7.369 | 2.901 | 7.150 | 2.815 | 7.587 | 2.987 | 7.379 | 2.905 |
| 12.700 | 5.000 | 7.696 | 3.030 | 7.041 | 2.772 | 7.877 | 3.101 | 7.221 | 2.843 |
| 13.335 | 5.250 | 8.070 | 3.177 | 6.863 | 2.703 | 8.242 | 3.245 | 7.038 | 2.771 |
| 13.970 | 5.500 | 8.397 | 3.306 | 6.688 | 2.633 | 8.542 | 3.363 | 6.833 | 2.690 |
| 14.605 | 5.750 | 8.636 | 3.400 | 6.482 | 2.552 | 8.771 | 3.453 | 6.617 | 2.605 |
| 15.240 | 6.000 | 8.799 | 3.464 | 6.256 | 2.463 | 8.933 | 3.517 | 6.391 | 2.516 |
| 15.875 | 6.250 | 8.903 | 3.505 | 6.020 | 2.370 | 9.037 | 3.558 | 6.154 | 2.423 |
| 16.510 | 6.500 | 8.959 | 3.527 | 5.773 | 2.273 | 9.099 | 3.580 | 5.999 | 2.326 |
| 17.145 | 6.750 | 8.981 | 3.536 | 5.525 | 2.175 | 9.116 | 3.589 | 5.659 | 2.228 |
| 17.780 | 7.000 | 8.976 | 3.534 | 5.260 | 2.071 | 9.111 | 3.587 | 5.395 | 2.124 |
| 18.160 | 7.150 | ----- | ----- | 5.095 | 2.006 | ----- | ----- | 5.230 | 2.059 |
| 18.415 | 7.250 | 8.905 | 3.506 | ----- | ----- | 9.040 | 3.559 | ----- | ----- |
| 19.202 | 7.560 | 8.750 | 3.445 | ----- | ----- | 8.885 | 3.498 | ----- | ----- |

(i) 24A mixer.

Figure 6. – Concluded.

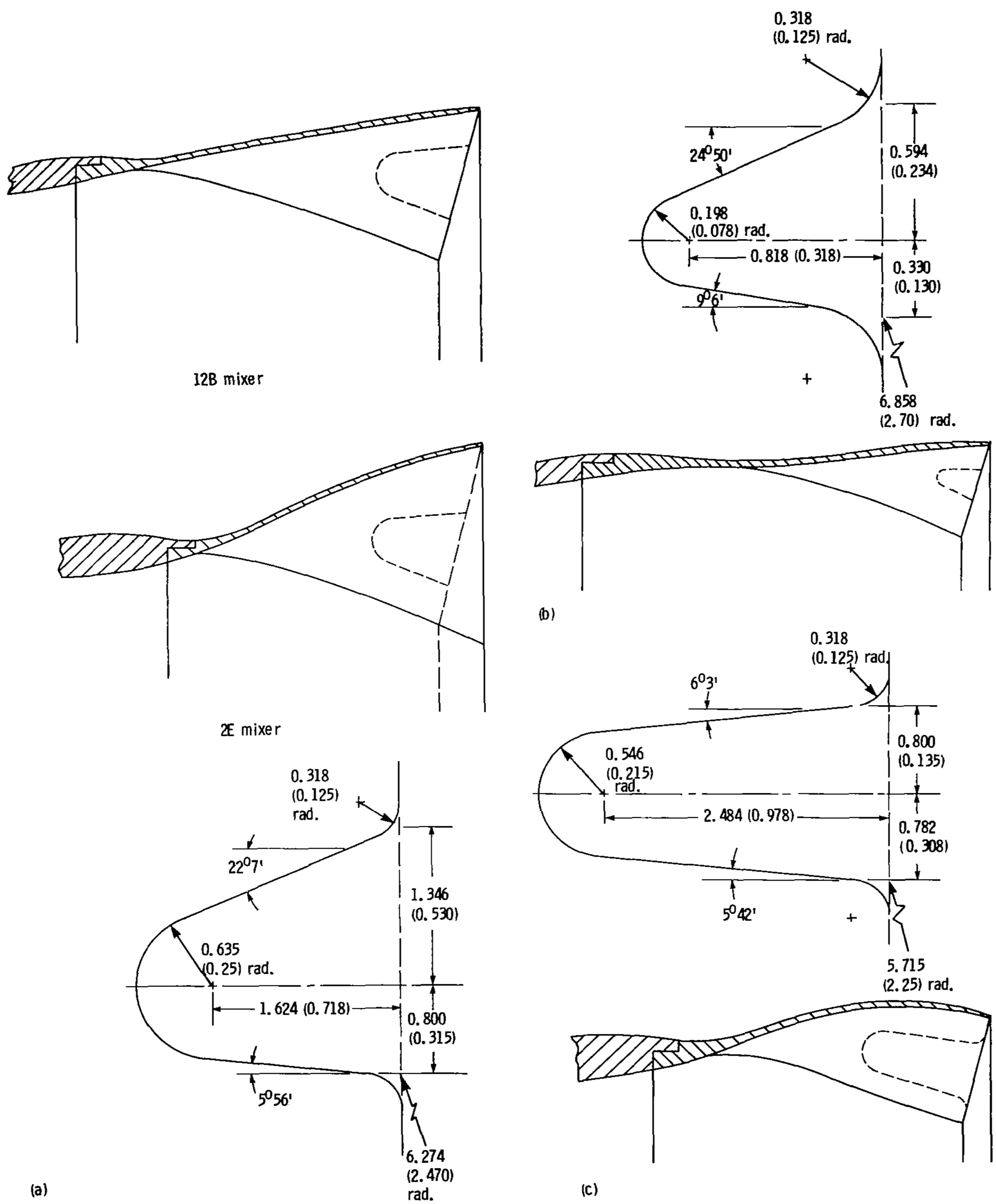


(a) Geometric details for 12B and 2E lobes.
(b) Details for 1E lobes.
(c) Details for 12C lobes.

Figure 7. – Geometric details of mixer lobe scalloping.

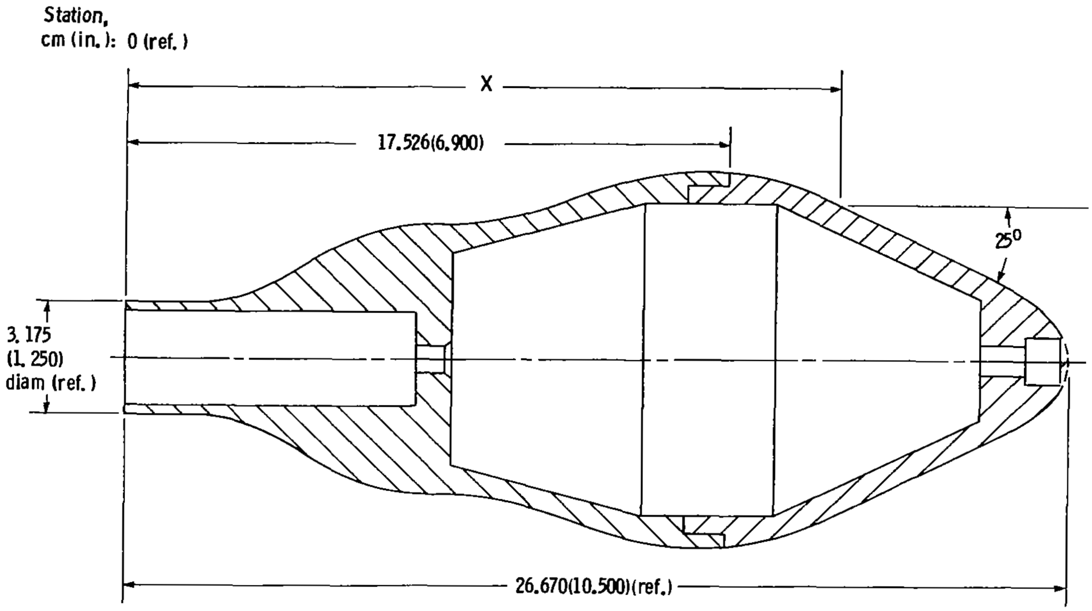


(a)

| X±0.002 | | $Y_r$±0.002 | | X±0.002 | | $Y_r$±0.002 | |
|---|---|---|---|---|---|---|---|
| cm | in. | cm | in. | cm | in. | cm | in. |
| 0 | 0 | 1.588 | 0.625 | 13.183 | 5.190 | 4.724 | 1.860 |
| 1.524 | .600 | 1.588 | .625 | 14.021 | 5.520 | 4.978 | 1.960 |
| 2.667 | 1.050 | 1.702 | .670 | 15.113 | 5.950 | 5.207 | 2.050 |
| 2.835 | 1.510 | 2.032 | .800 | 15.875 | 6.250 | 5.283 | 2.080 |
| 4.928 | 1.940 | 2.591 | 1.020 | 16.713 | 6.580 | 5.309 | 2.090 |
| 5.842 | 2.300 | 3.099 | 1.220 | 17.424 | 6.860 | 5.271 | 2.075 |
| 6.756 | 2.660 | 3.454 | 1.360 | 17.958 | 7.070 | 5.182 | 2.040 |
| 7.747 | 3.050 | 3.734 | 1.470 | 18.923 | 7.450 | 4.928 | 1.940 |
| 8.433 | 3.320 | 3.810 | 1.500 | 20.396 | 8.030 | 4.293 | 1.690 |
| 9.271 | 3.650 | 3.810 | 1.500 | 22.377 | 8.810 | 3.353 | 1.320 |
| 10.236 | 4.030 | 3.874 | 1.525 | 24.663 | 9.710 | 2.184 | .860 |
| 11.278 | 4.440 | 4.115 | 1.620 | 25.908 | 10.200 | 1.270 | .500 |
| 12.243 | 4.820 | 4.394 | 1.730 | 26.670 | 10.500 | 0 | 0 |

(a) Reference centerbody.

Figure 8. – Centerbody contours and dimensions.

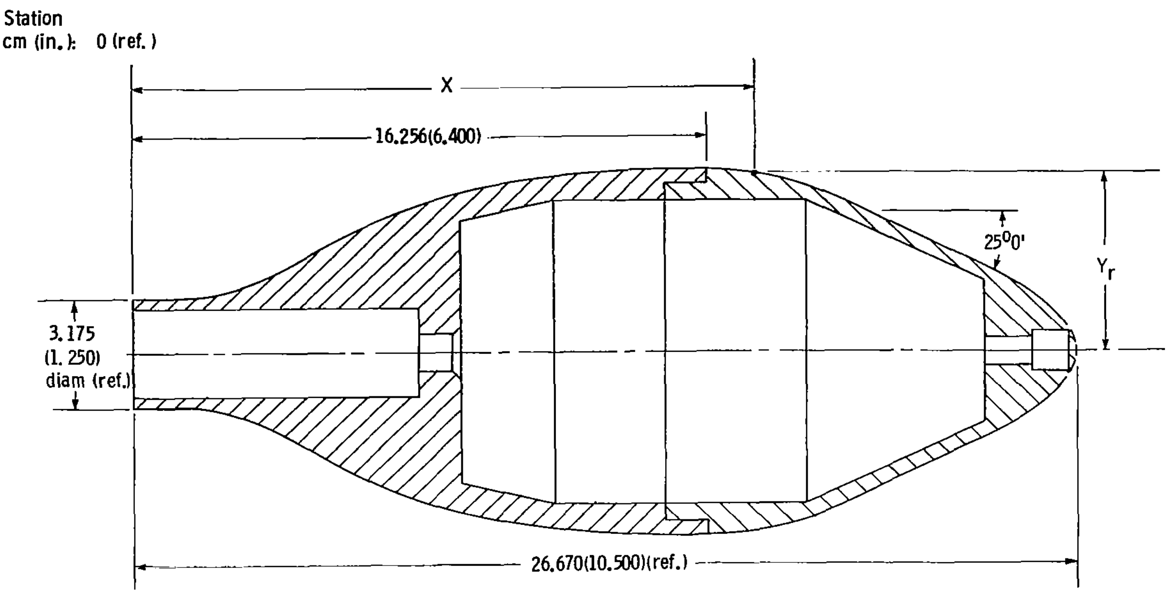


| $X \pm 0.002$ | | $Y_r \pm 0.002$ | | $X \pm 0.002$ | | $Y_r \pm 0.002$ | |
|---|---|---|---|---|---|---|---|
| cm | in. | cm | in. | cm | in. | cm | in. |
| 0 | 0 | 1.588 | 0.625 | 13.716 | 5.400 | 5.324 | 2.096 |
| .508 | .400 | 1.588 | .625 | 14.478 | 5.700 | 5.359 | 2.110 |
| 1.778 | .700 | 1.623 | .639 | 15.240 | 6.000 | 5.377 | 2.117 |
| 2.540 | 1.000 | 1.758 | .692 | 15.748 | 6.200 | 5.375 | 2.116 |
| 3.302 | 1.300 | 2.007 | .790 | 16.256 | 6.400 | 5.362 | 2.111 |
| 4.064 | 1.600 | 2.357 | .928 | 16.764 | 6.600 | 5.334 | 2.100 |
| 4.826 | 1.900 | 2.771 | 1.091 | 17.526 | 6.900 | 5.253 | 2.068 |
| 5.334 | 2.100 | 3.058 | 1.204 | 18.288 | 7.200 | 5.105 | 2.010 |
| 6.096 | 2.400 | 3.475 | 1.368 | 19.050 | 7.500 | 4.879 | 1.921 |
| 6.858 | 2.700 | 3.848 | 1.515 | 19.812 | 7.800 | 4.569 | 1.799 |
| 7.620 | 3.000 | 4.173 | 1.643 | 22.352 | 8.800 | 3.363 | 1.324 |
| 8.382 | 3.300 | 4.448 | 1.751 | 23.114 | 9.100 | 3.000 | 1.181 |
| 9.144 | 3.600 | 4.674 | 1.840 | 23.876 | 9.400 | 2.621 | 1.032 |
| 9.906 | 3.900 | 4.856 | 1.912 | 24.638 | 9.700 | 2.207 | .869 |
| 10.668 | 4.200 | 5.001 | 1.969 | 25.400 | 10.000 | 1.697 | .668 |
| 11.430 | 4.500 | 5.116 | 2.014 | 26.162 | 10.300 | .508 | .400 |
| 12.192 | 4.800 | 5.204 | 2.049 | 26.670 | 10.500 | 0 | 0 |
| 12.954 | 5.100 | 5.273 | 2.076 | | | | |

(b)

(b) 3B centerbody.

Figure 8. – Continued.

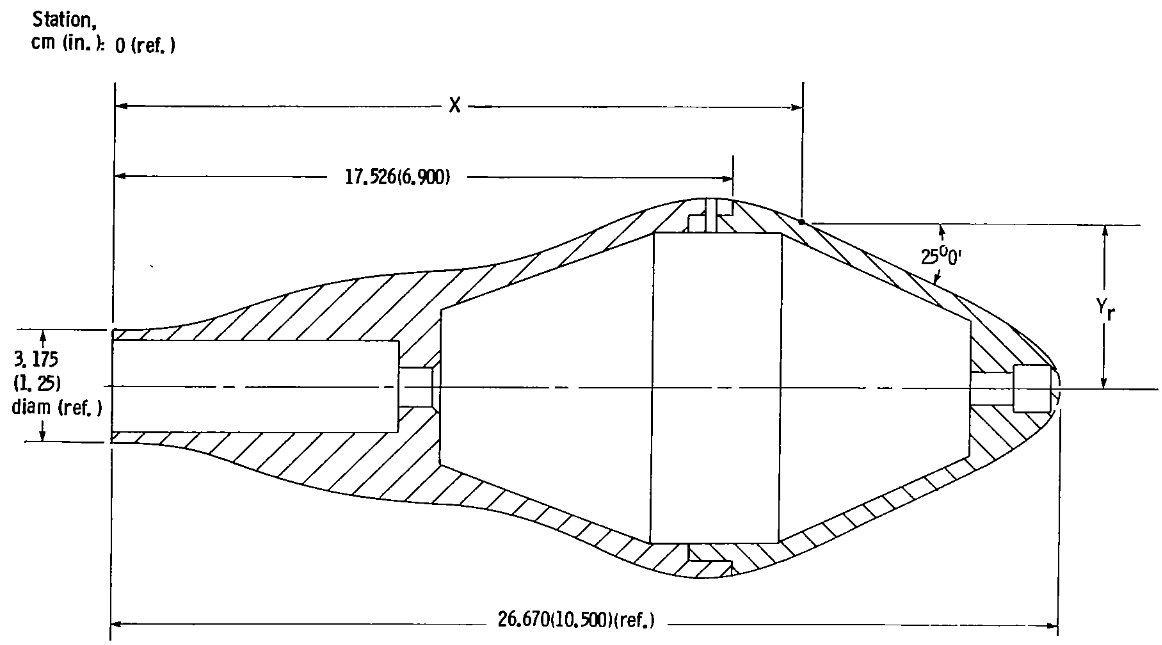


| X±0.002 | | $Y_r$±0.002 | | X±0.002 | | $Y_r$±0.002 | |
|---|---|---|---|---|---|---|---|
| cm | in. | cm | in. | cm | in. | cm | in. |
| 0 | 0 | 1.588 | 0.625 | 13.970 | 5.550 | 4.653 | 1.832 |
| .762 | .300 | 1.588 | .625 | 14.732 | 5.800 | 4.963 | 1.954 |
| 1.270 | .500 | 1.631 | .642 | 15.494 | 6.100 | 5.207 | 2.050 |
| 1.778 | .700 | 1.707 | .672 | 16.400 | 6.400 | 5.354 | 2.108 |
| 2.540 | 1.000 | 1.877 | .739 | 16.764 | 6.600 | 5.364 | 2.122 |
| 3.302 | 1.300 | 2.101 | .827 | 17.272 | 6.800 | 5.372 | 2.115 |
| 4.064 | 1.600 | 2.355 | .927 | 17.526 | 6.900 | 5.344 | 2.104 |
| 4.826 | 1.900 | 2.604 | 1.025 | 18.034 | 7.100 | 5.248 | 2.066 |
| 5.588 | 2.200 | 2.824 | 1.112 | 18.542 | 7.300 | 5.105 | 2.010 |
| 6.350 | 2.500 | 2.997 | 1.180 | 19.304 | 7.600 | 4.813 | 1.895 |
| 7.112 | 2.800 | 3.112 | 1.225 | 20.066 | 7.900 | 4.460 | 1.756 |
| 7.874 | 3.100 | 3.180 | 1.252 | 23.114 | 9.100 | 3.000 | 1.181 |
| 8.636 | 3.400 | 3.223 | 1.269 | 23.876 | 9.400 | 2.621 | 1.032 |
| 9.398 | 3.700 | 3.274 | 1.289 | 24.638 | 9.700 | 2.207 | .869 |
| 10.160 | 4.000 | 3.360 | 1.323 | 25.400 | 10.000 | 1.697 | .668 |
| 10.922 | 4.300 | 3.503 | 1.379 | 25.908 | 10.200 | 1.270 | .500 |
| 11.684 | 4.600 | 3.719 | 1.464 | 26.162 | 10.300 | 1.016 | .400 |
| 12.446 | 4.900 | 3.995 | 1.573 | 26.670 | 10.500 | 0 | 0 |
| 13.208 | 5.200 | 4.321 | 1.701 | | | | |

(c)

(c) 2AC centerbody.

Figure 8. – Concluded.

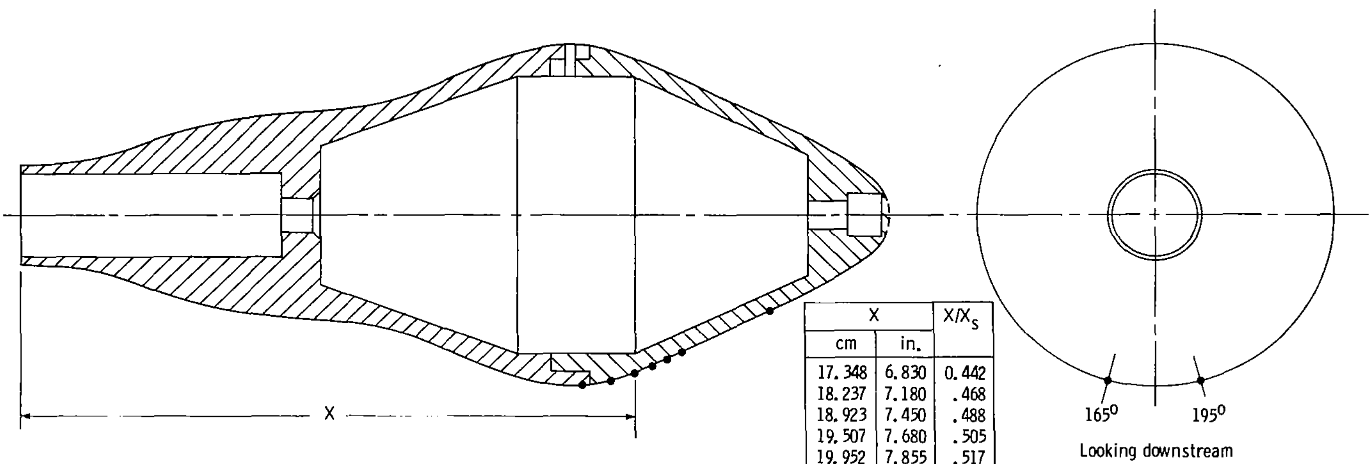


| X | | $X/X_s$ |
|---|---|---|
| cm | in. | |
| 17.348 | 6.830 | 0.442 |
| 18.237 | 7.180 | .468 |
| 18.923 | 7.450 | .488 |
| 19.507 | 7.680 | .505 |
| 19.952 | 7.855 | .517 |
| 20.396 | 8.030 | .530 |
| 23.063 | 9.080 | .607 |

Figure 9. – Centerbody static pressure instrumentation details.

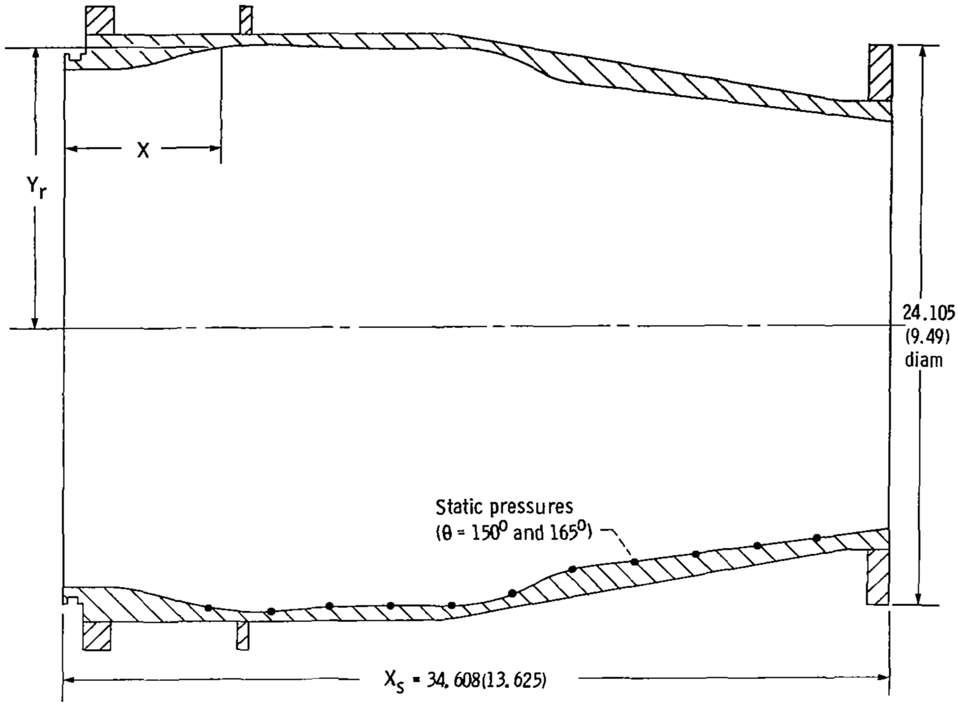


| Contour coordinates | | | |
|---|---|---|---|
| X ± 0.005 | | $Y_r$ ± 0.005 | |
| cm | in. | cm | in. |
| 0 | 0 | 11.100 | 4.370 |
| 1.334 | .525 | 11.100 | 4.370 |
| 2.350 | .925 | 11.151 | 4.390 |
| 3.239 | 1.275 | 11.227 | 4.420 |
| 4.102 | 1.615 | 11.455 | 4.510 |
| 5.093 | 2.005 | 11.709 | 4.610 |
| 6.058 | 2.385 | 11.887 | 4.680 |
| 7.226 | 2.845 | 12.040 | 4.740 |
| 8.166 | 3.215 | 12.116 | 4.770 |
| 9.284 | 3.655 | 12.090 | 4.760 |
| 10.325 | 4.065 | 12.040 | 4.740 |
| 11.316 | 4.455 | 11.938 | 4.700 |
| 16.091 | 6.335 | 11.938 | 4.700 |
| 17.005 | 6.695 | 11.875 | 4.675 |
| 17.894 | 7.045 | 11.684 | 4.600 |
| 18.733 | 7.375 | 11.405 | 4.490 |
| 19.368 | 7.645 | 11.151 | 4.390 |
| 20.053 | 7.895 | 10.846 | 4.270 |
| 20.688 | 8.145 | 10.566 | 4.160 |
| 21.323 | 8.395 | 10.414 | 4.100 |
| 34.608 | 13.625 | 8.738 | 3.440 |

| Static pressures | | |
|---|---|---|
| X | | $X/X_s$ |
| cm | in. | cm |
| 6.033 | 2.375 | 0.174 |
| 8.573 | 3.375 | .248 |
| 11.113 | 4.375 | .321 |
| 13.653 | 5.375 | .395 |
| 16.193 | 6.375 | .468 |
| 18.733 | 7.375 | .541 |
| 21.273 | 8.375 | .615 |
| 23.813 | 9.375 | .688 |
| 26.353 | 10.375 | .762 |
| 28.893 | 11.375 | .835 |
| 31.433 | 12.375 | .908 |

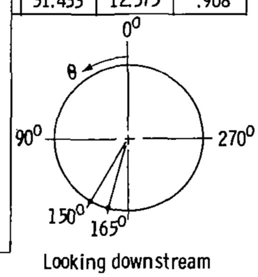


Figure 10. – Rotatable shroud contour coordinates and instrumentation details.

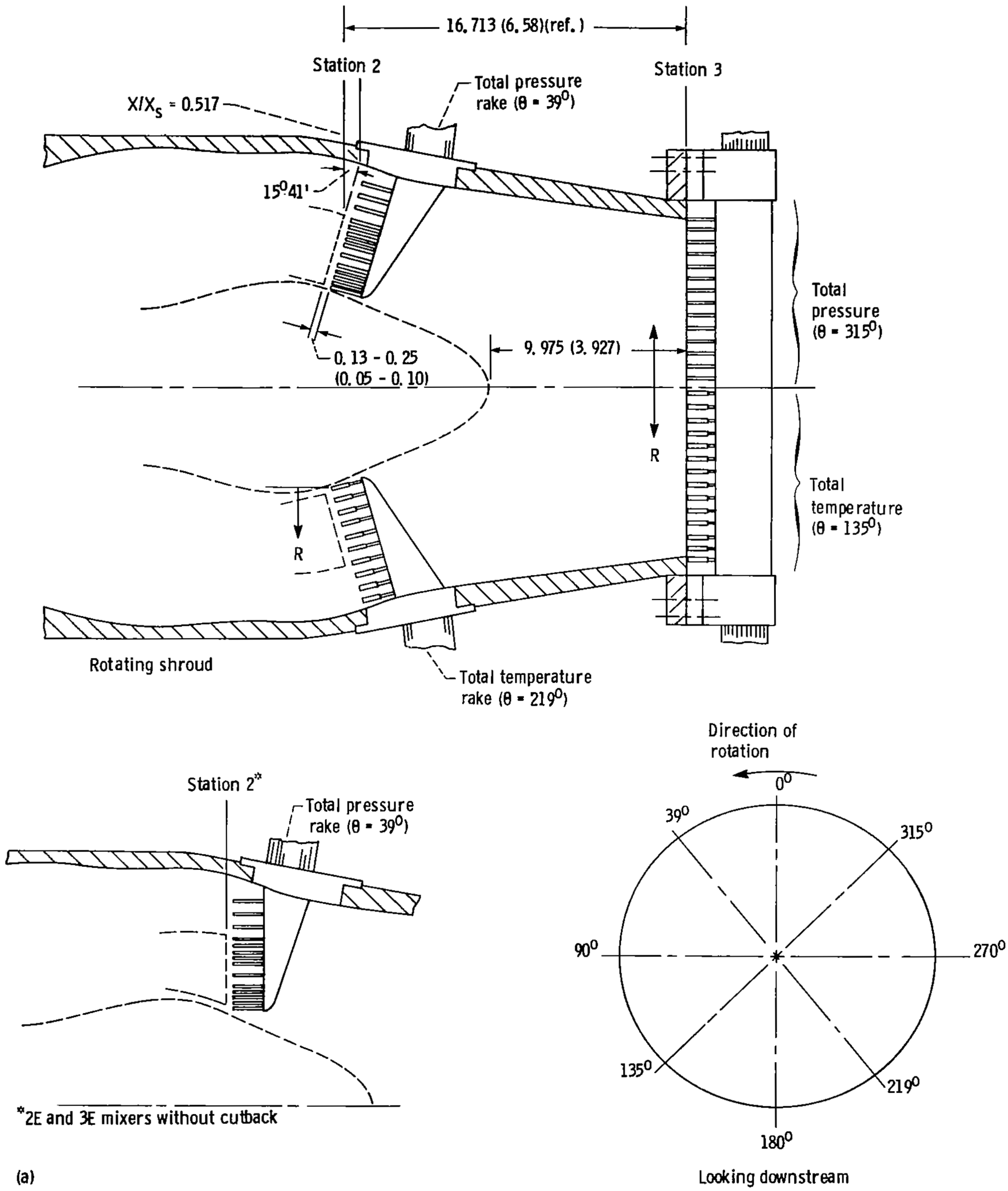


(a) Stations 2 and 3.

**Figure 11. – Total pressure and temperature rake instrumentation details.**

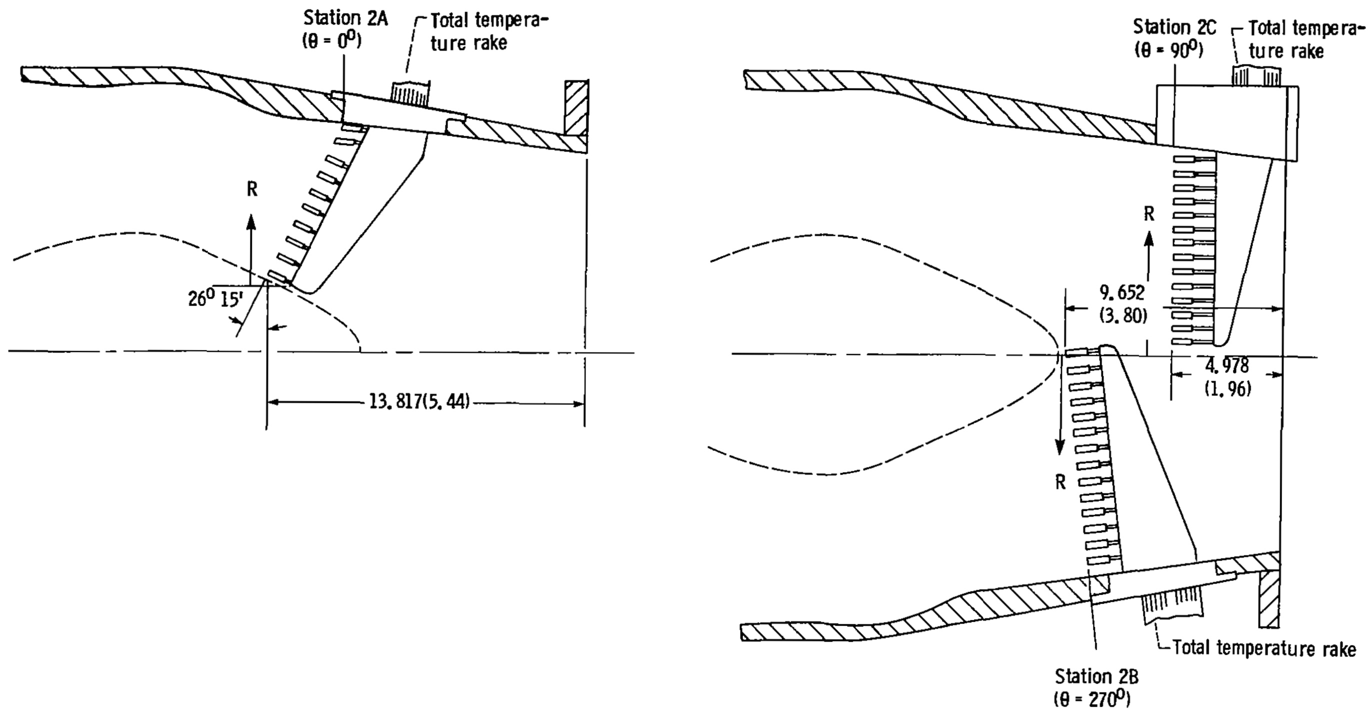


| Tube | Station | | | | | | | |
|---|---|---|---|---|---|---|---|---|
| | 2 | | | 2A | 2B | 2C | 3 | |
| | Temperature | Pressure | Pressure[a] | Temperature | | | Temperature | Pressure |
| | Radial distance, $R/R_{max}$ | | | | | | | |
| 1 | 0.444 | 0.444 | 0.400 | 0.291 | 0 | 0.043 | 0.043 | 0.043 |
| 2 | .498 | .471 | .427 | .356 | .063 | .099 | .099 | .099 |
| 3 | .552 | .498 | .454 | .420 | .125 | .156 | .156 | .156 |
| 4 | .606 | .525 | .481 | .485 | .188 | .212 | .212 | .212 |
| 5 | .660 | .552 | .508 | .549 | .250 | .268 | .268 | .268 |
| 6 | .714 | .606 | .562 | .614 | .313 | .324 | .324 | .324 |
| 7 | .769 | .660 | .616 | .679 | .375 | .381 | .381 | .381 |
| 8 | .823 | .687 | .643 | .743 | .438 | .437 | .437 | .437 |
| 9 | .877 | .714 | .670 | .808 | .500 | .493 | .493 | .493 |
| 10 | .931 | .741 | .697 | .873 | .563 | .549 | .549 | .549 |
| 11 | ----- | .769 | .724 | ----- | .626 | .606 | .606 | .606 |
| 12 | ----- | .823 | .778 | ----- | .688 | .662 | .662 | .662 |
| 13 | ----- | .877 | .832 | ----- | .751 | .719 | .719 | .719 |
| 14 | ----- | .931 | .886 | ----- | .813 | .775 | .775 | .775 |

(b)

[a]2E and 3E mixers without cutback.

(b) Stations 2A, 2B, and 2C and rake dimensions.

Figure 11. – Concluded.

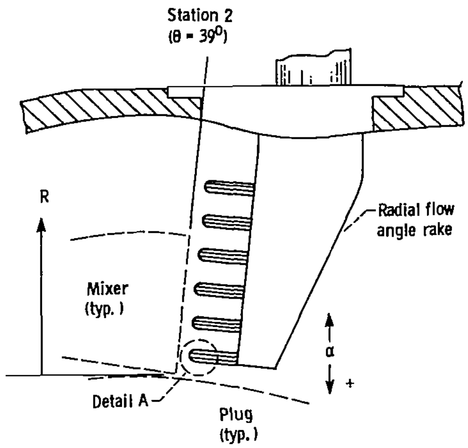


| Tube | $R/R_{max}$ |
| --- | --- |
| 1 | 0.447 |
| 2 | .525 |
| 3 | .603 |
| 4 | .681 |
| 5 | .759 |
| 6 | .842 |

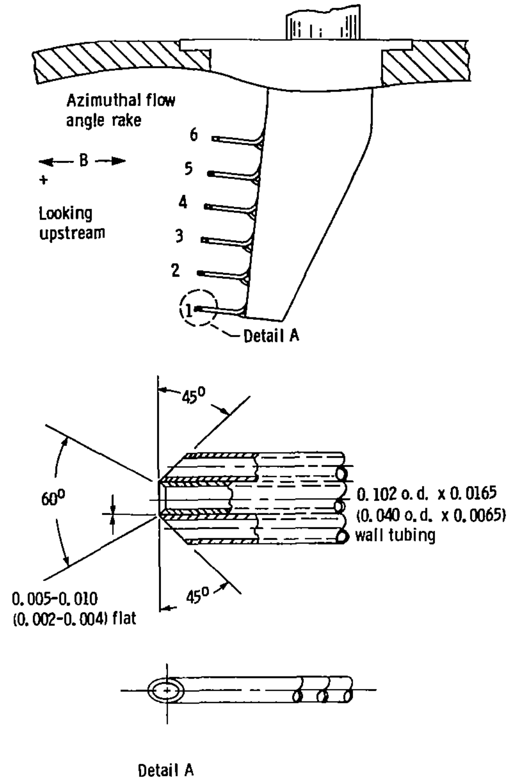


(a)

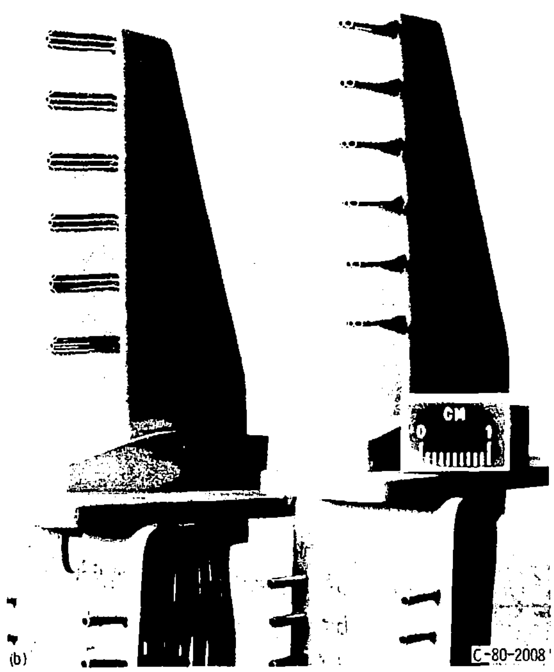


(b)

(a) Rake dimensions and detail.
(b) Flow angularity rakes.

Figure 12. – Flow angularity rake dimensions and details.

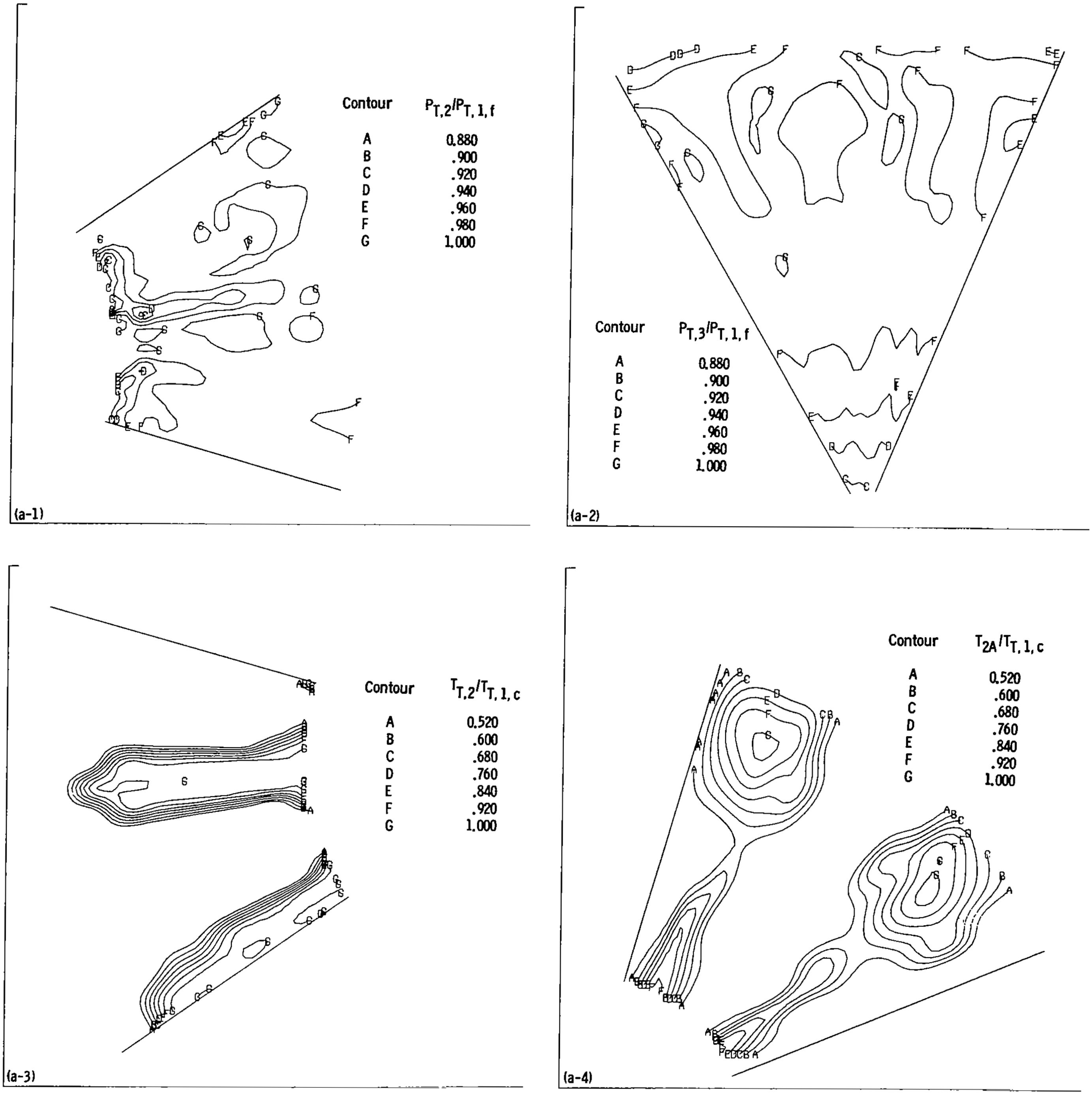


(a) 12B/3B mixer configuration.

Figure 13. – Contour plots of total pressure and temperature ratios at various nozzle stations in mixing region for nozzle pressure ratio of 2.4 and temperature ratio of 2.5 (cruise condition).

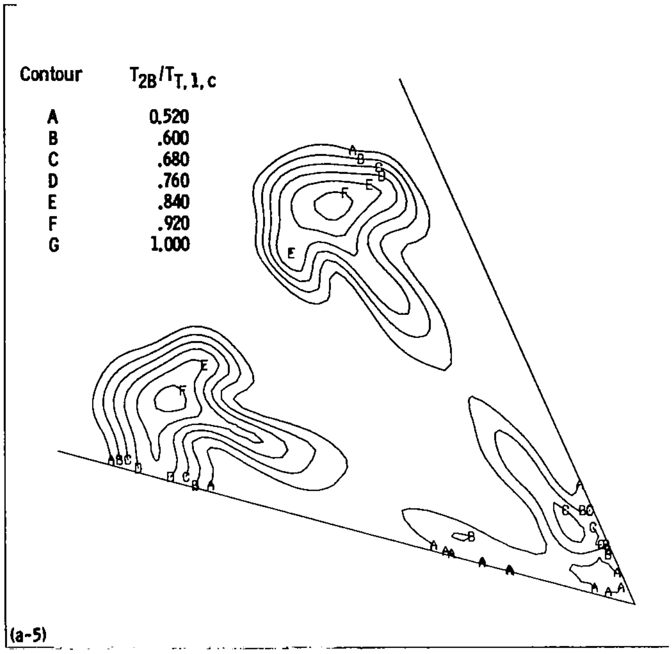


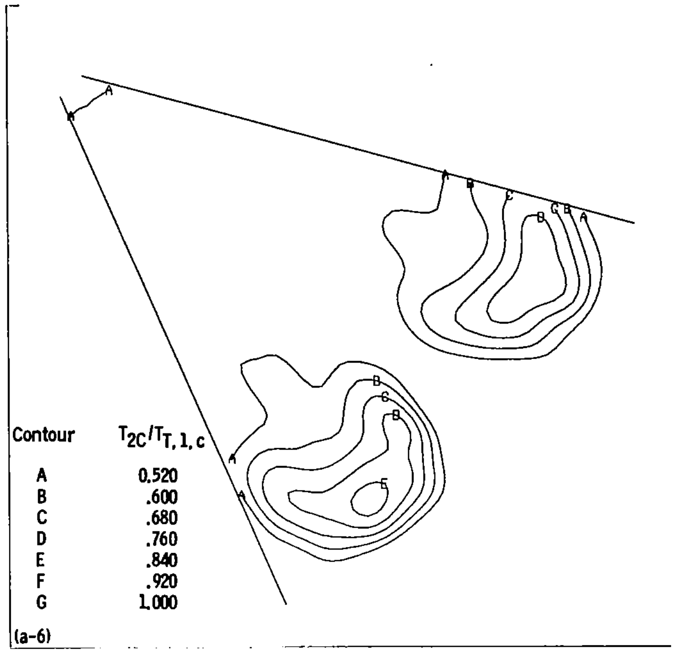


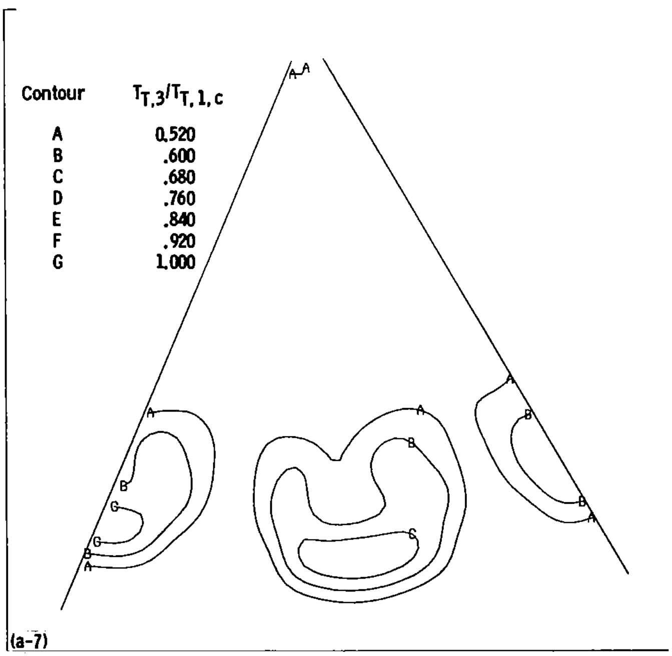


(a) Concluded.

Figure 13. – Continued.

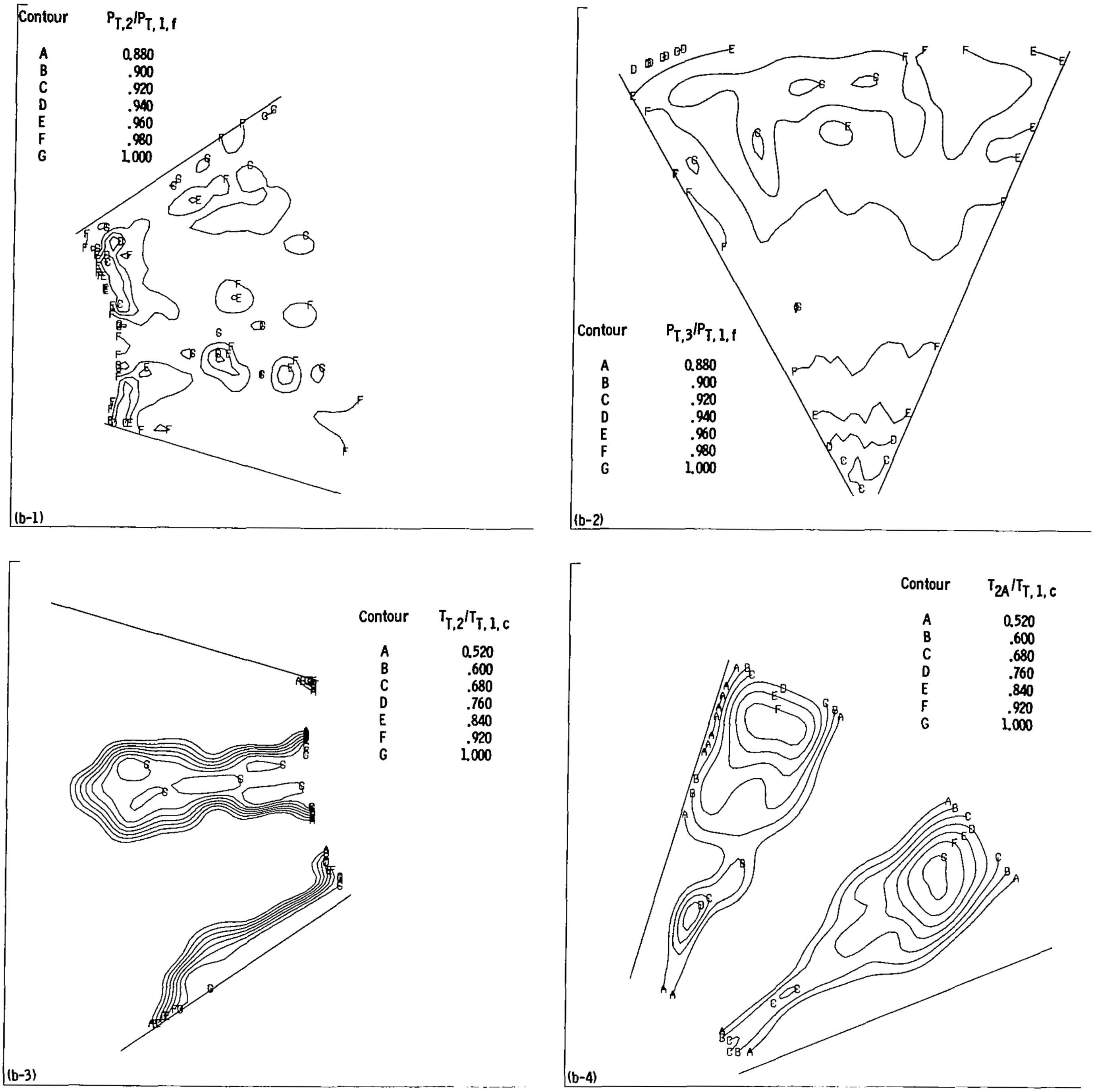


(b) 12B/3B-S mixer configuration.

Figure 13. – Continued.

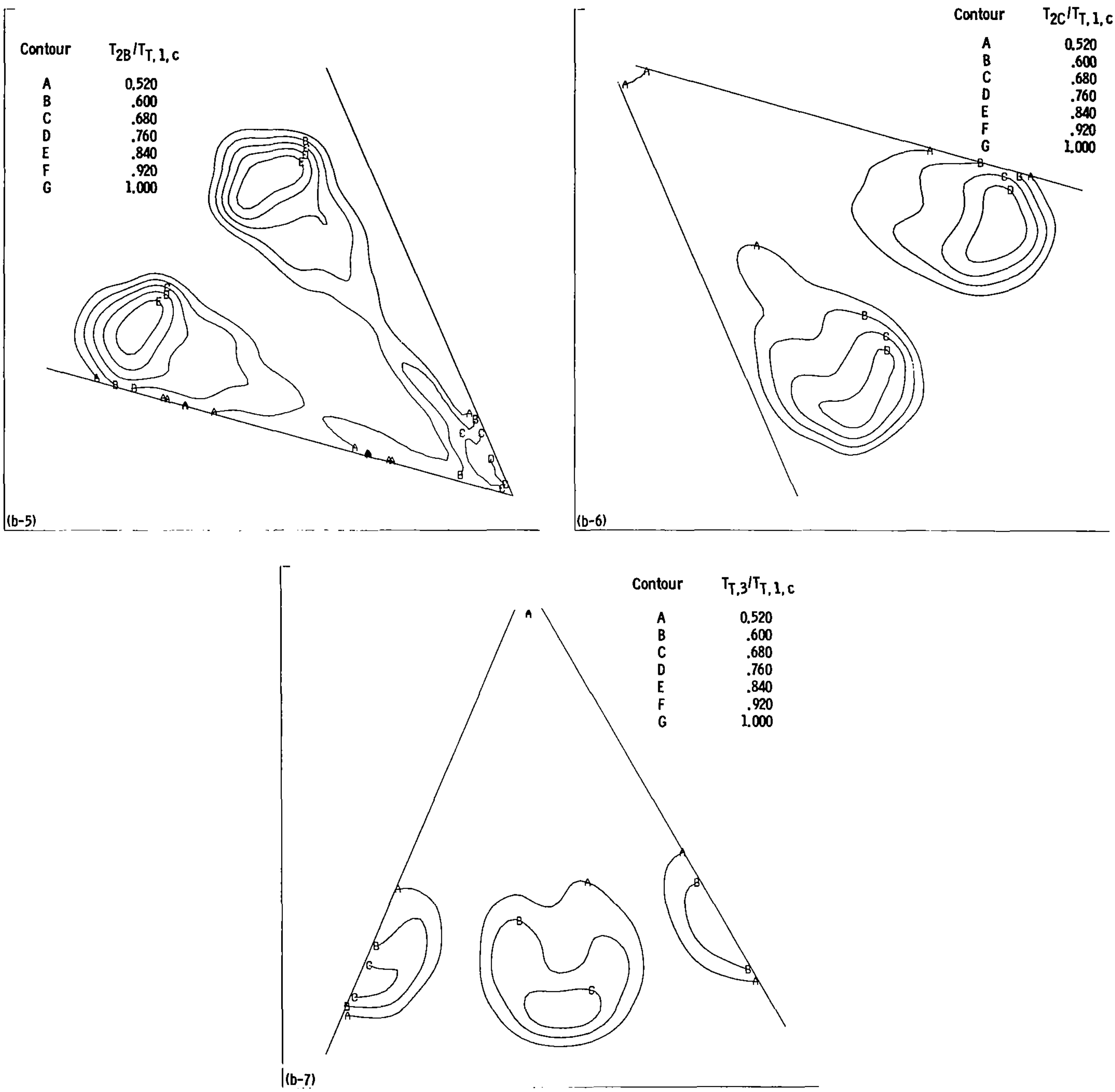


(b) Concluded.

Figure 13. – Continued.

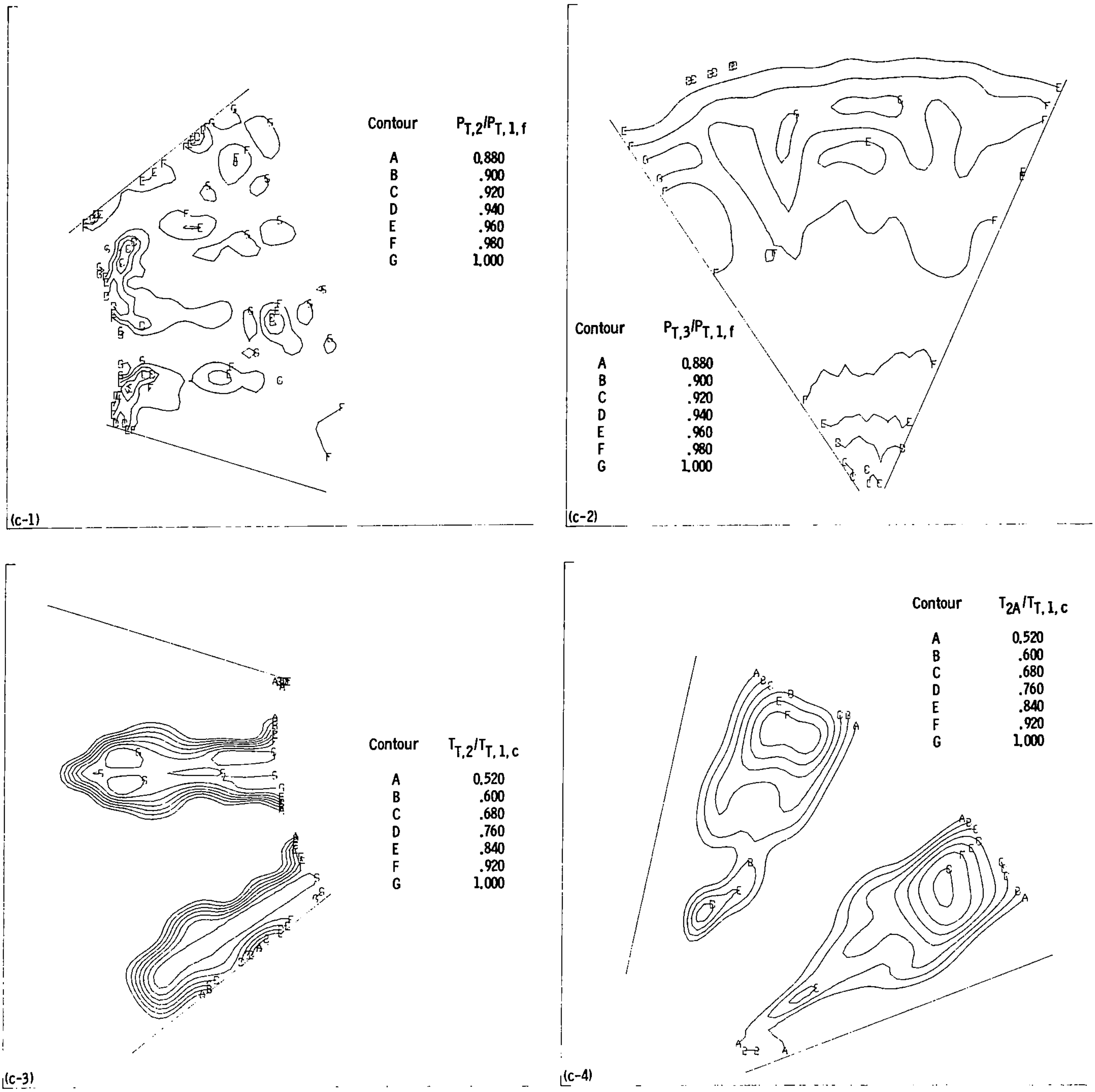


(c) 12B/REF-S mixer configuration.

Figure 13. – Continued.

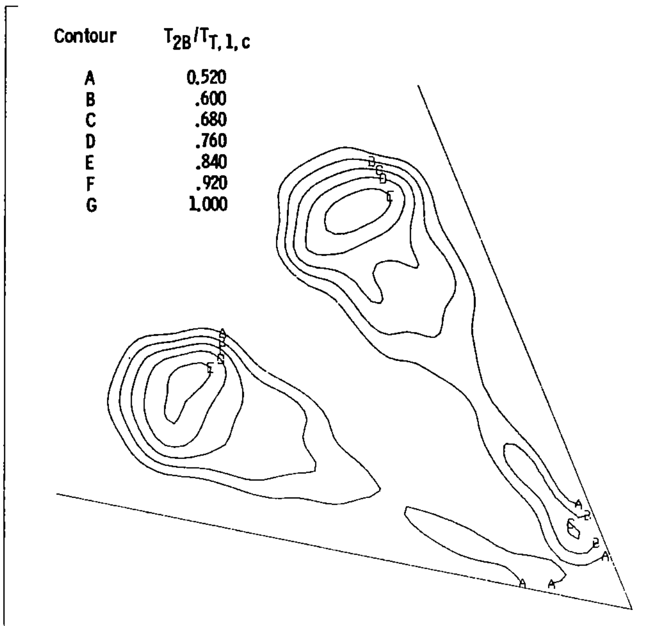


(c-5)

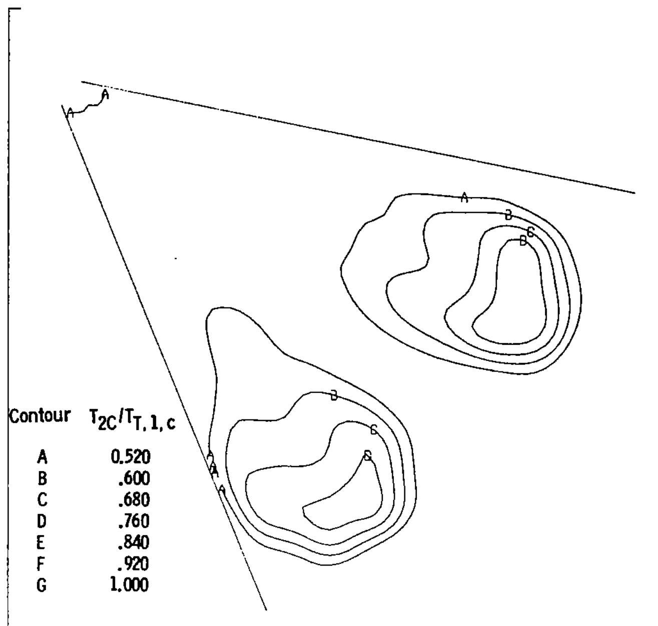


(c-6)

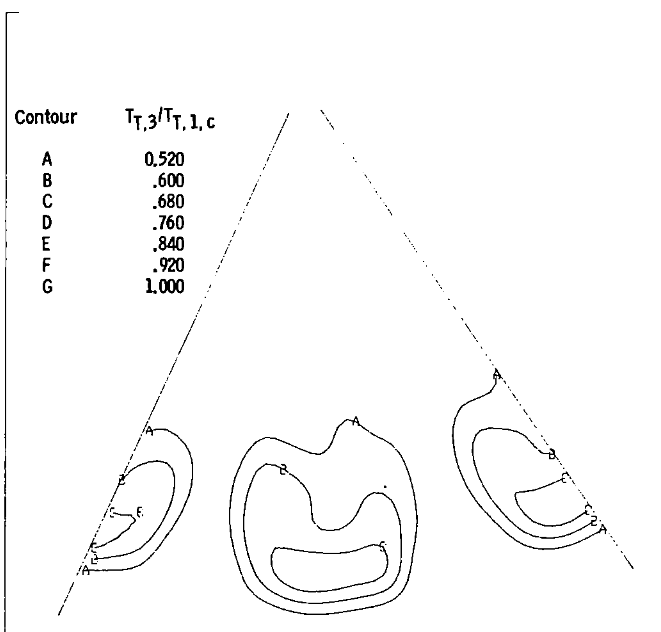


(c-7)

(c) Concluded.

Figure 13. – Continued.

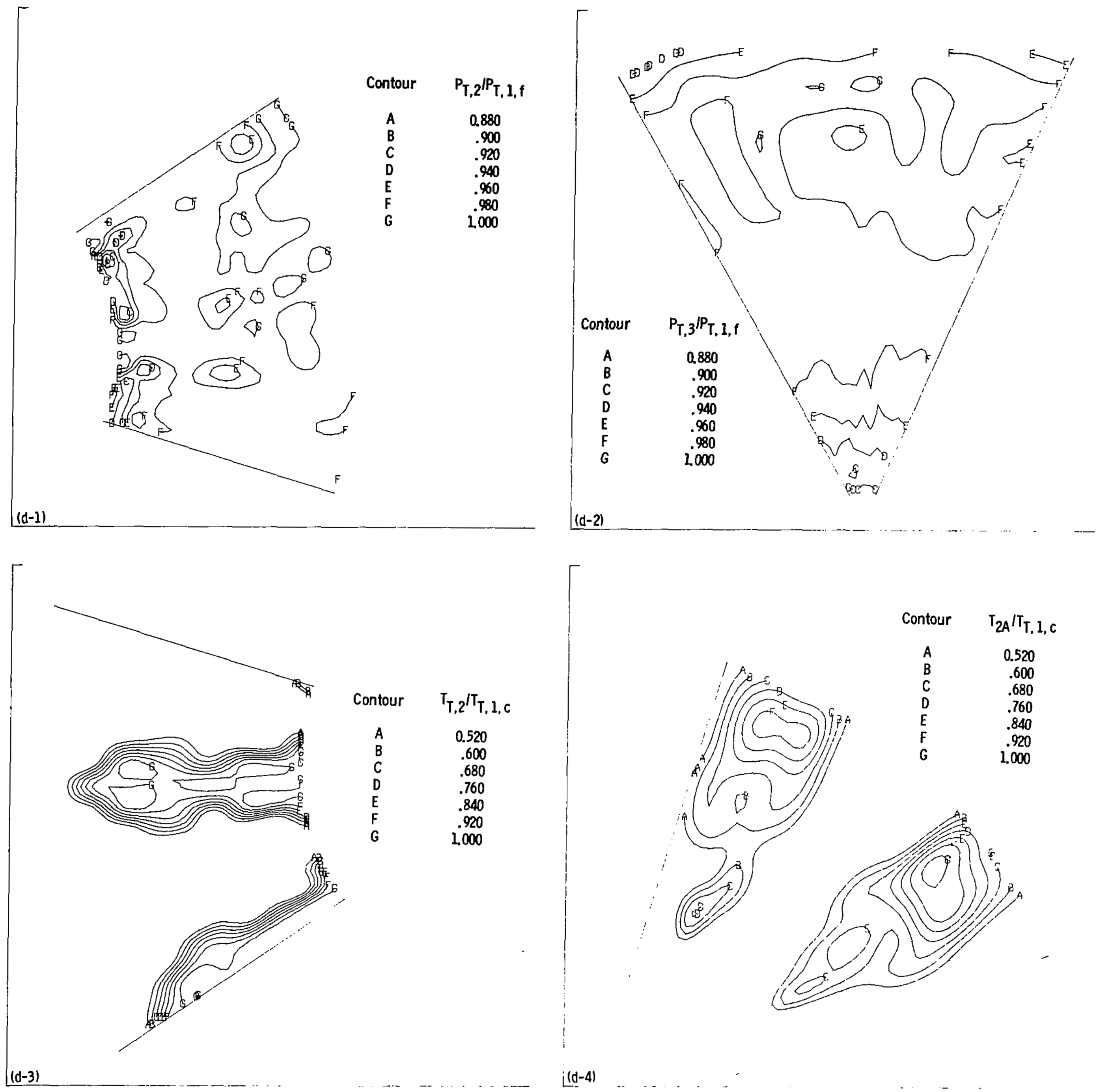


(d) 12B/2AC-S mixer configuration.

Figure 13. – Continued.

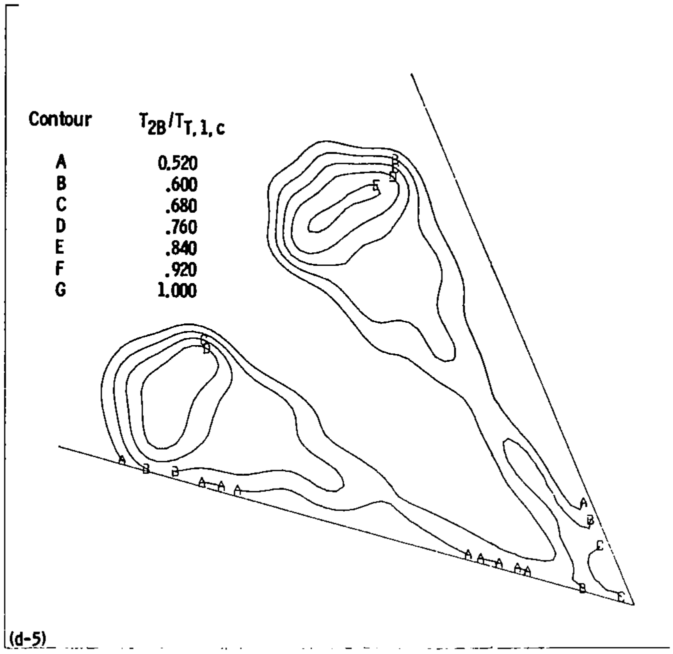


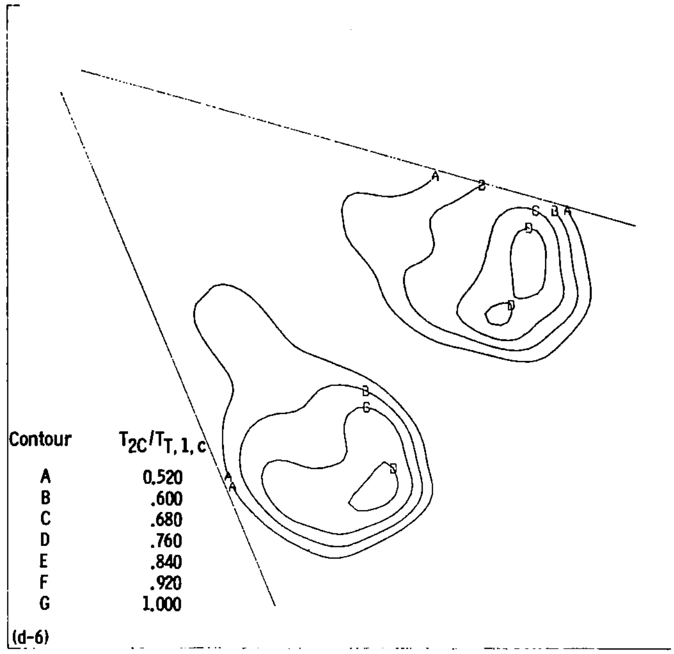


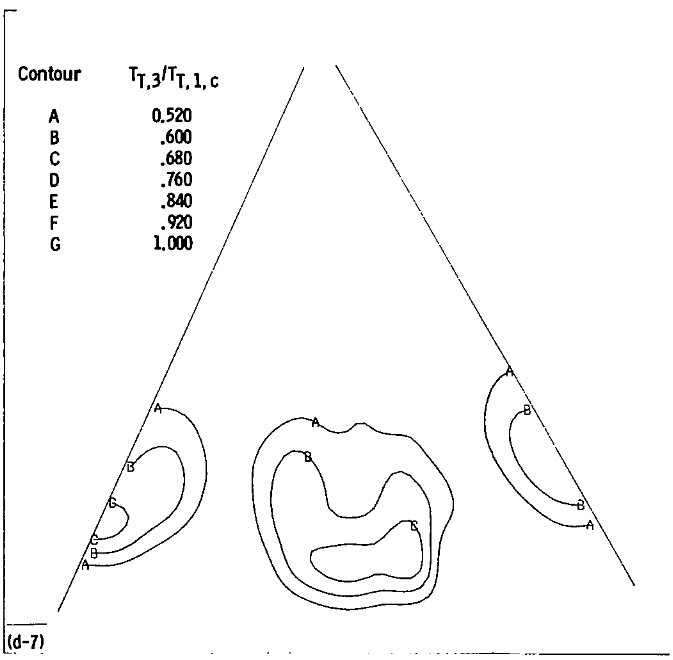


(d) Concluded.

Figure 13. – Continued.

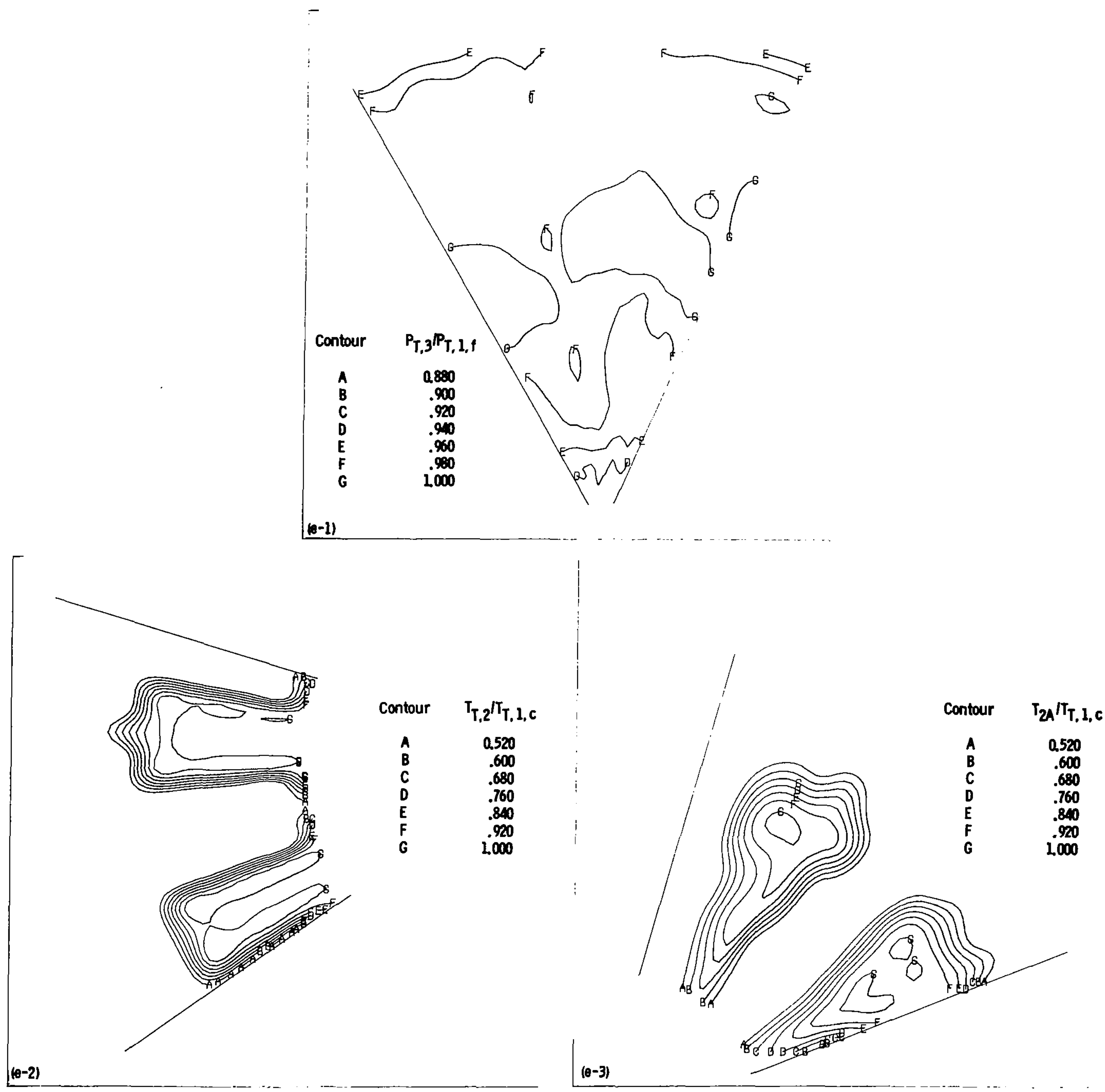


(e) 12A/REF mixer configuration.

Figure 13. – Continued.

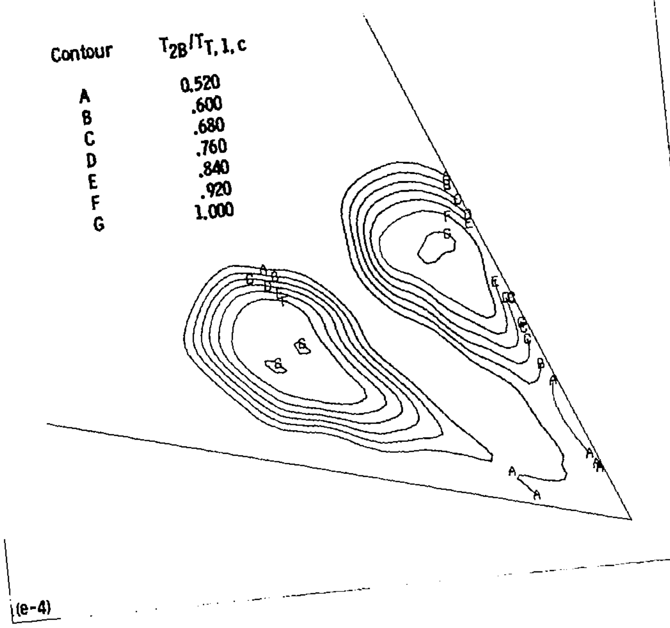


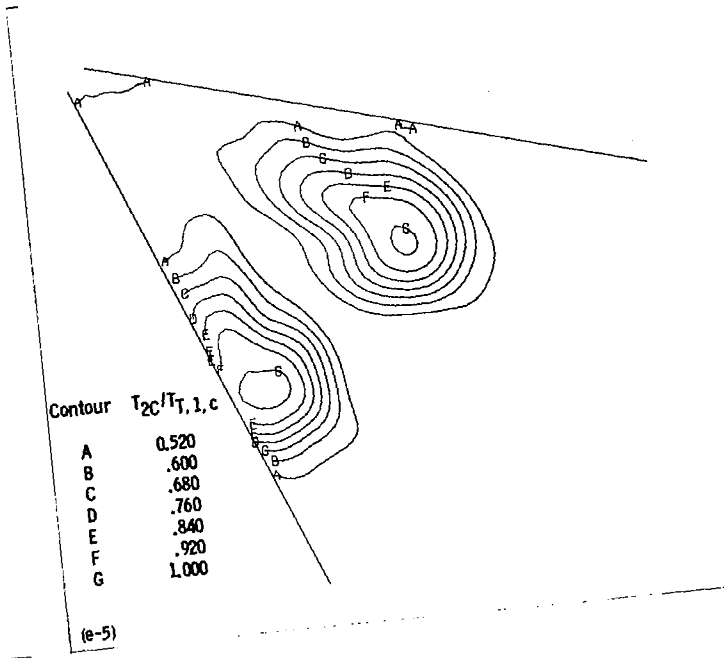


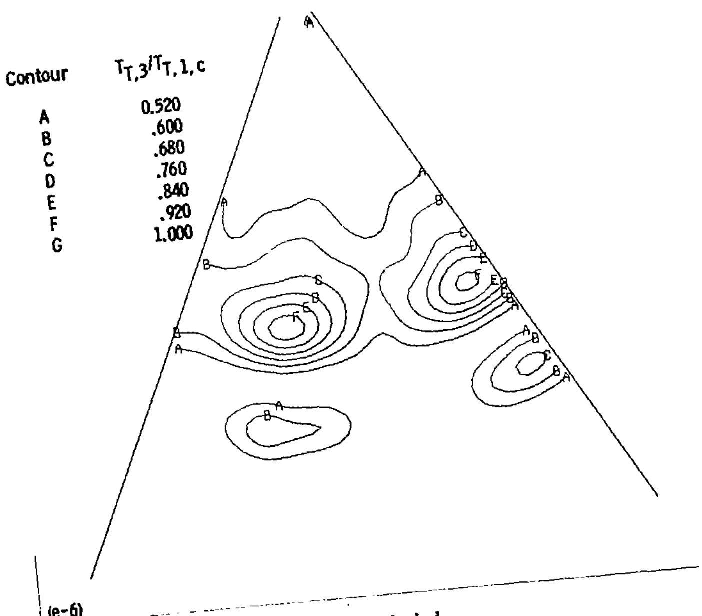


(e) Concluded.

Figure 13. – Continued.

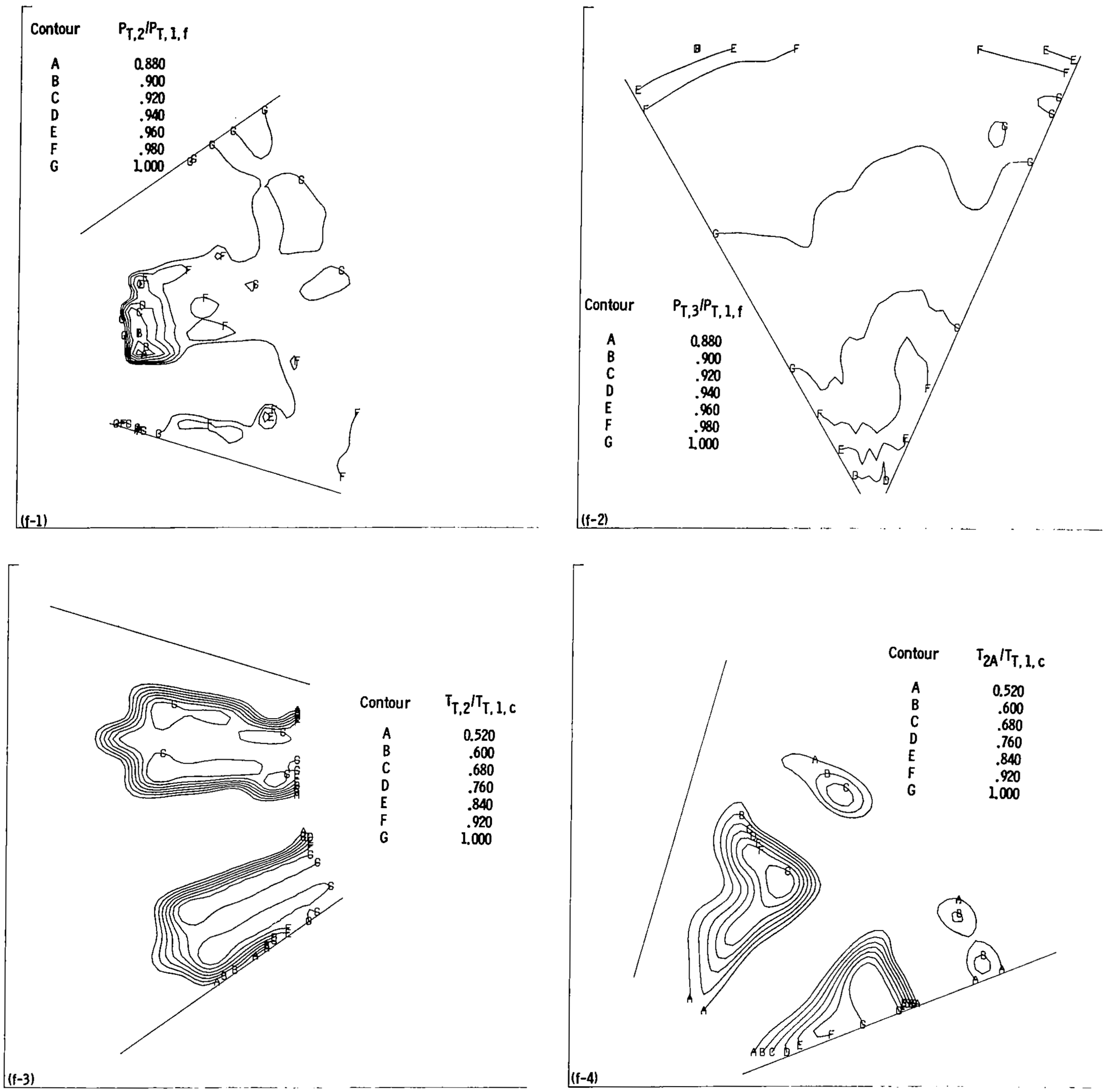


(f) 12A/2AC mixer configuration.

Figure 13. – Continued.

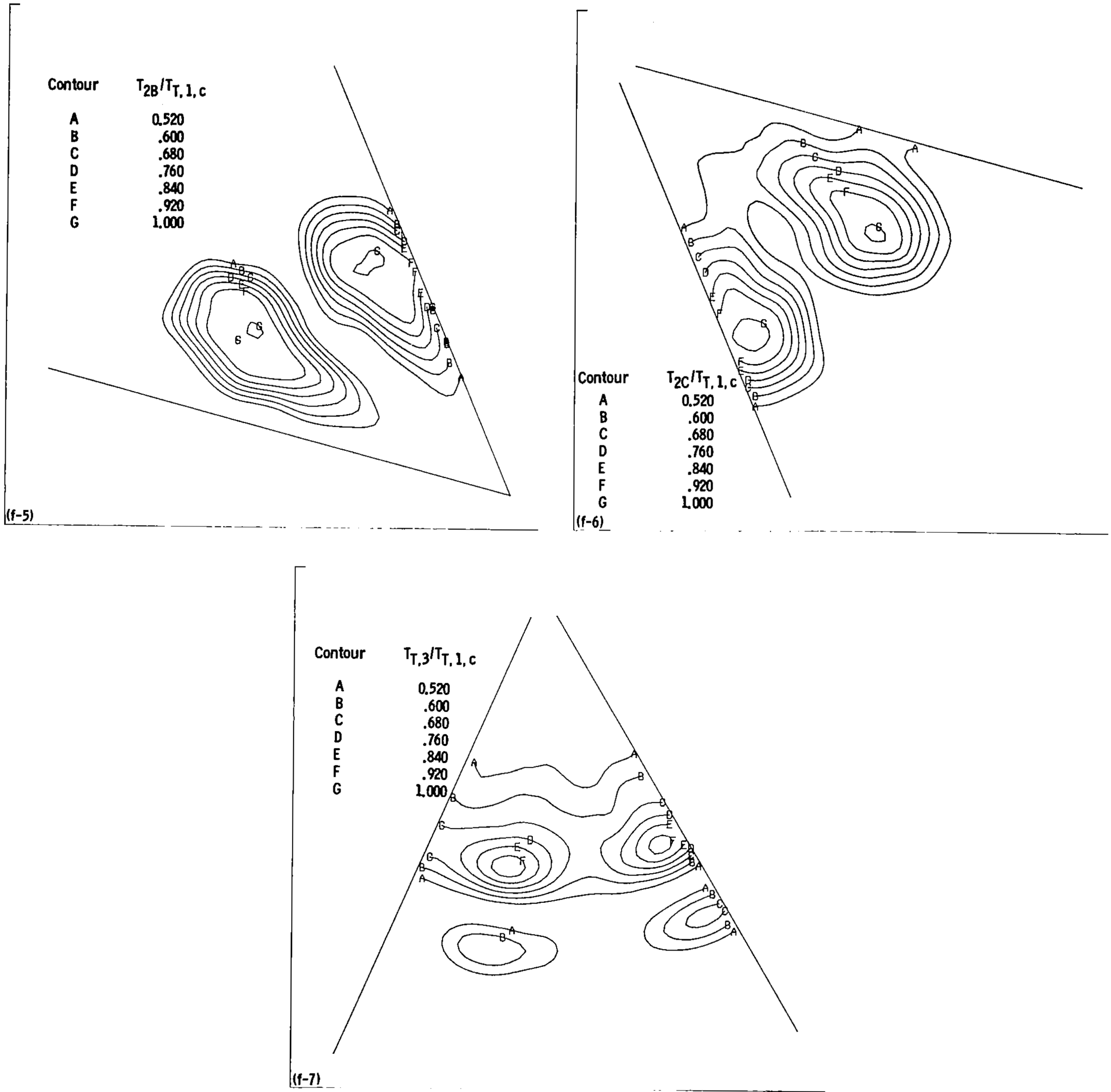


(f) Concluded.

Figure 13. – Continued.

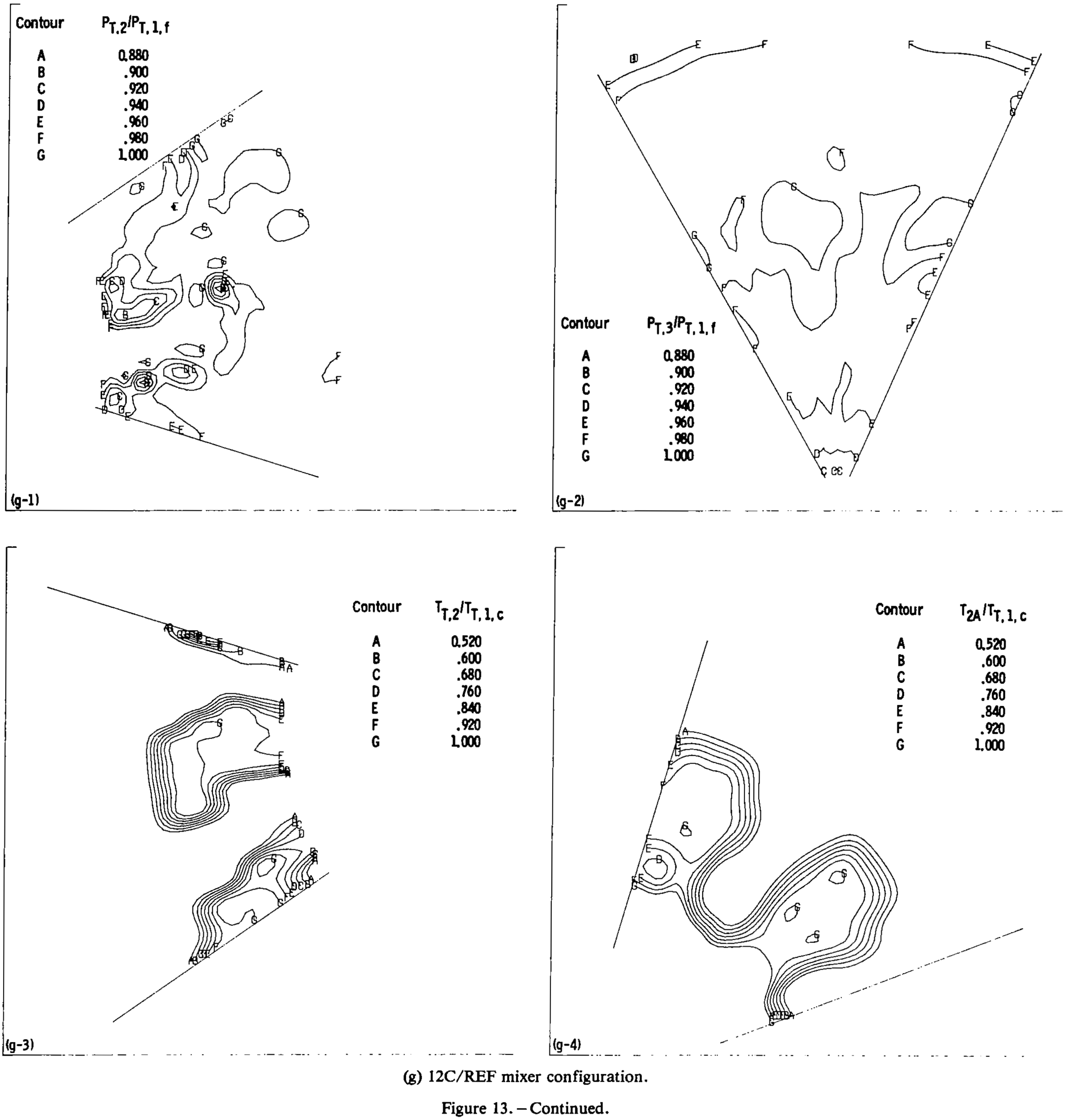


(g) 12C/REF mixer configuration.

Figure 13. – Continued.

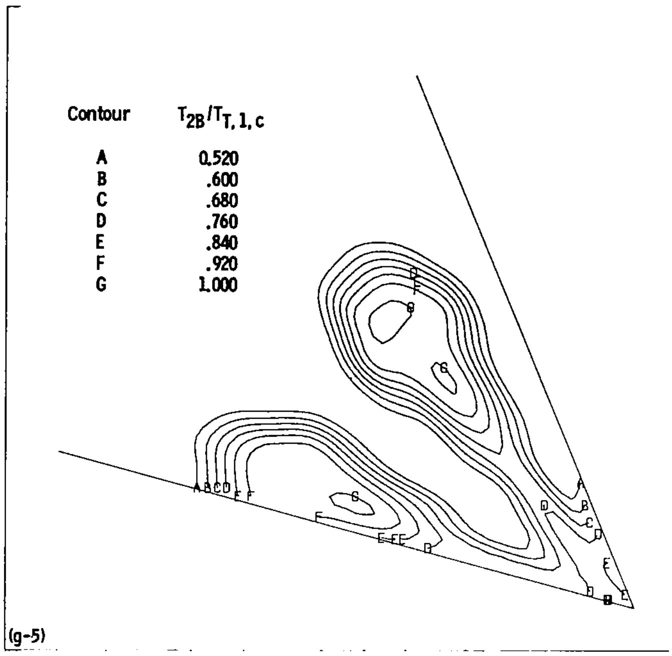


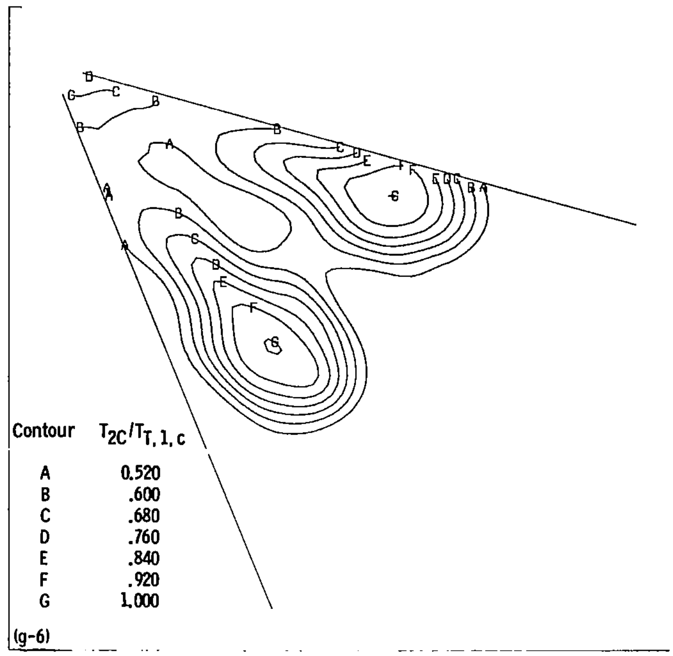


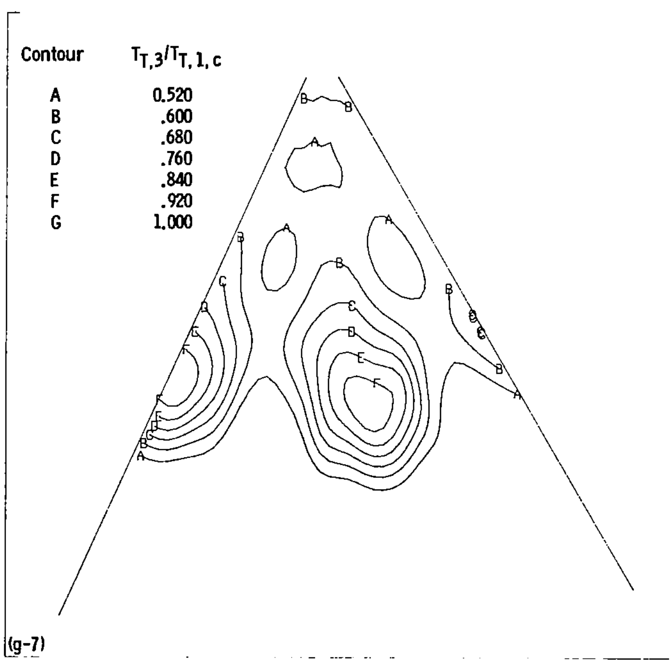


(g) Concluded.

Figure 13. – Continued.

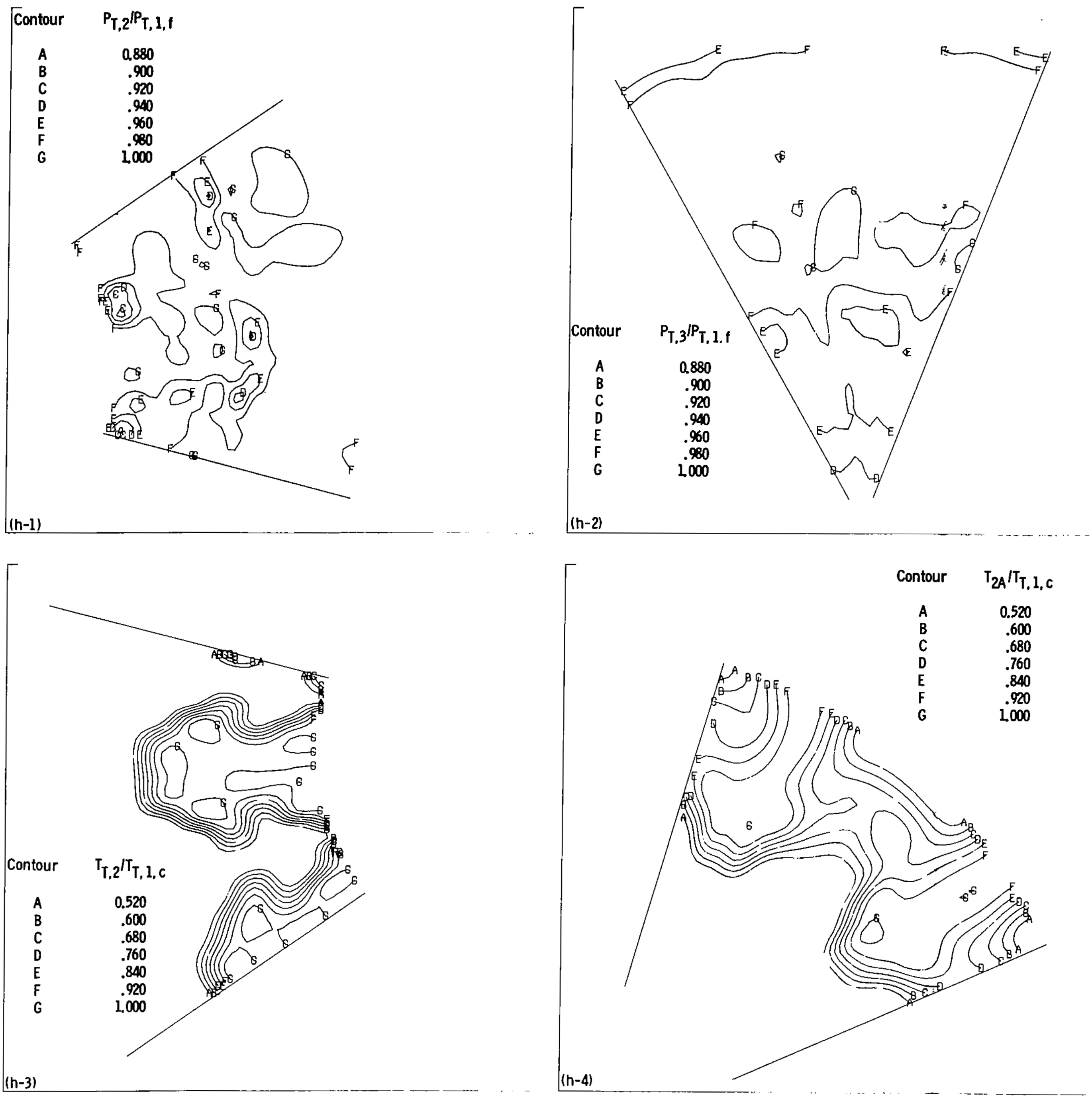


(h) 12C/REF-S mixer configuration.

Figure 13. – Continued.

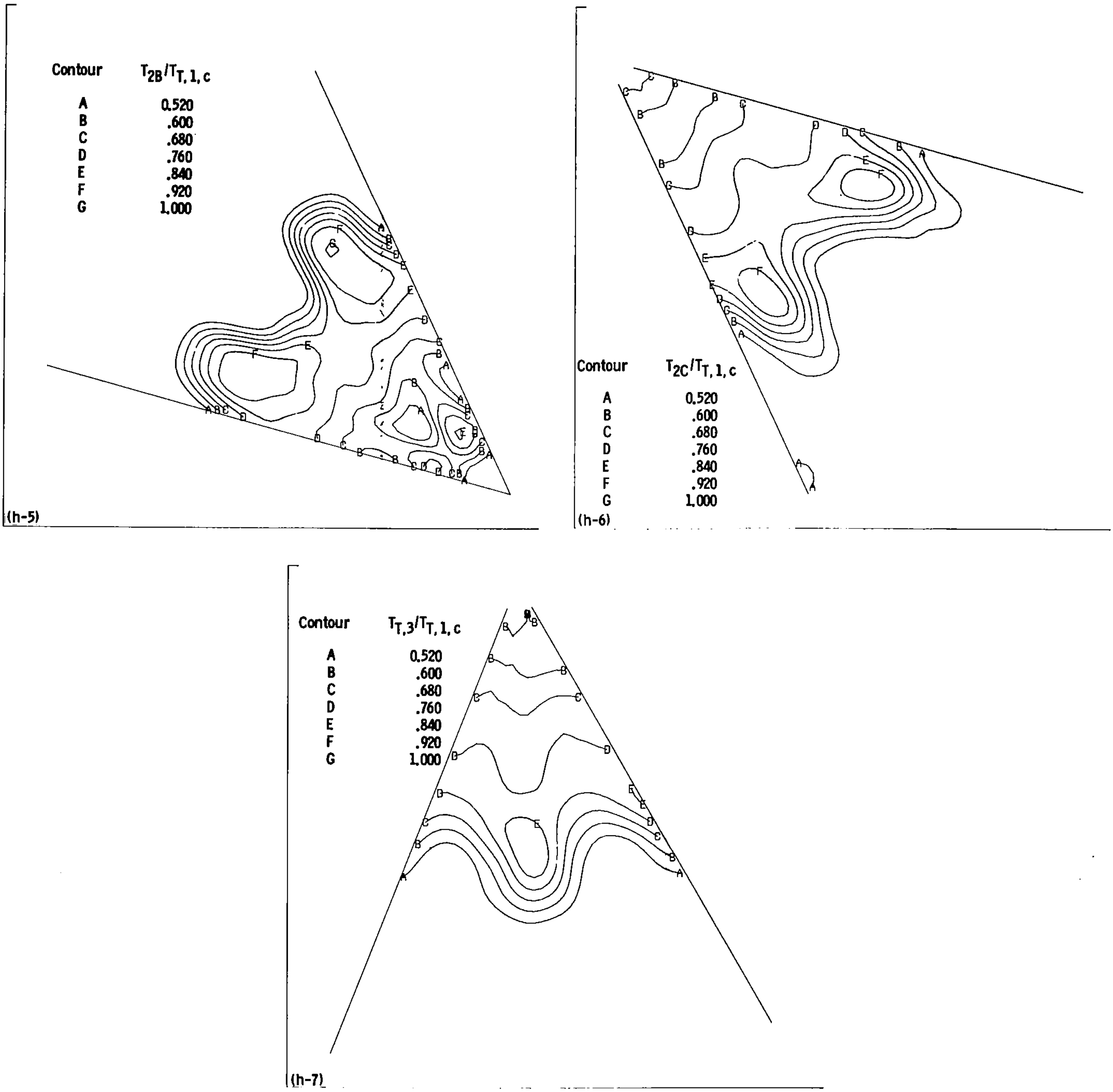


(h) Concluded.

Figure 13. – Continued.

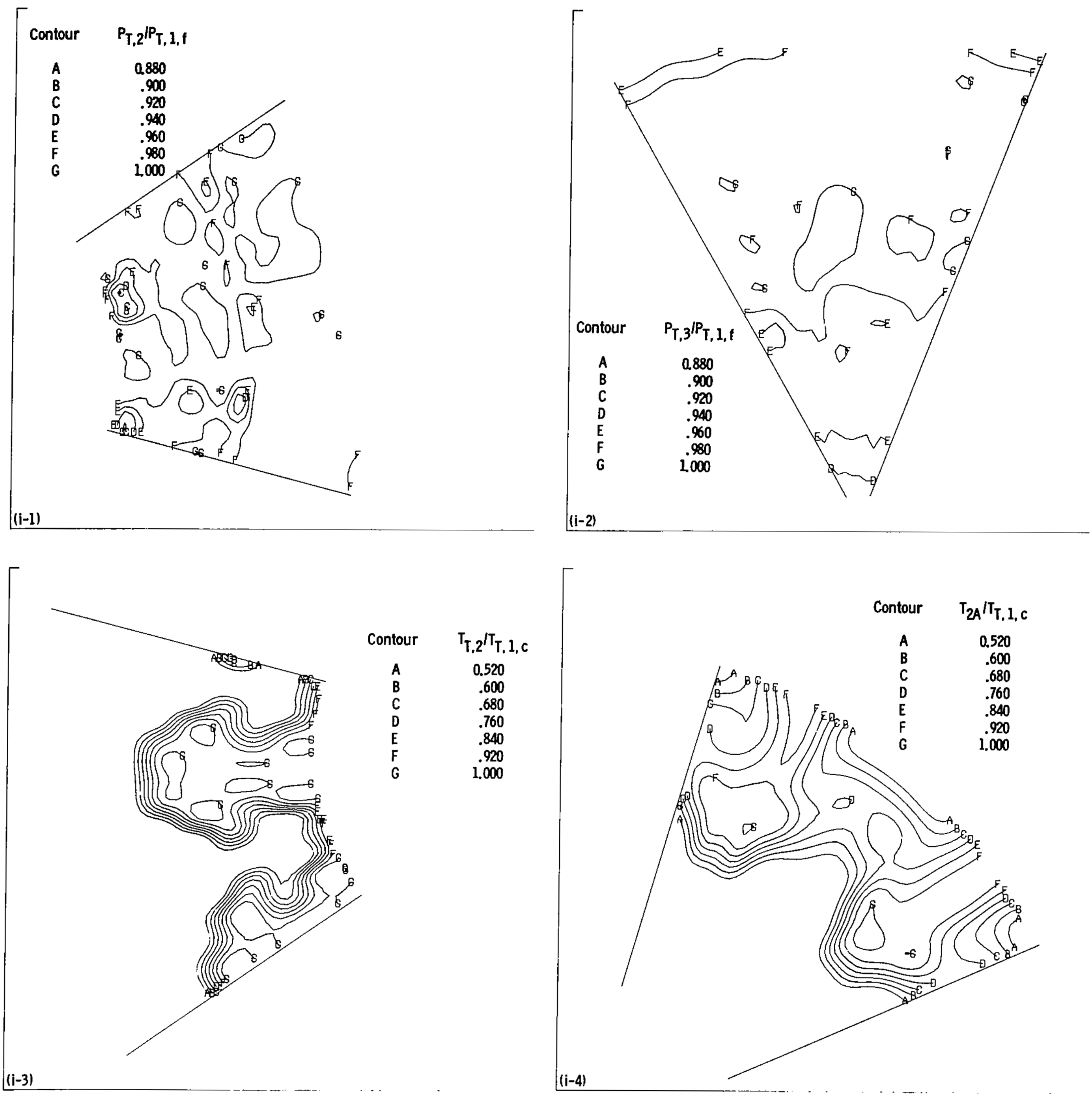


(i) 12C/2AC–S mixer configuration.

Figure 13. – Continued.

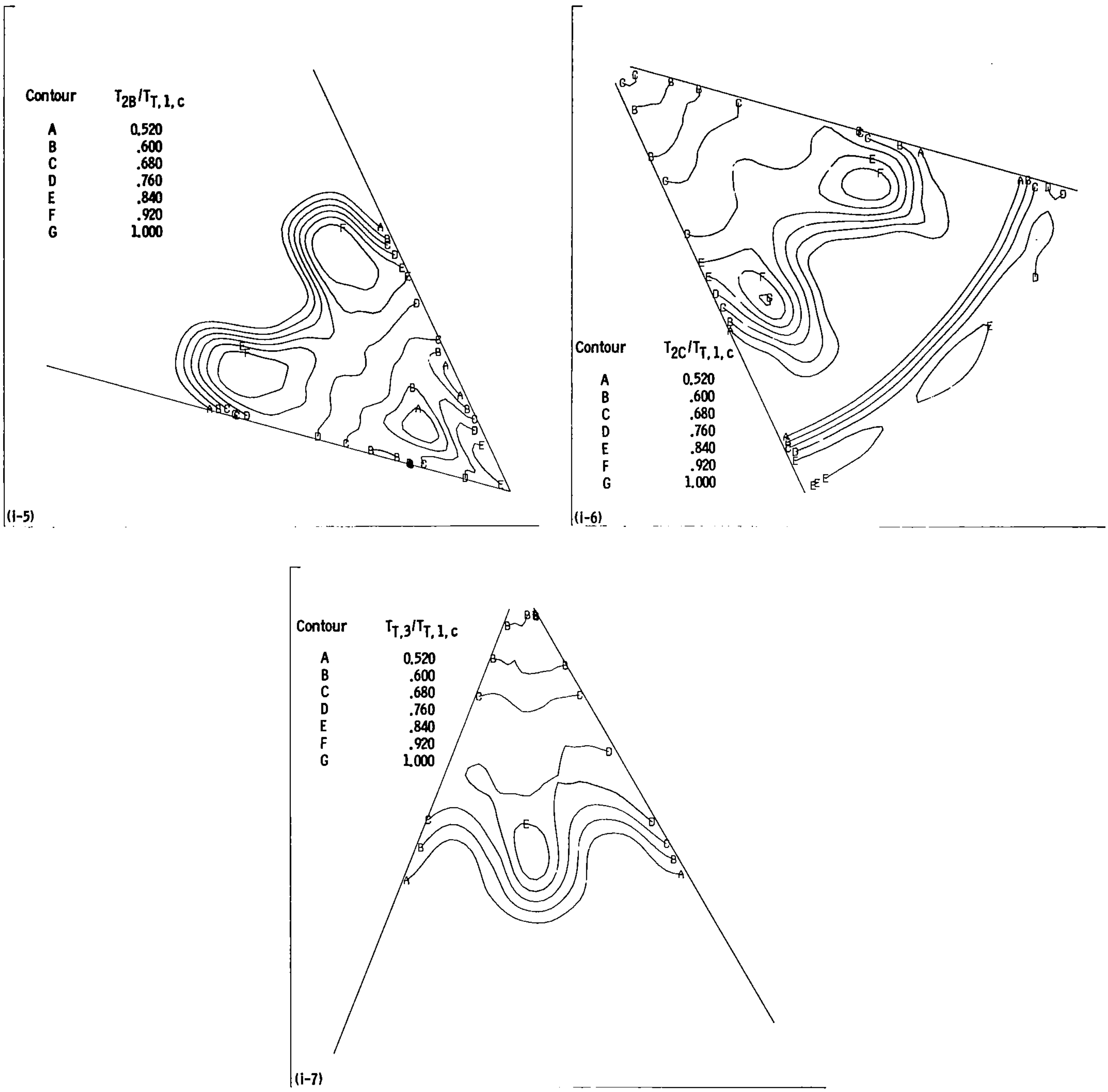


(i) Concluded.

Figure 13. – Continued.

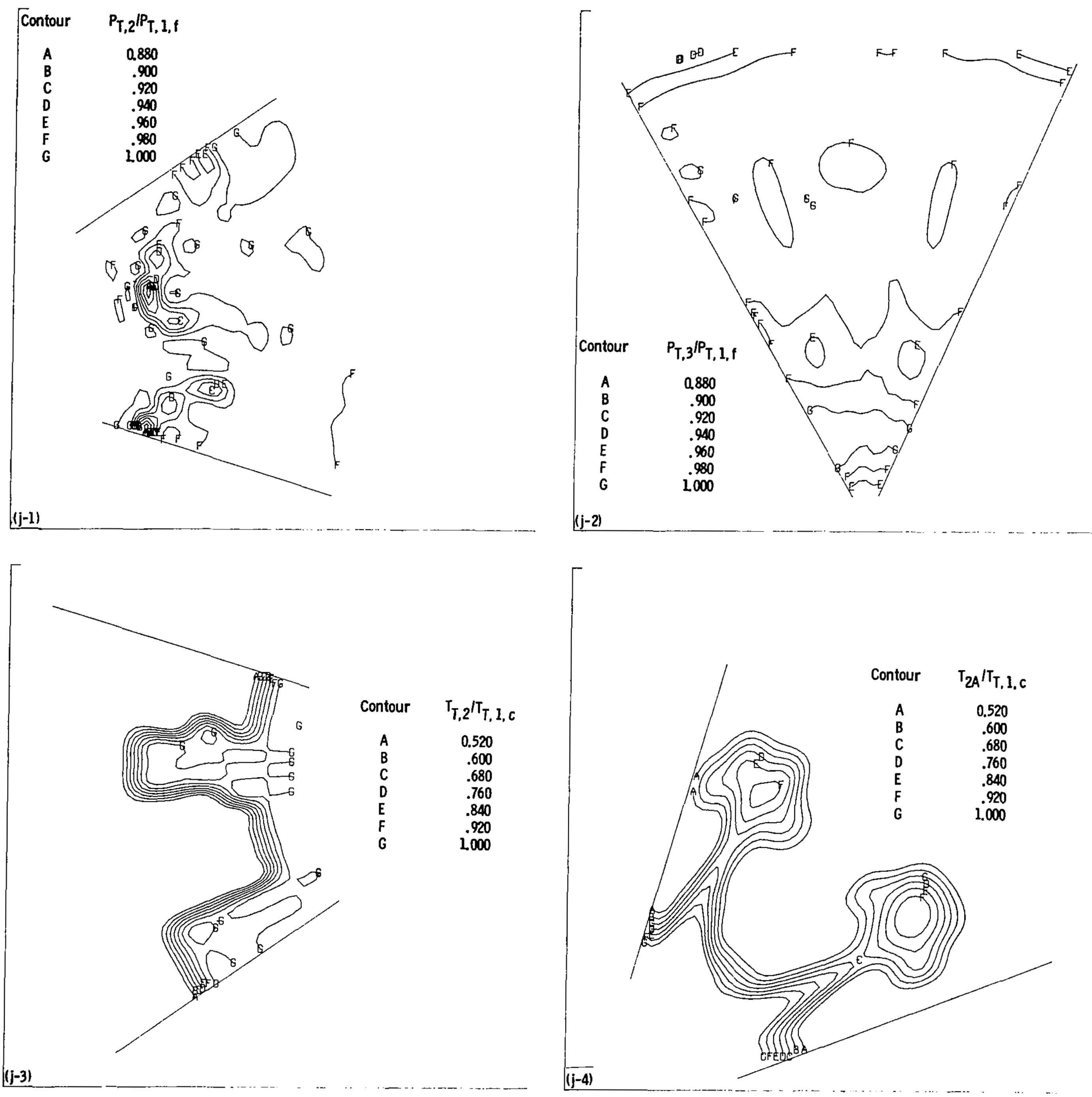


(j) 1E/2AC mixer configuration.

Figure 13. – Continued.

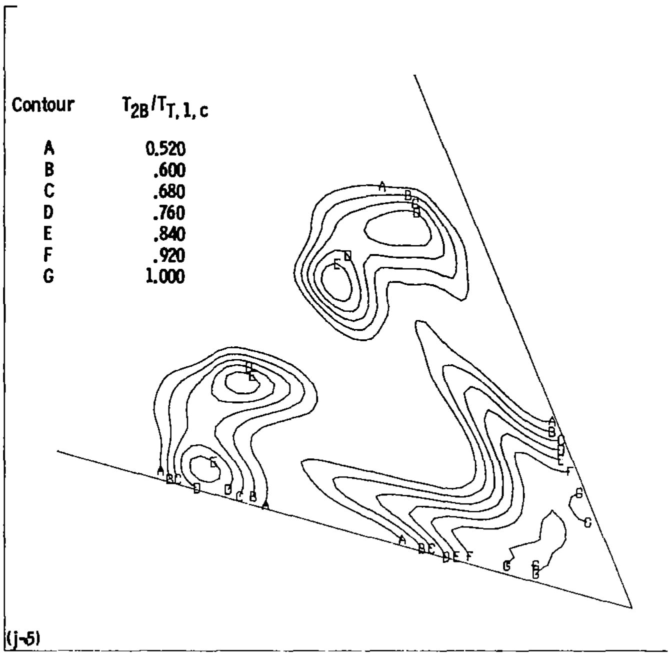


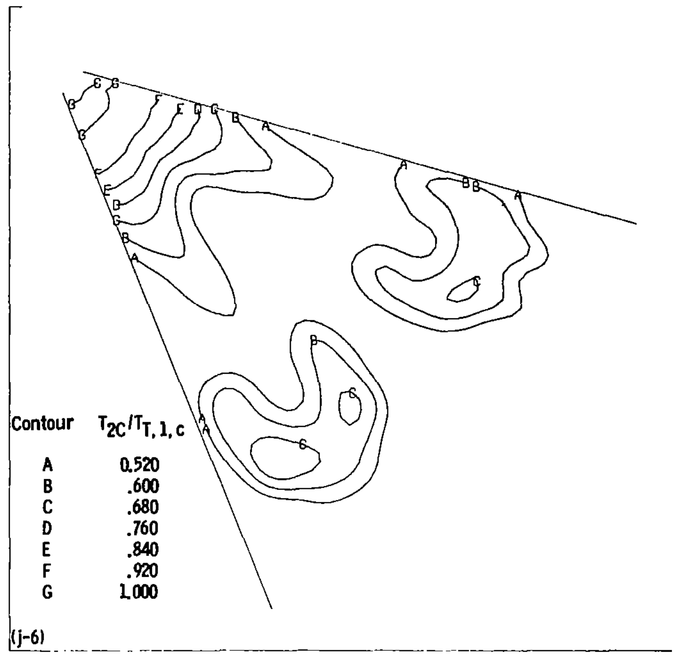


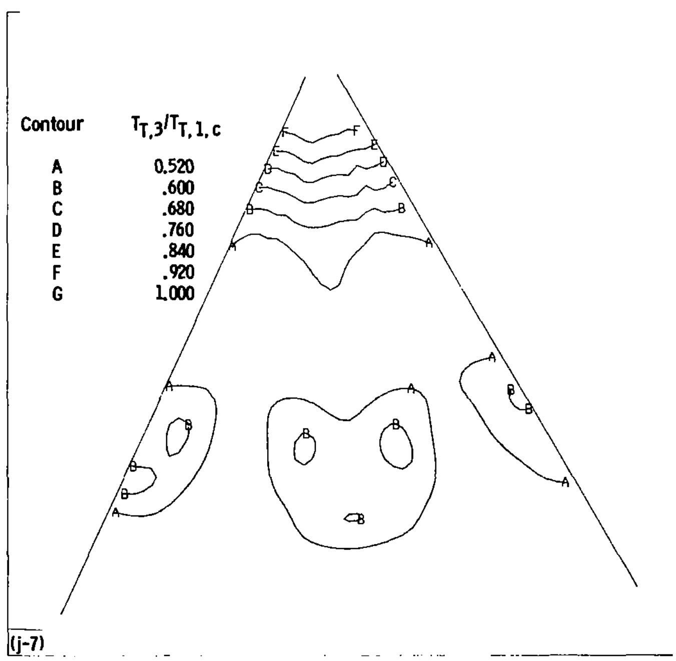


(j) Concluded.

Figure 13. – Continued.

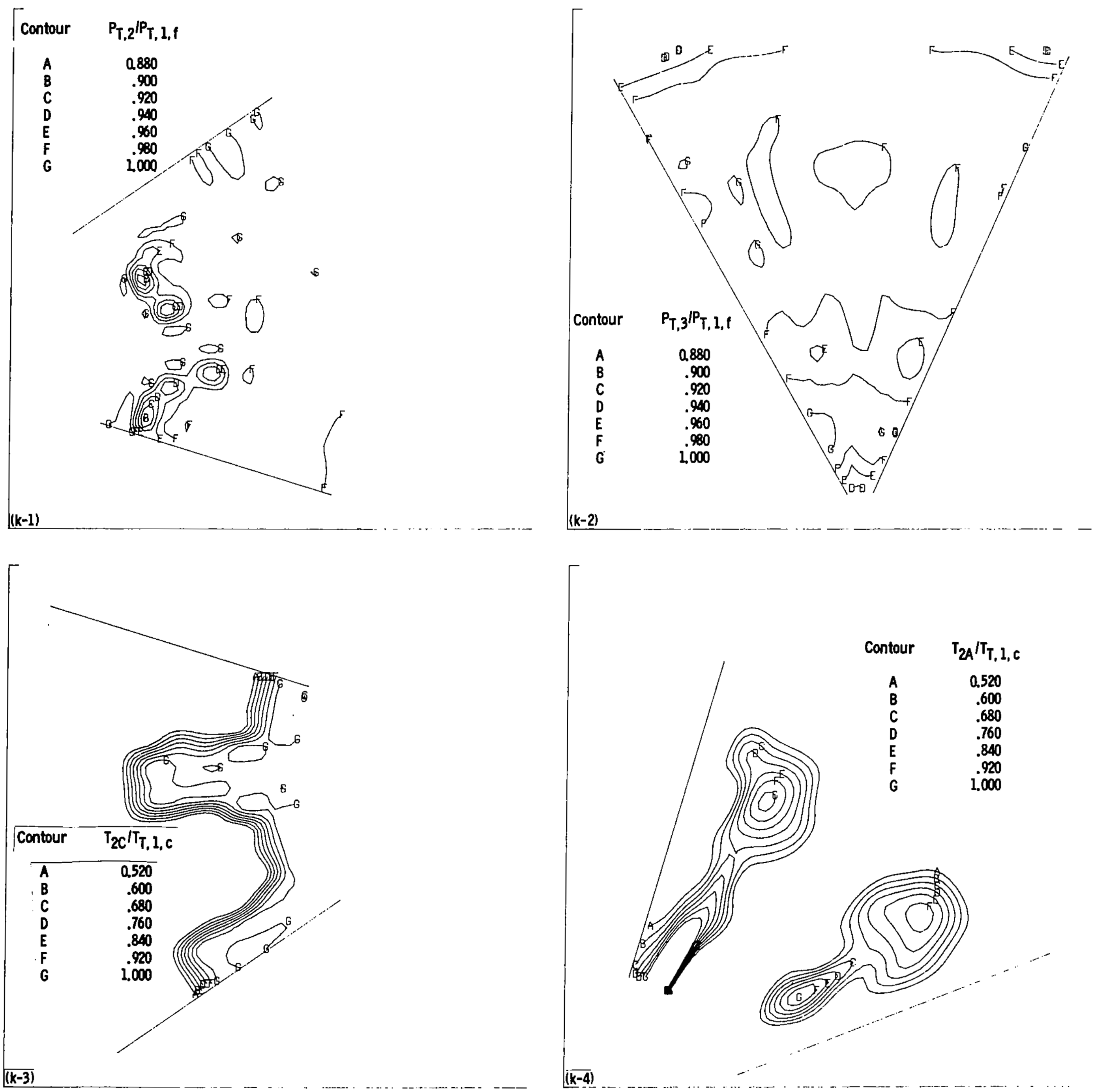


(k) 1E/2AC–S mixer configuration.

Figure 13. – Continued.

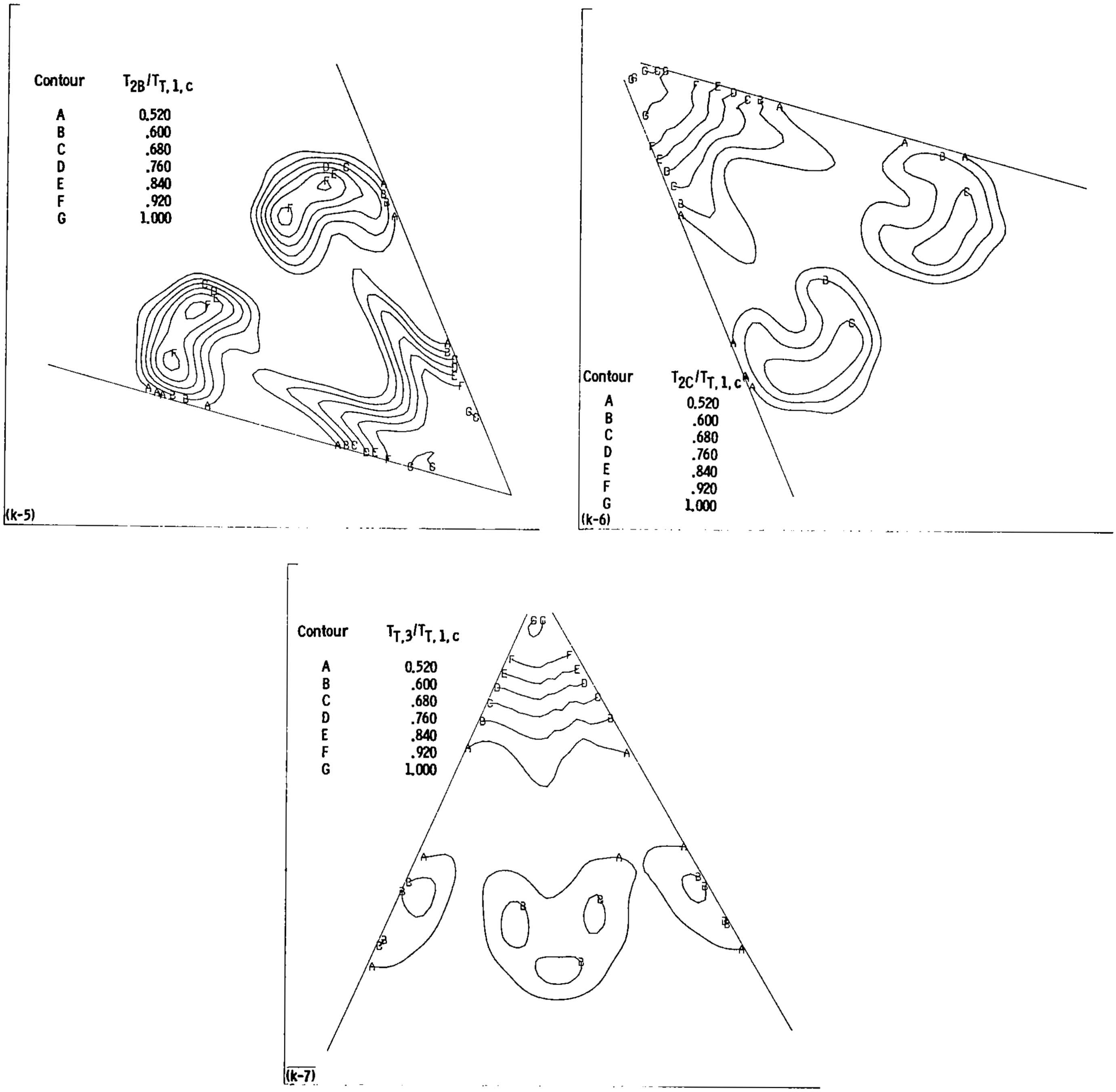


(k) Concluded.

Figure 13. – Continued.

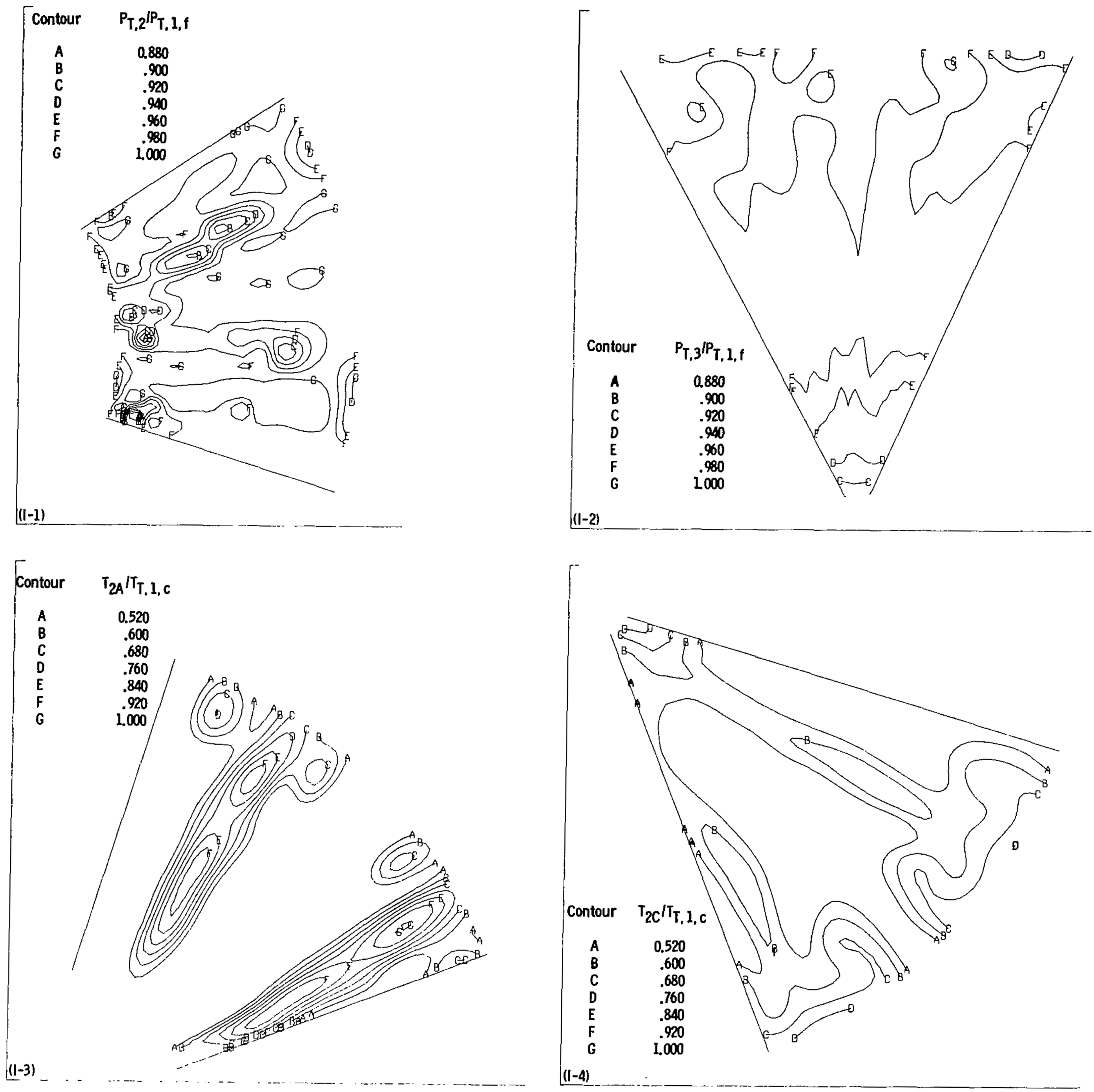


(l) 2E/REF mixer configuration.

Figure 13. – Continued.

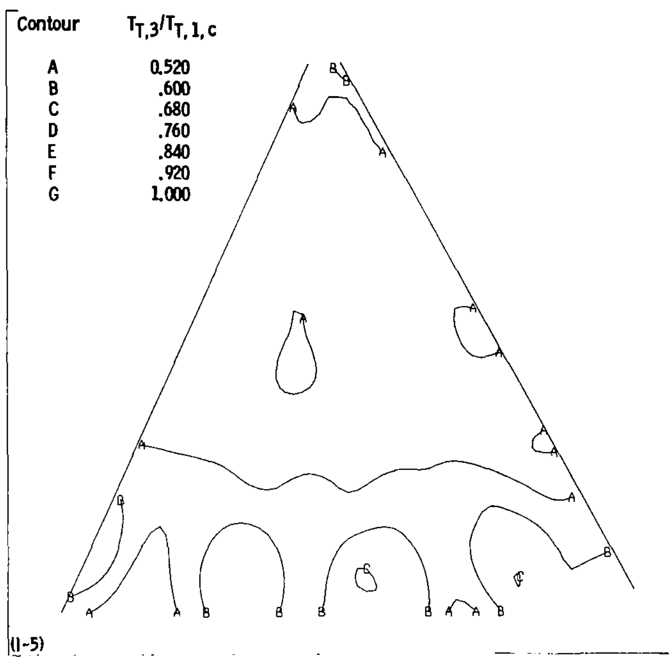


(l) Concluded.

Figure 13. – Continued.

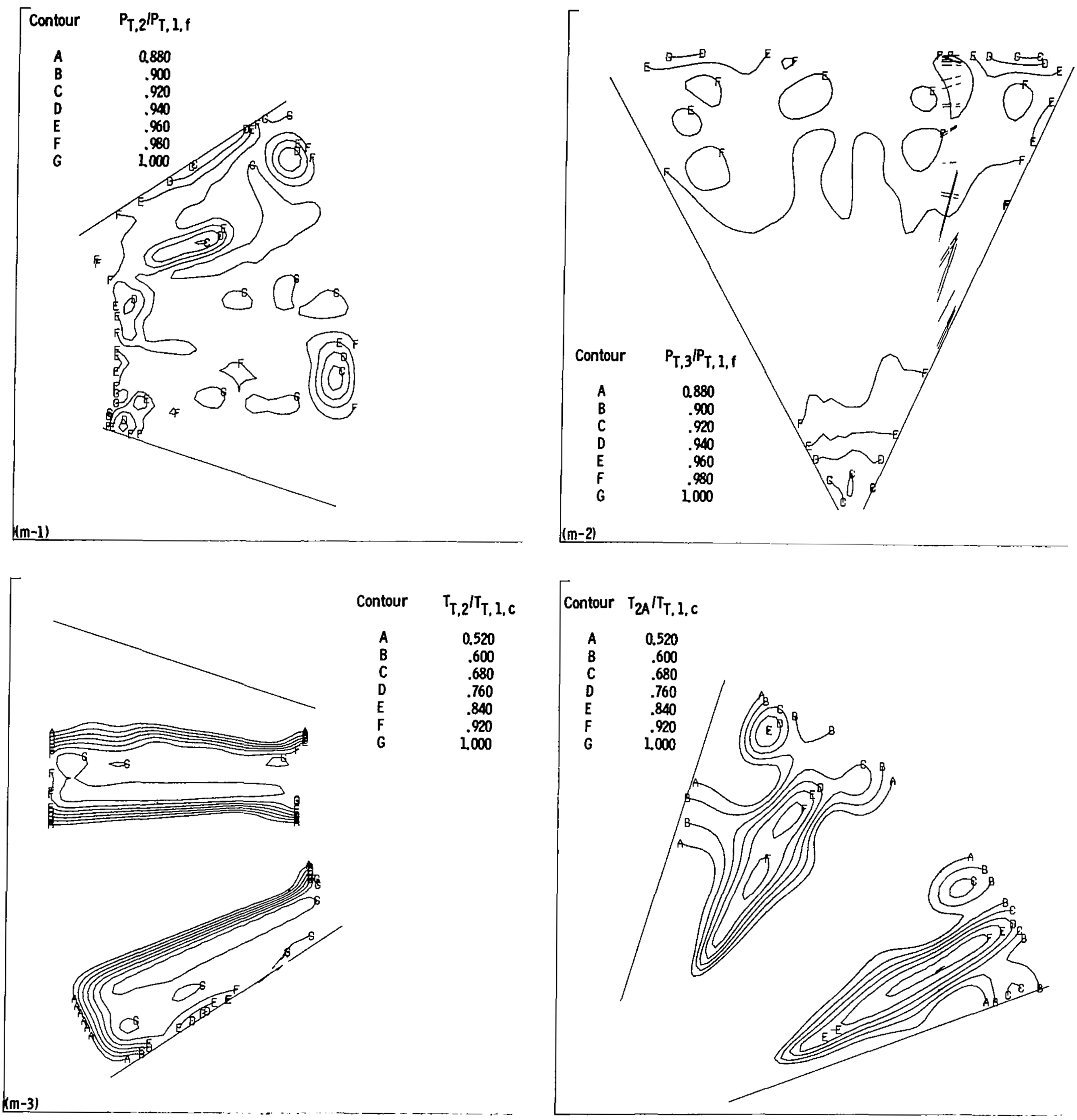


(m) 2E/REF–CB mixer configuration.

Figure 13. – Continued.

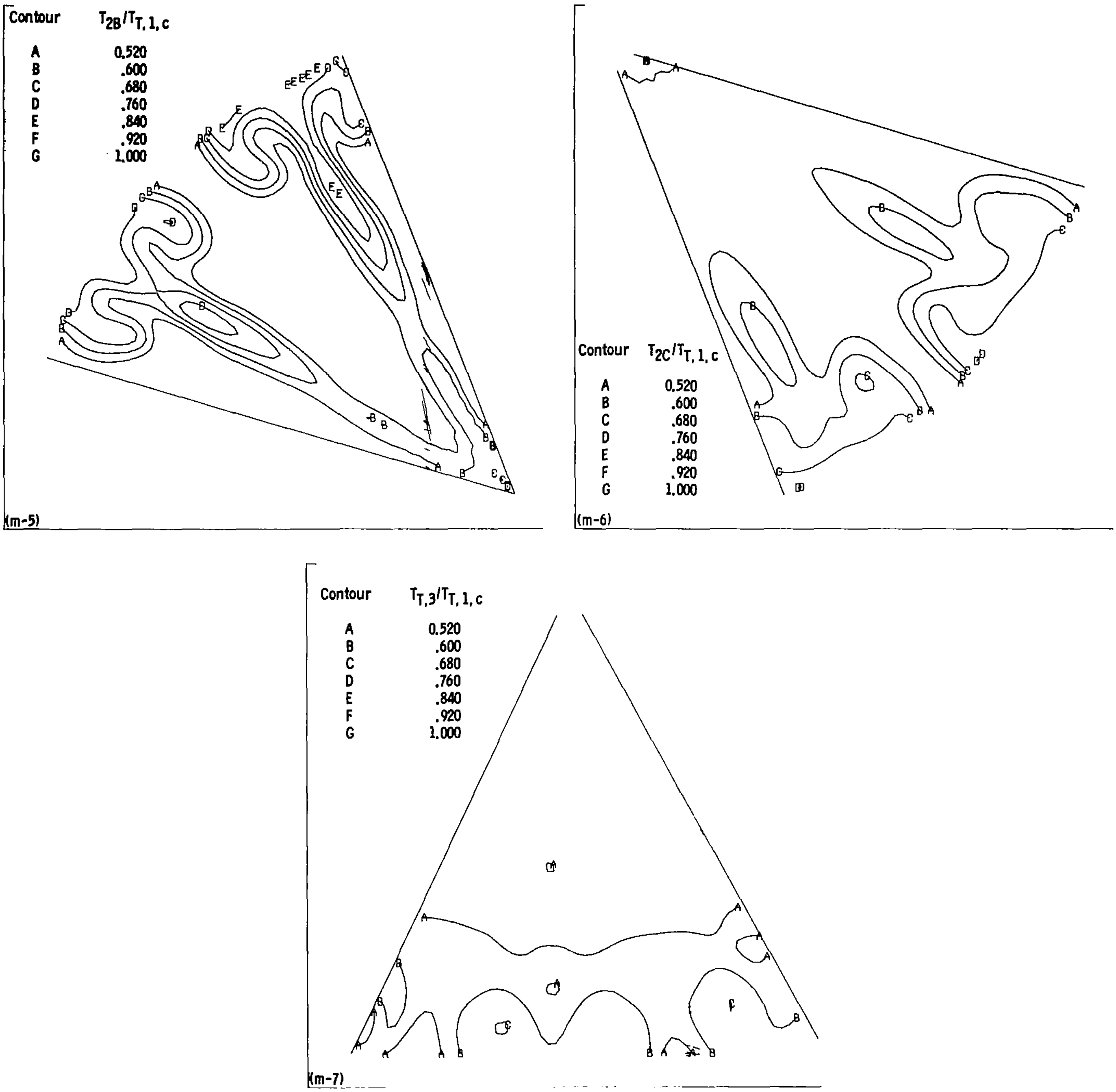


(m) Concluded.

Figure 13. – Continued.

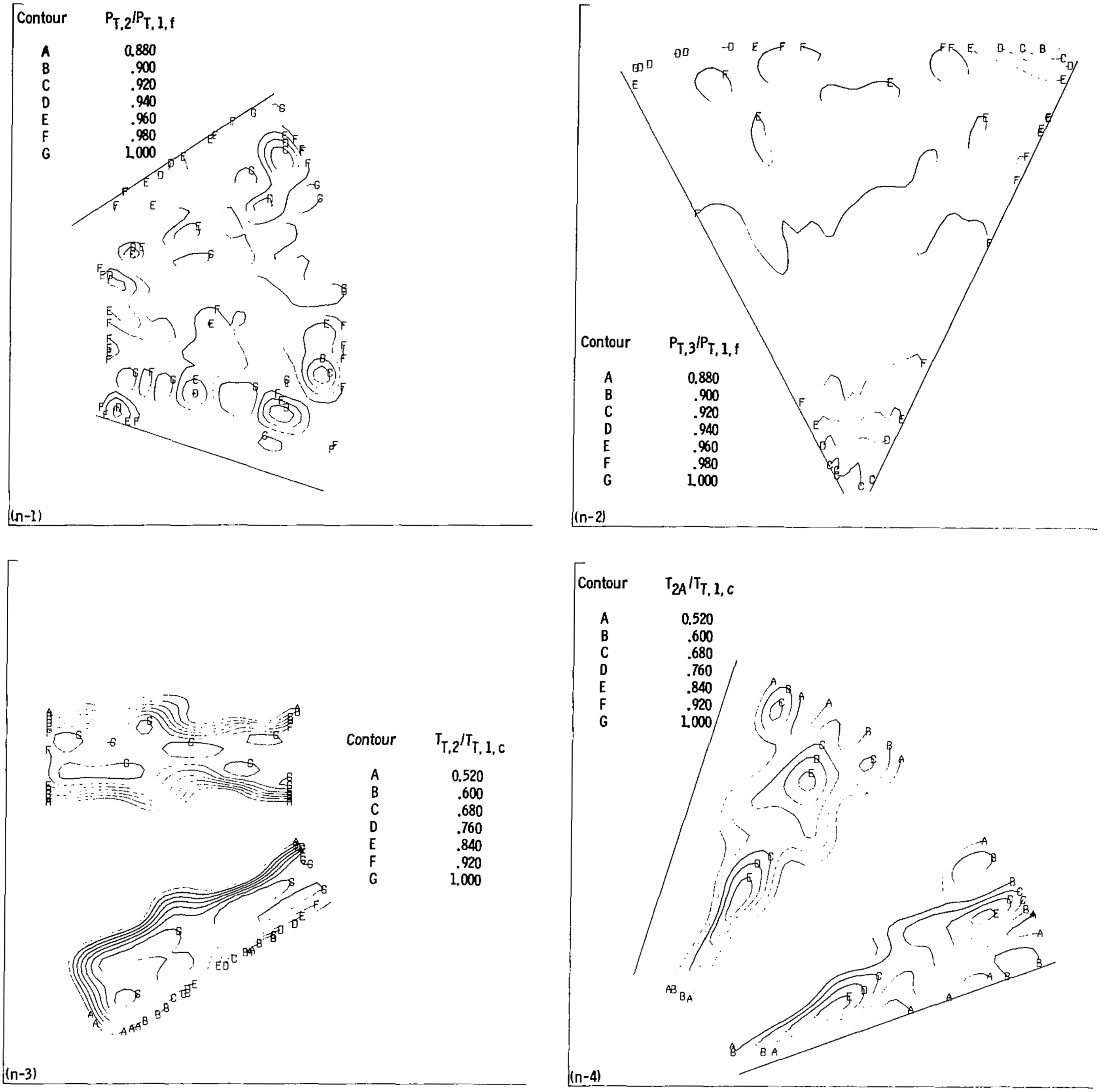


(n) 2E/REF-CB-S mixer configuration.

Figure 13. – Continued.

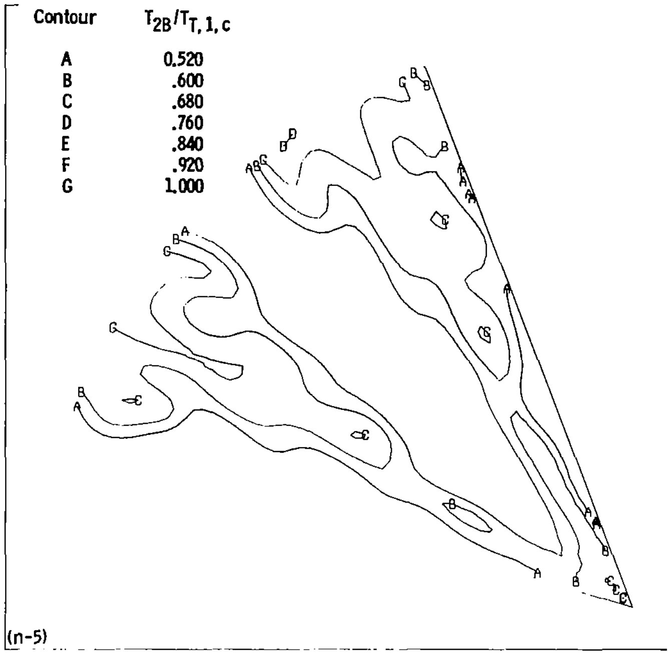


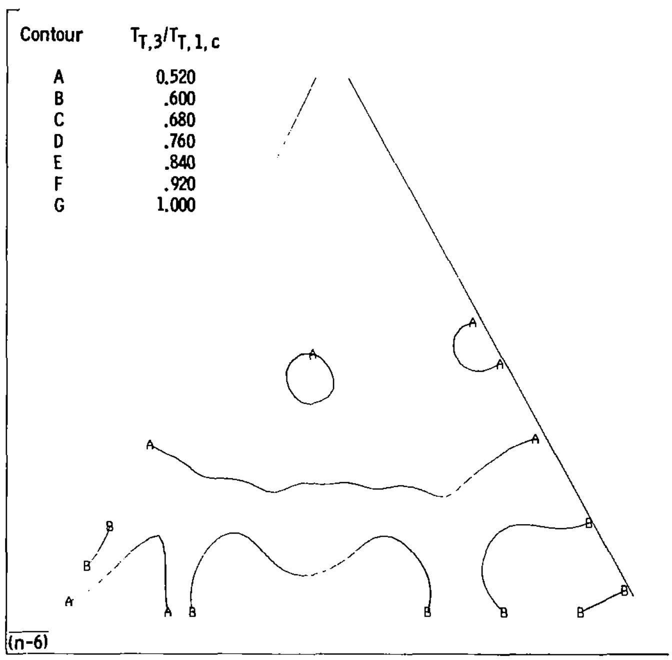


(n) Concluded.

Figure 13. – Continued.

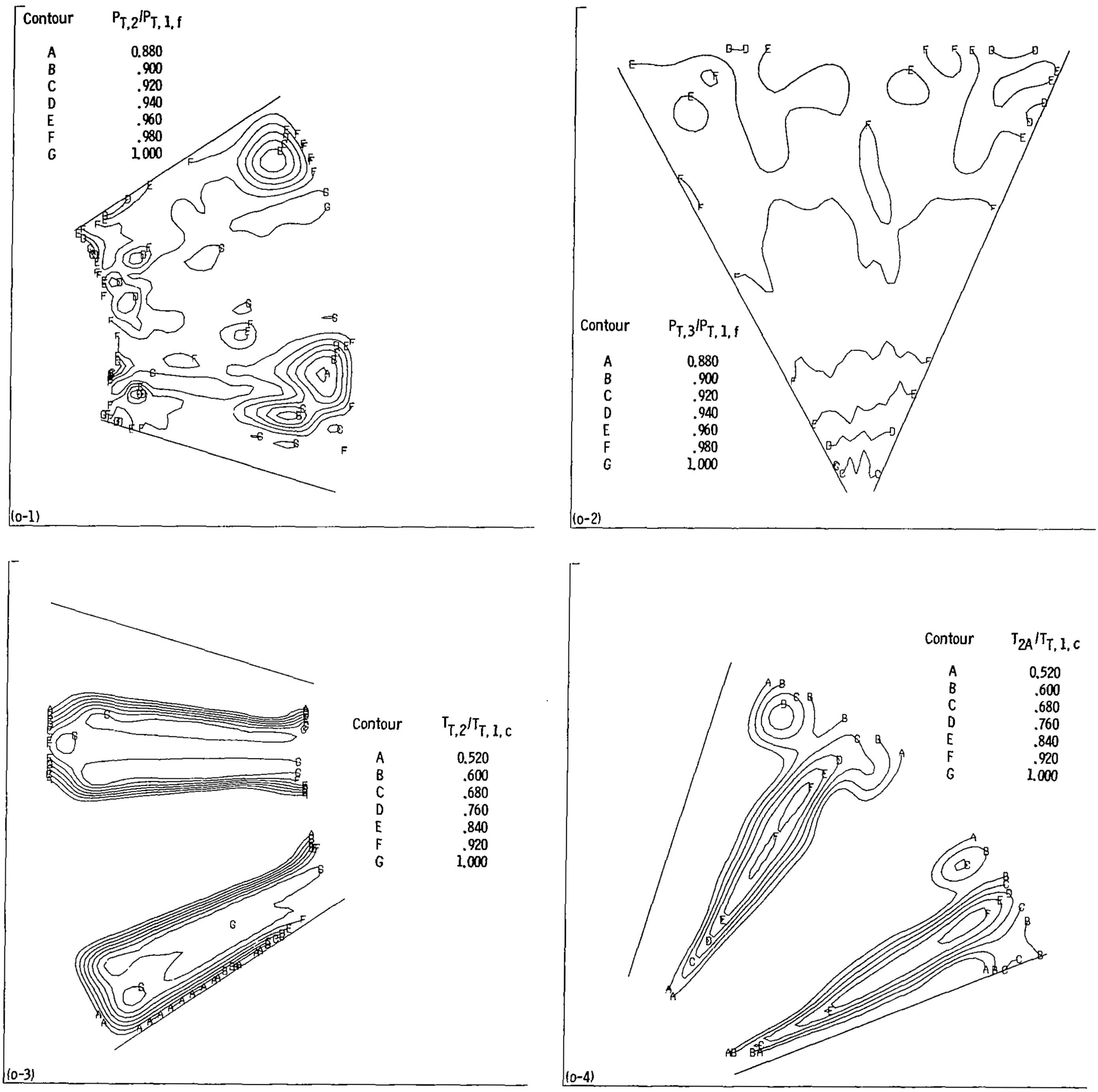


(o) 2E/3B-CB mixer configuration.

Figure 13. – Continued.

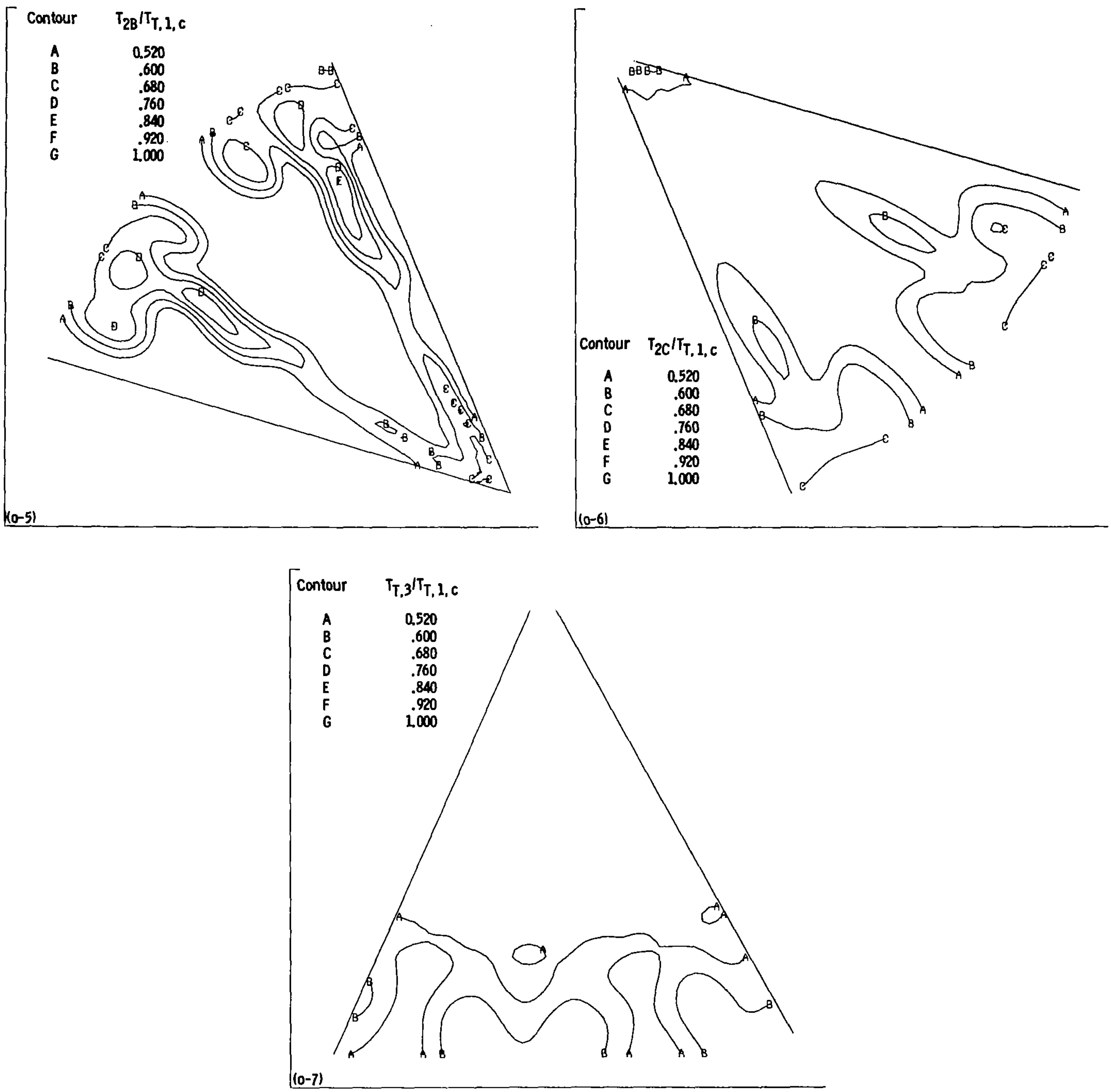


(o) Concluded.

Figure 13. – Continued.

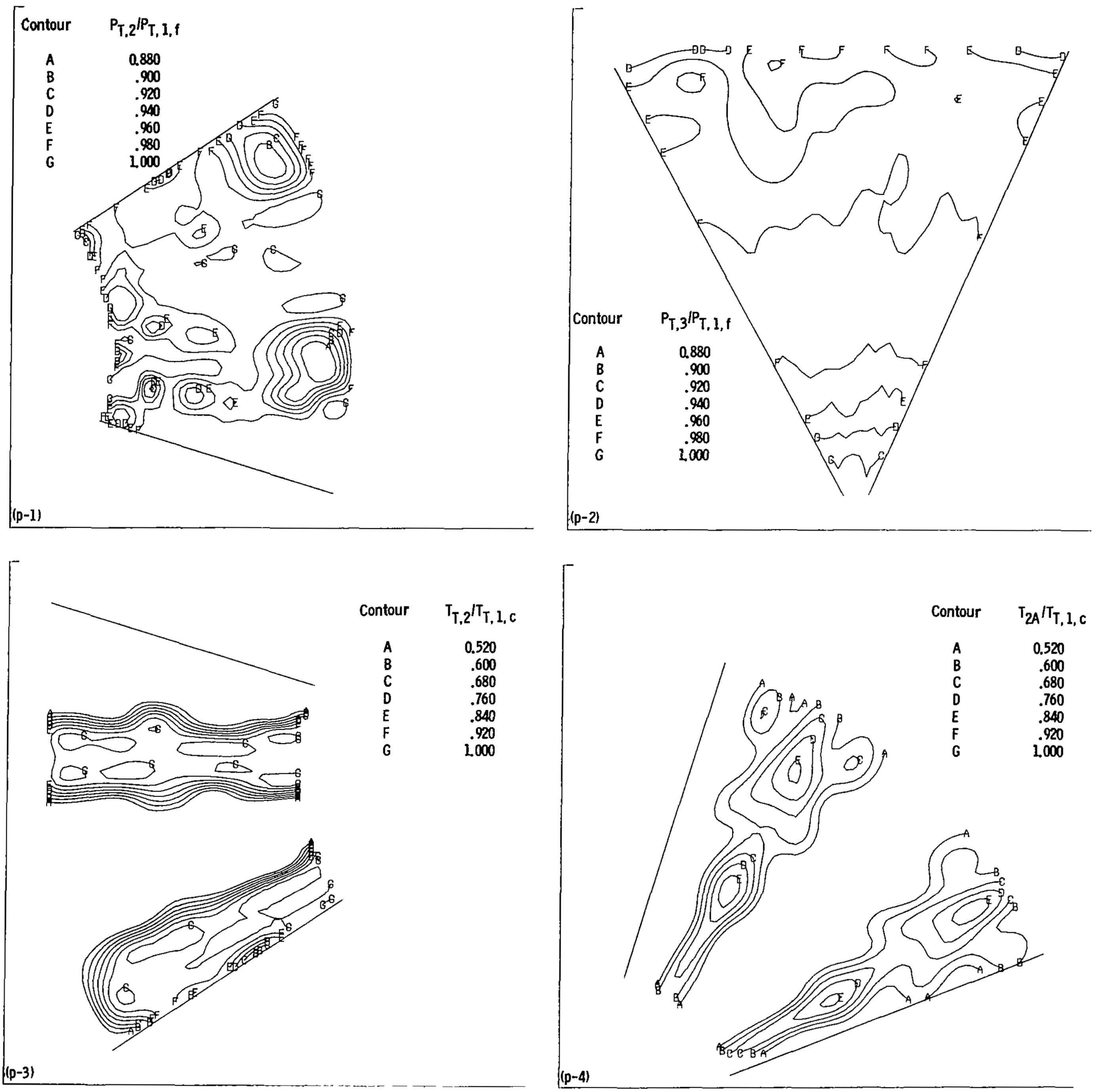


(p) 2E/3B-CB-S mixer configuration.

Figure 13. – Continued.

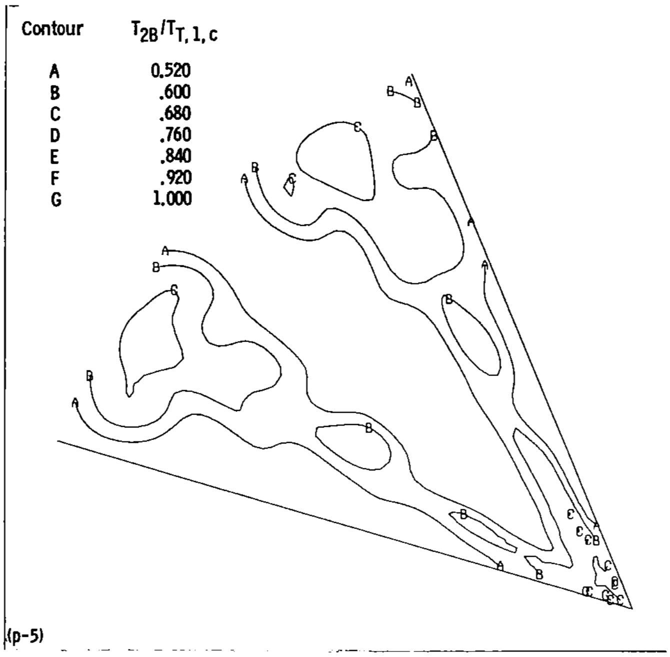


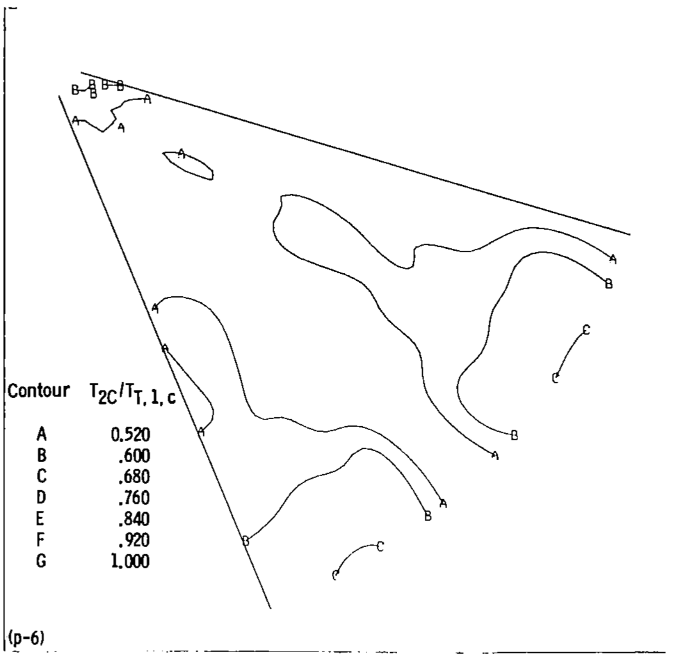


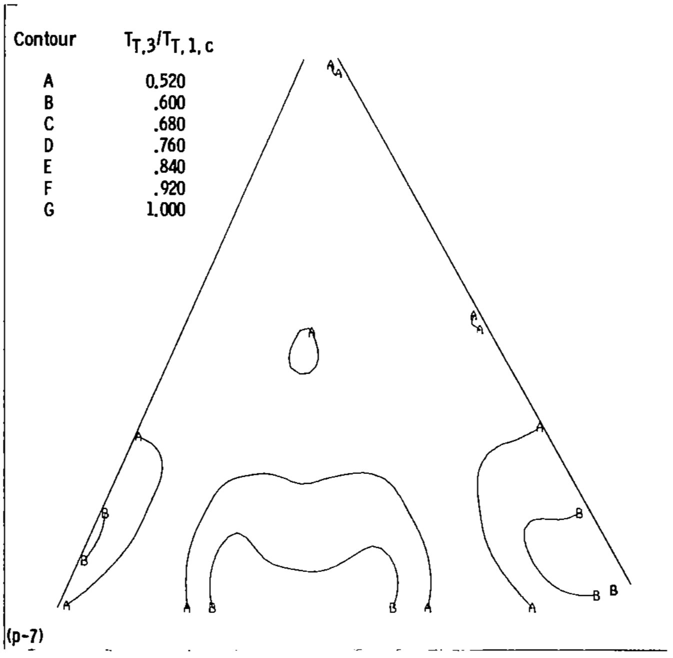


(p) Concluded.

Figure 13. – Continued.

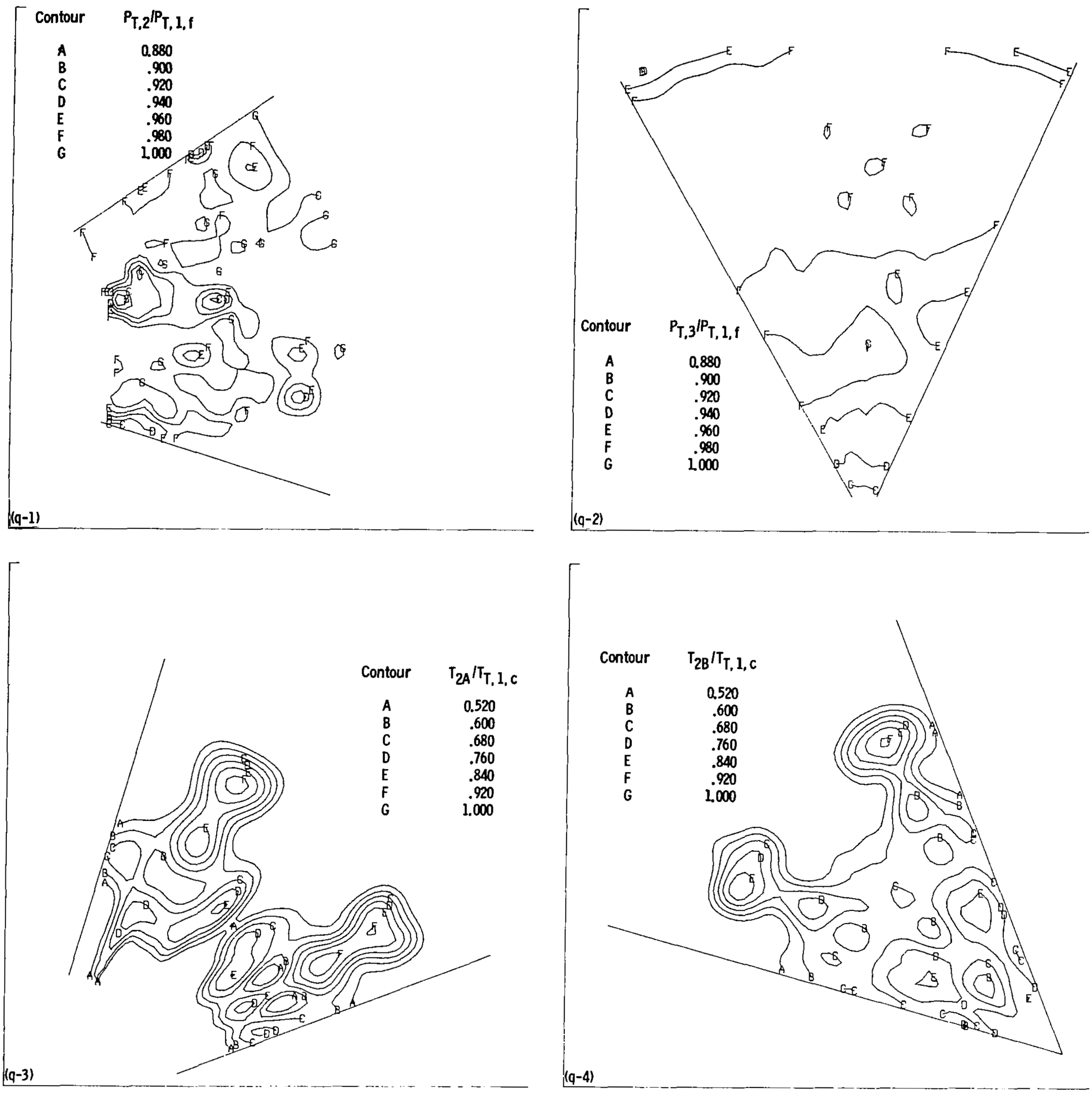


(q) 3E/2AC mixer configuration.

Figure 13. – Continued.

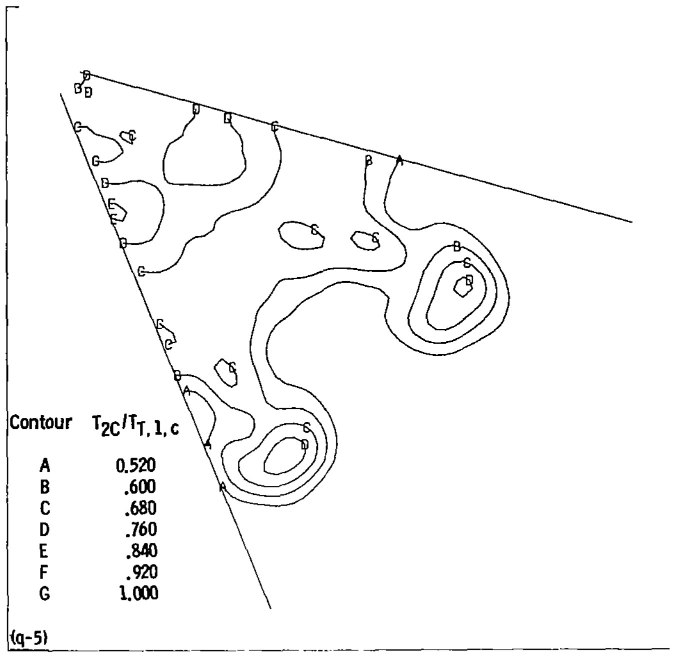


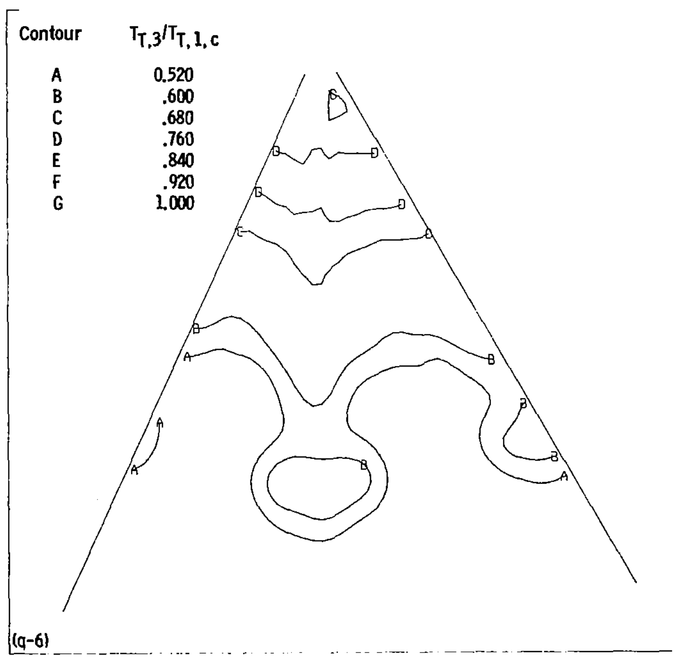


(q) Concluded.

Figure 13. – Concluded.

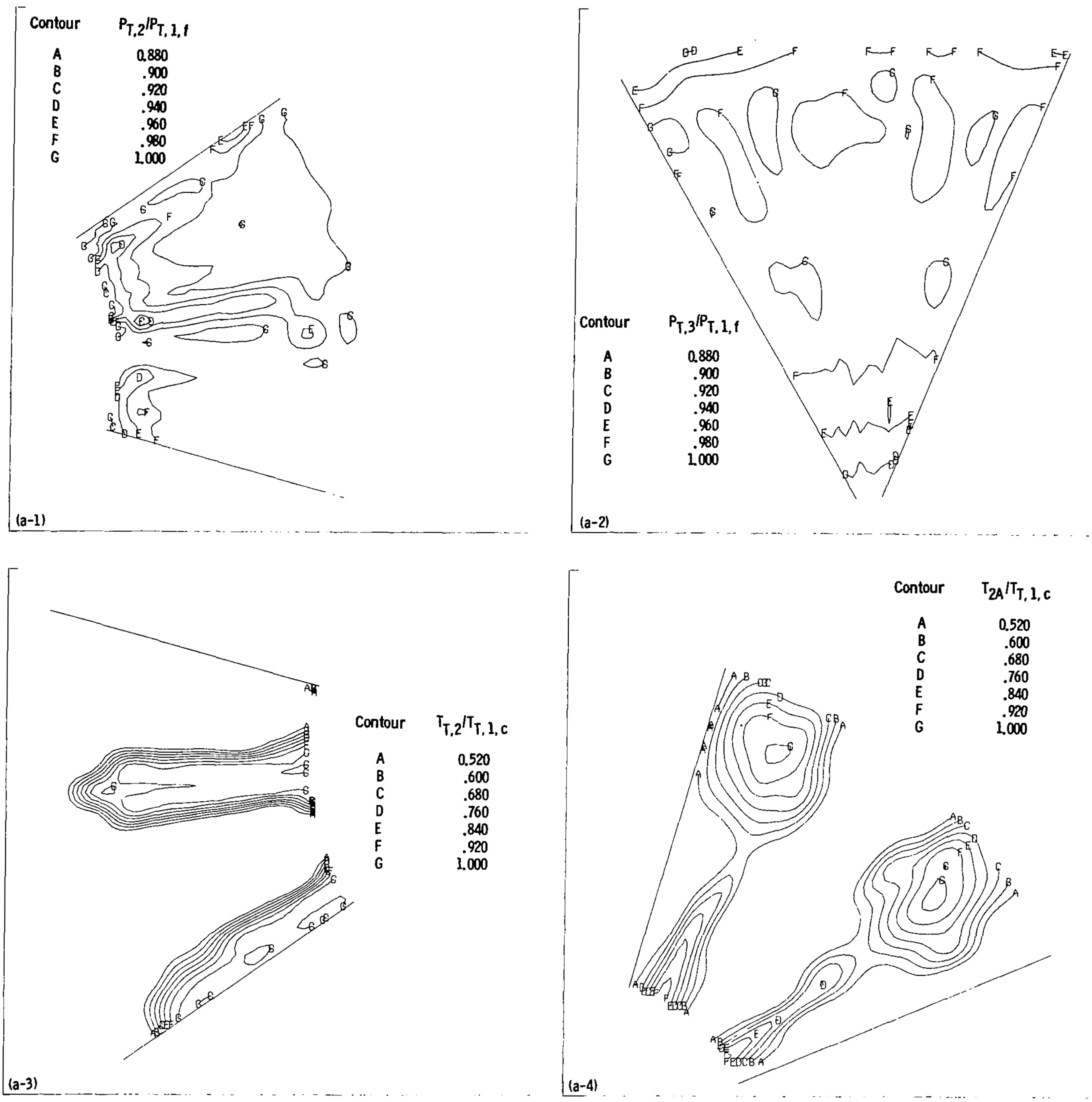


(a) 12B/3B mixer configuration.

Figure 14. – Contour plots of total pressure and temperature ratios at various nozzle stations in mixing region for nozzle pressure ratio of 1.6 and temperature ratio of 2.5 (takeoff condition).

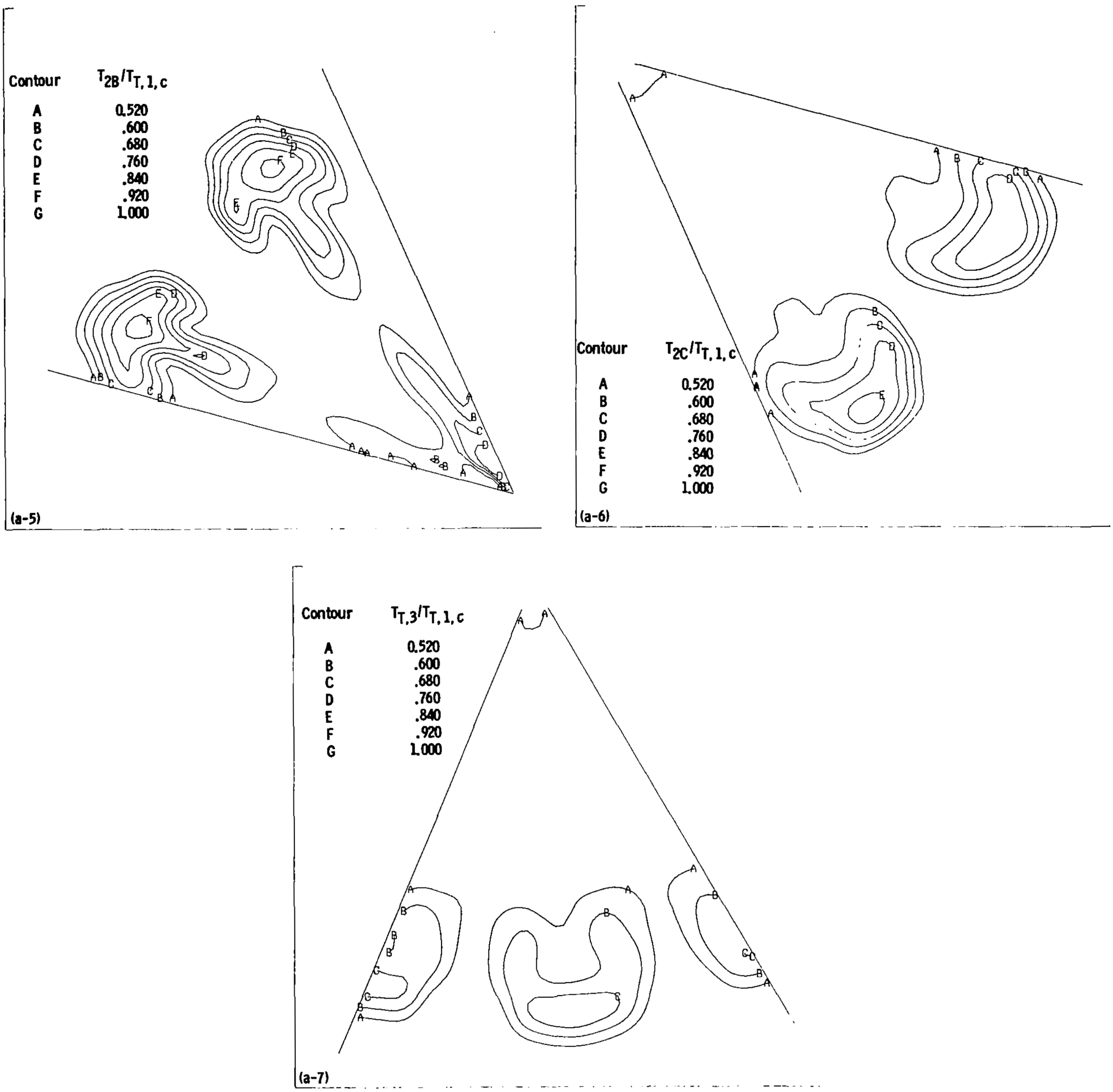


(a) Concluded.

Figure 14. – Continued.

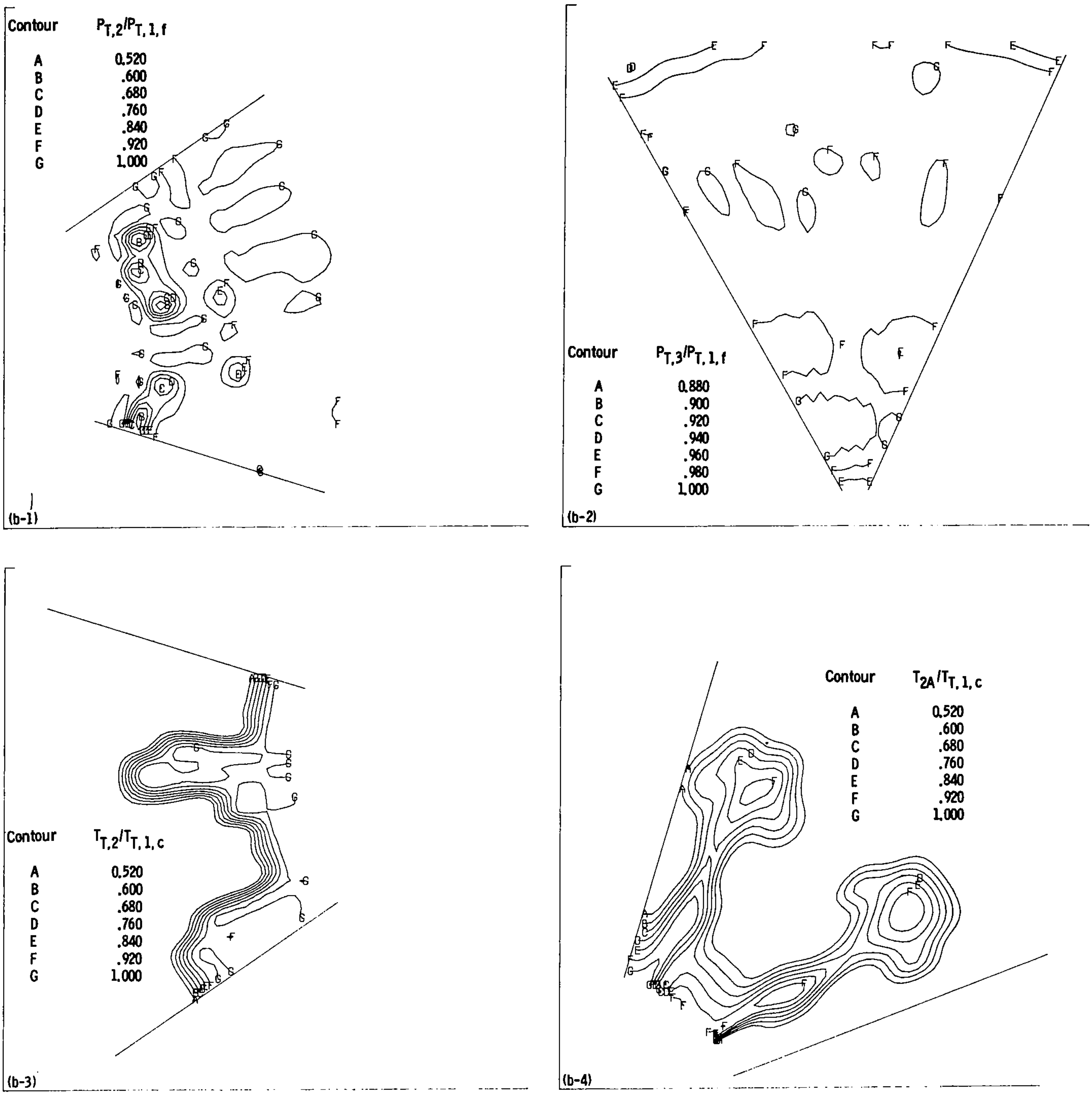


(b) 1E/2AC mixer configuration.

Figure 14. – Continued.

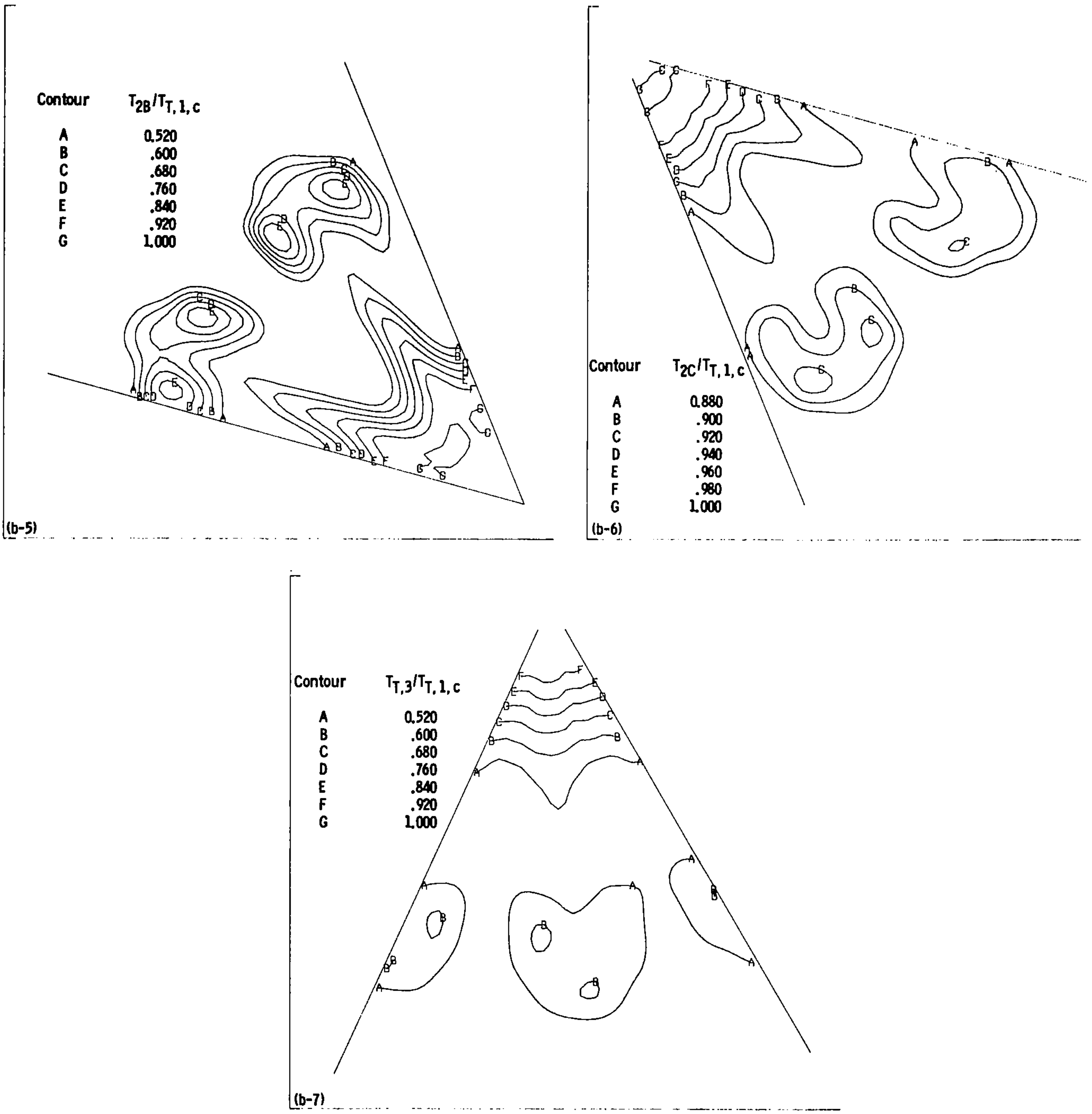


(b) Concluded.

Figure 14. – Continued.

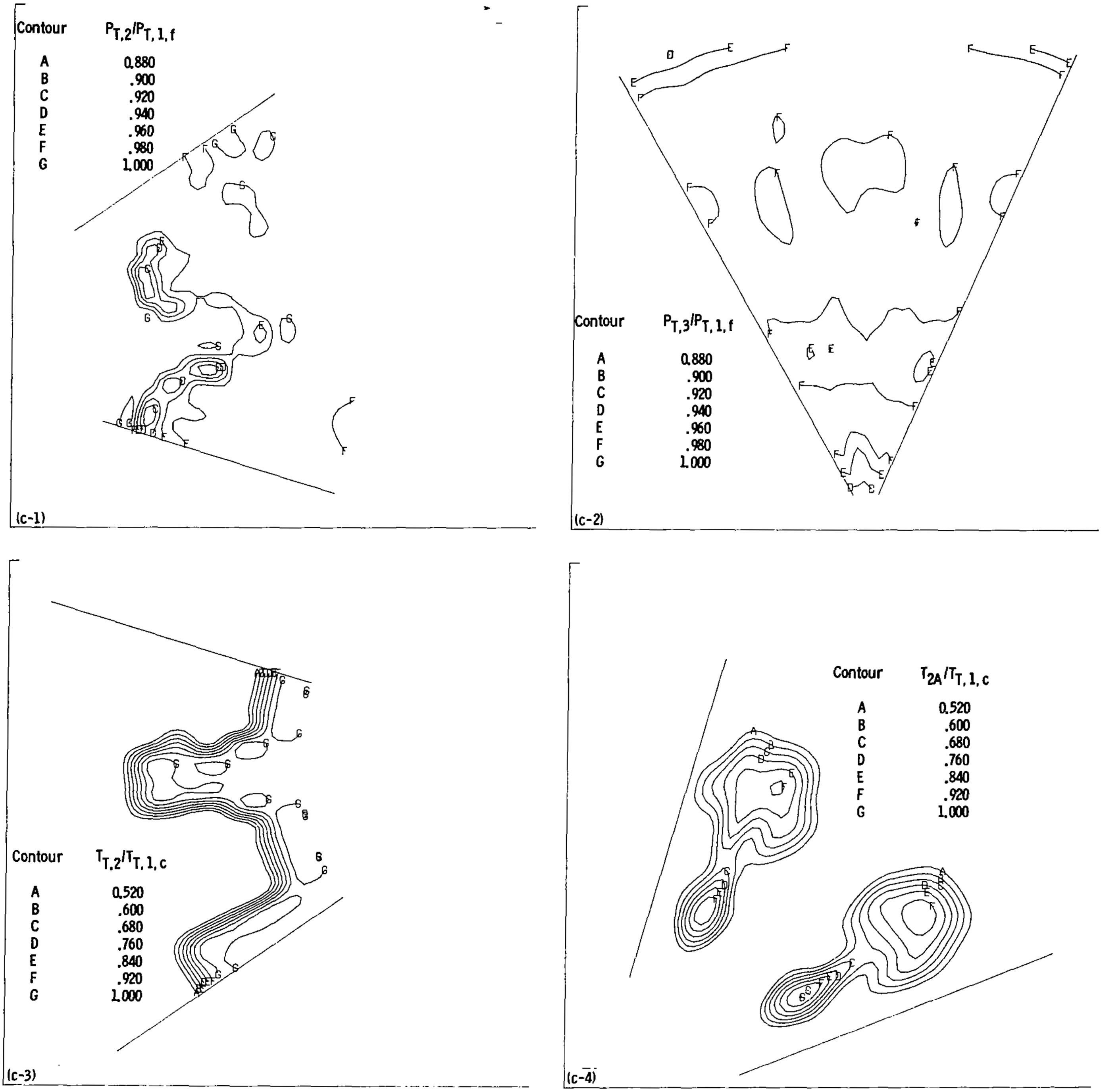


(c) 1E/2AC-S mixer configuration.

Figure 14. – Continued.

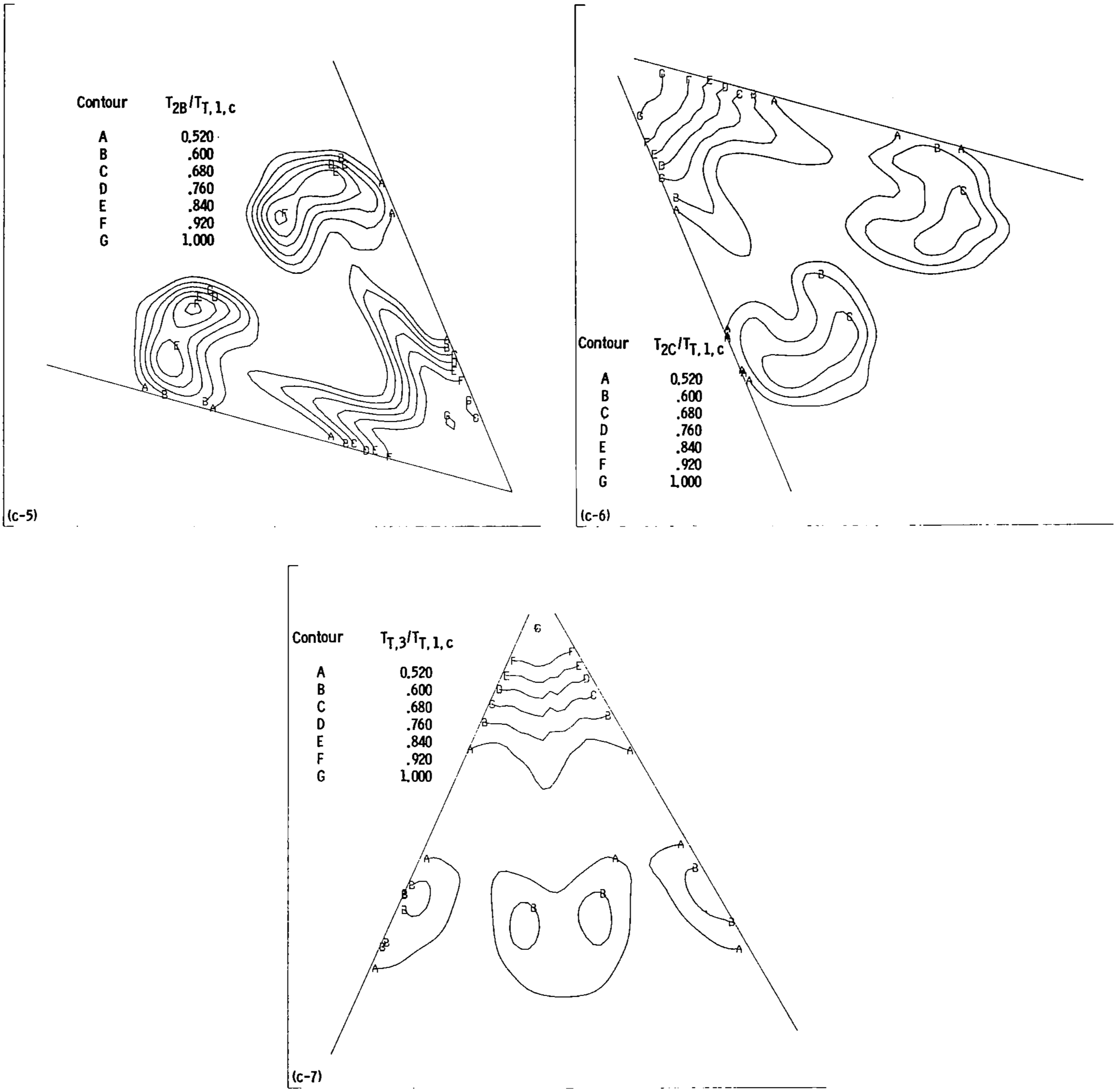


(c) Concluded.

Figure 14. – Continued.

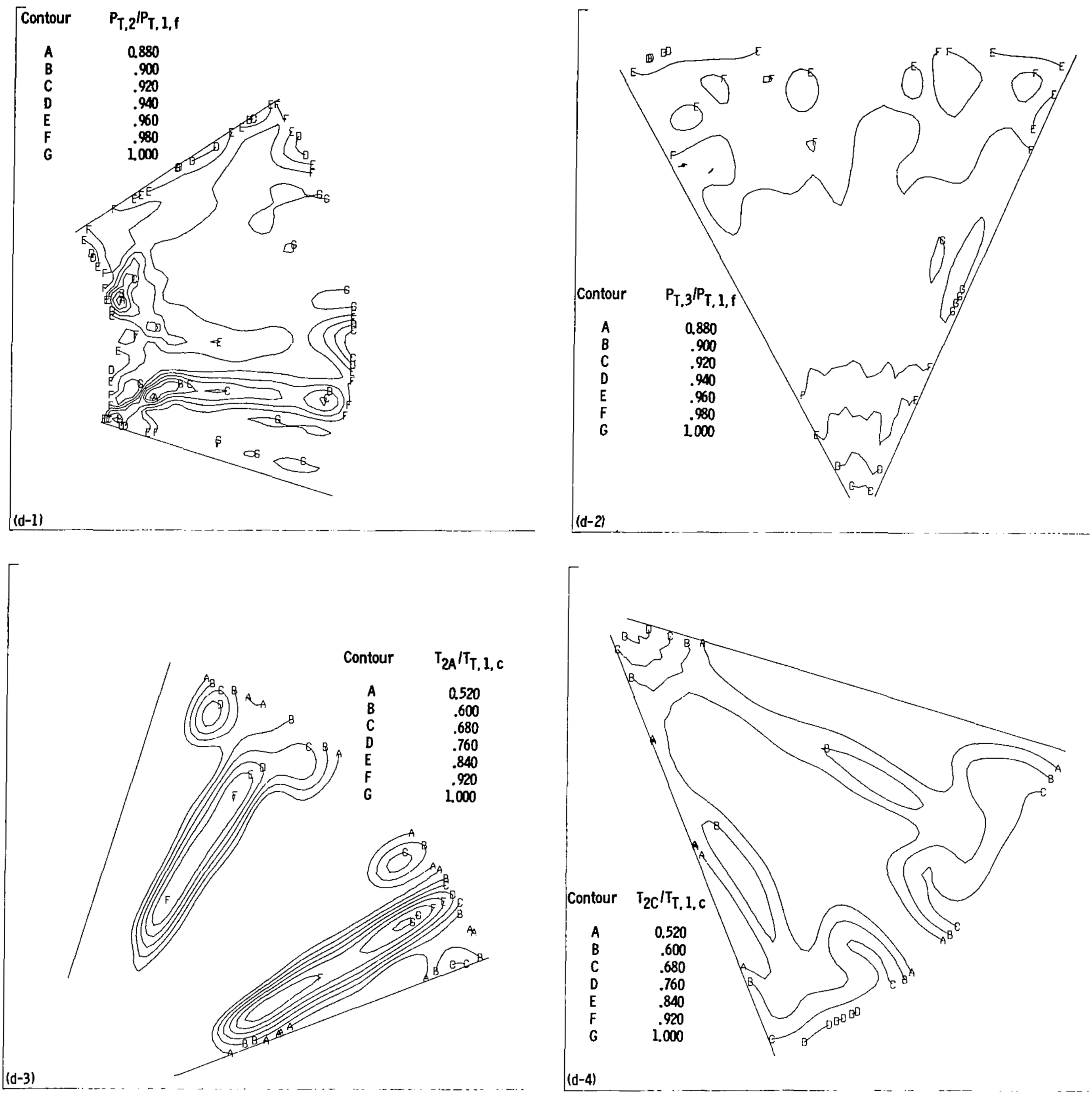


(d) 2E/REF mixer configuration.

Figure 14. – Continued.

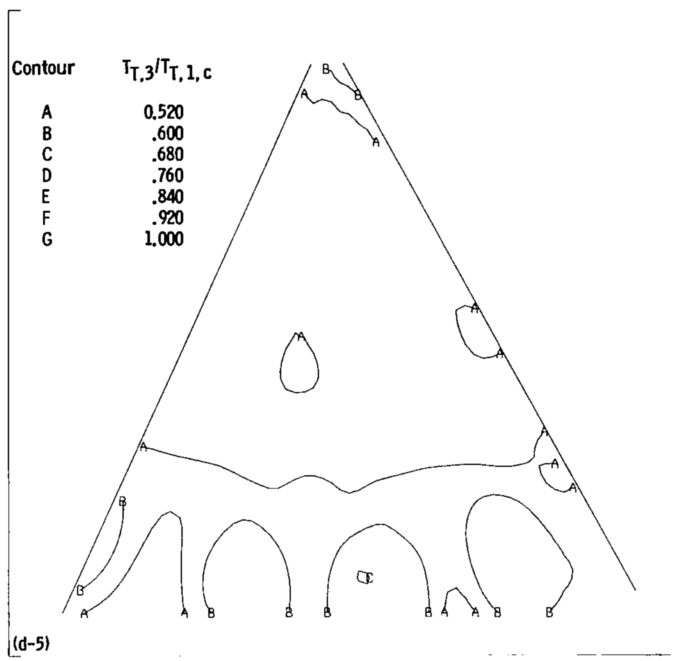


(d) Concluded.

Figure 14. – Continued.

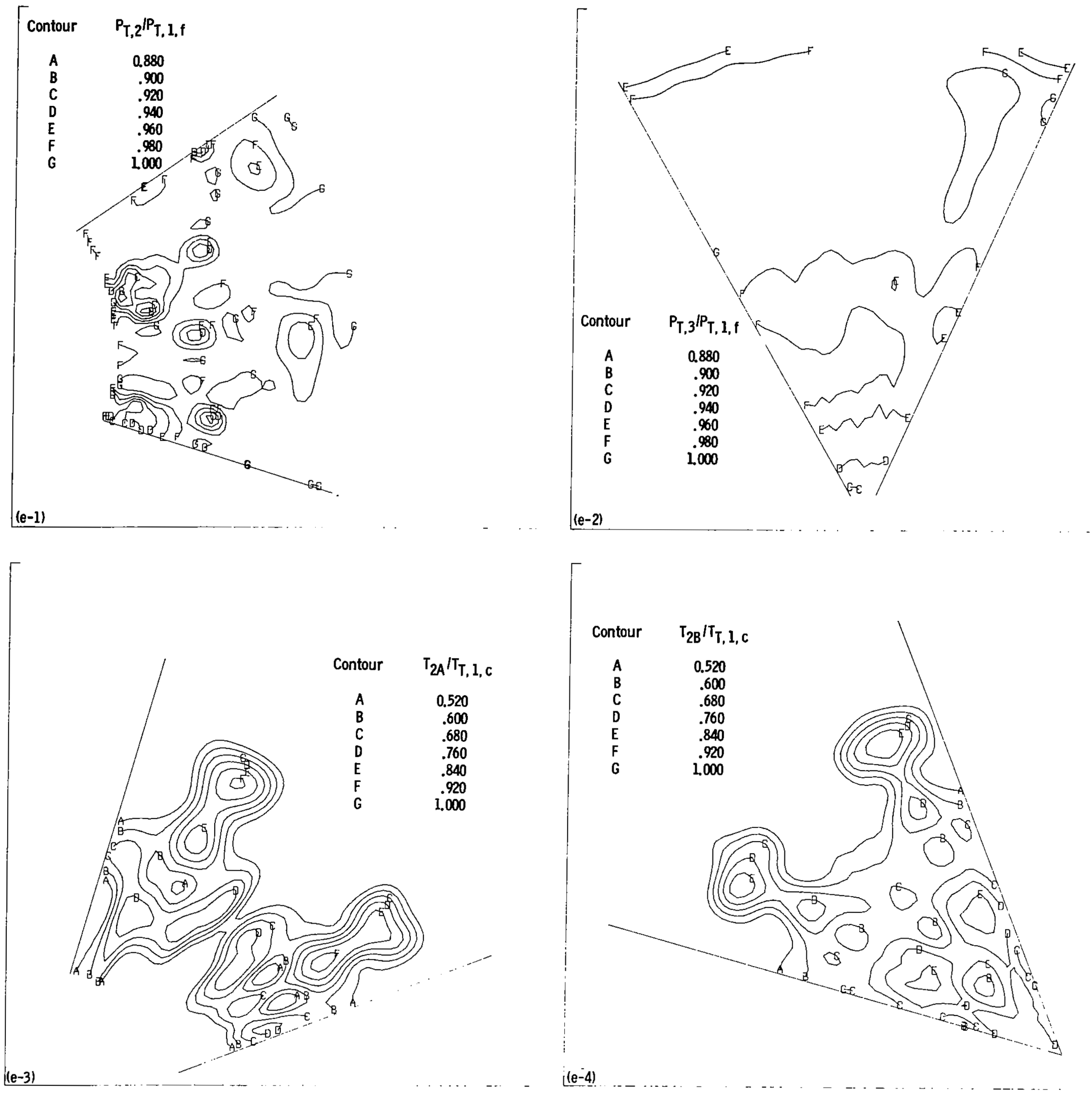


(e) 3E/2AC mixer configuration.

Figure 14. – Continued.

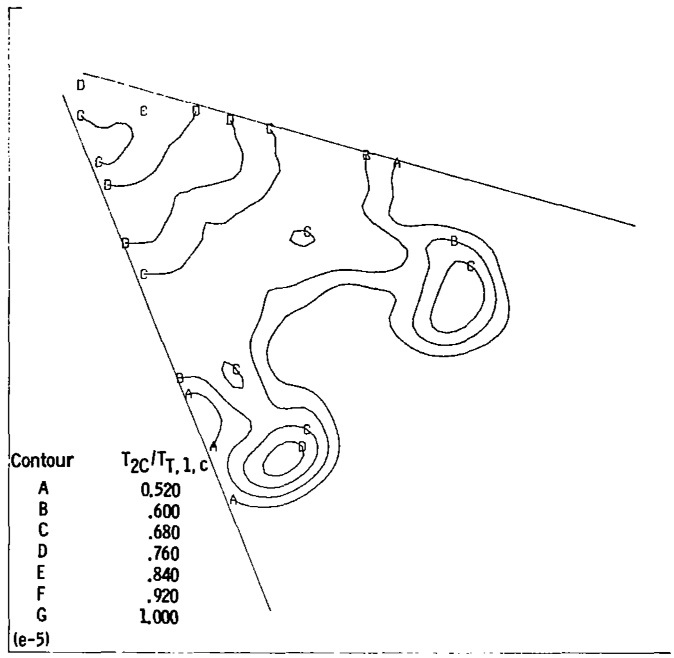


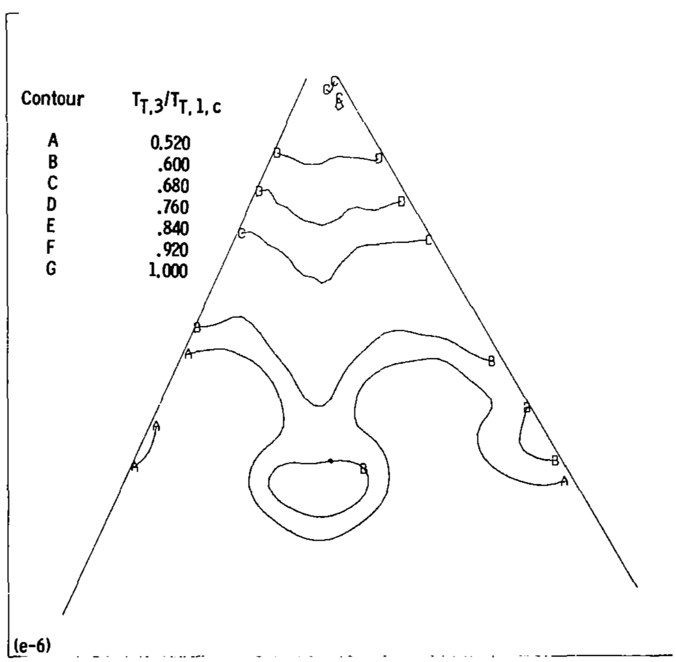


(e) Concluded.

Figure 14. – Concluded.

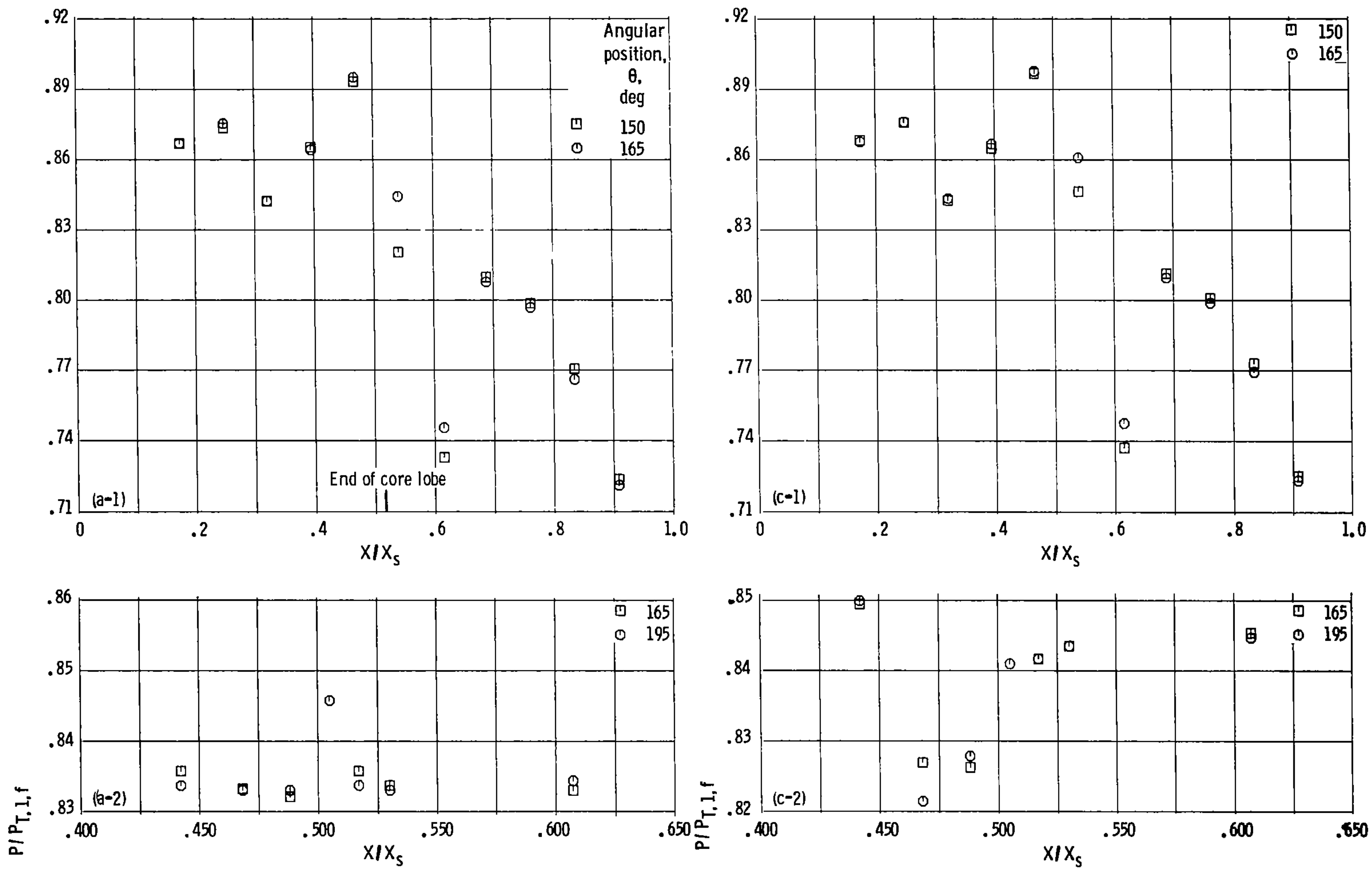

Angular position, θ, deg
150
165
End of core lobe
(a-1)
(c-1)
X/X$_s$
165
195
(a-2)
(c-2)
P/P$_{T,1,f}$
X/X$_s$

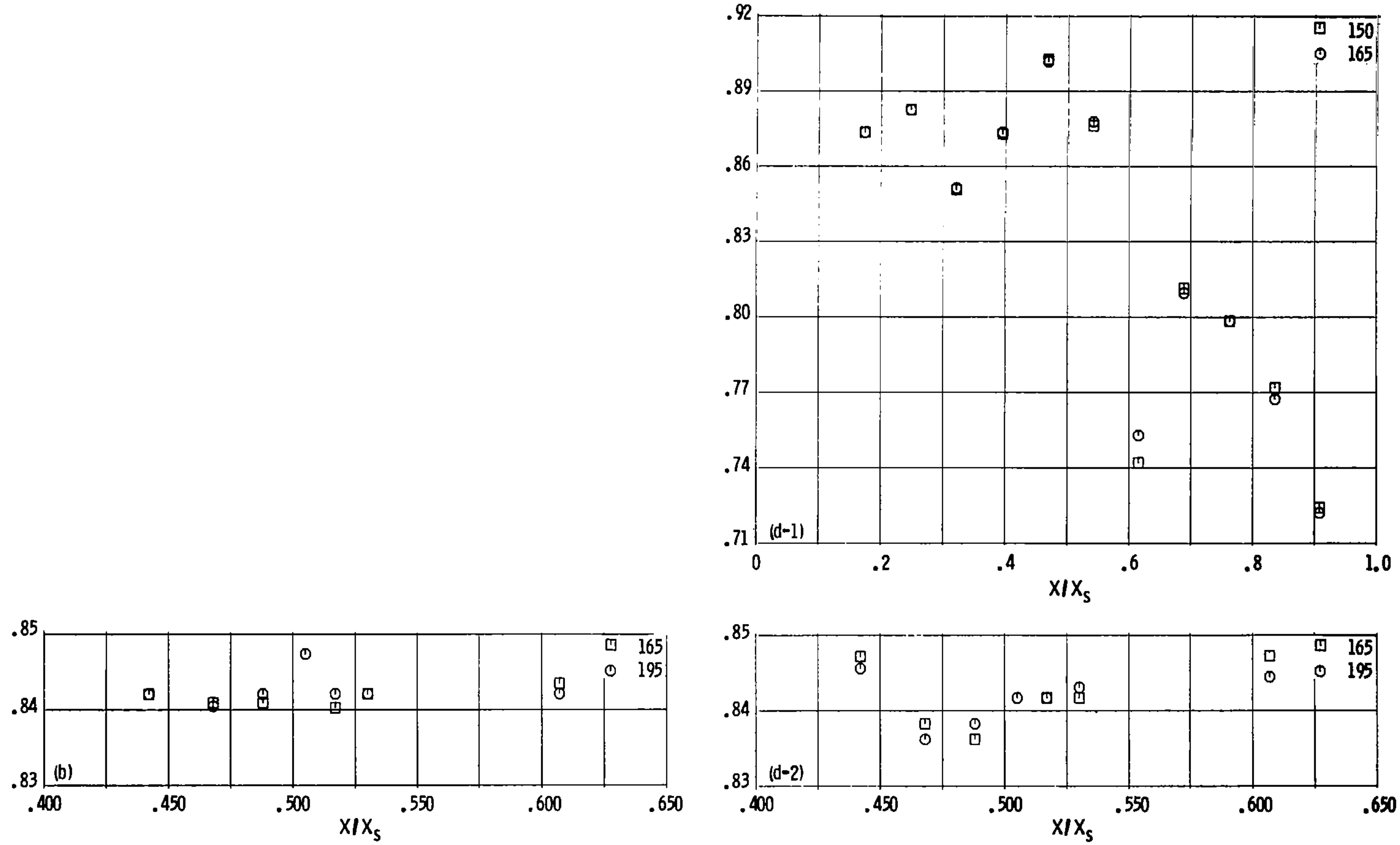


(a-1) Shroud statics. (a-2) Plug statics.
(a) 12B/3B mixer configuration.
(b) 12B/3B–S mixer configuration (plug statics).
(c-1) Shroud statics. (c-2) Plug statics.
(c) 12B/REF mixer configuration.
(d-1) Shroud statics. (d-2) Plug statics.
(d) 12B/REF–S mixer configuration.

Figure 15. – Static pressure distribution for nozzle shroud and centerbody. Nozzle pressure ratio, 2.4; temperature ratio, 2.5 (cruise condition).

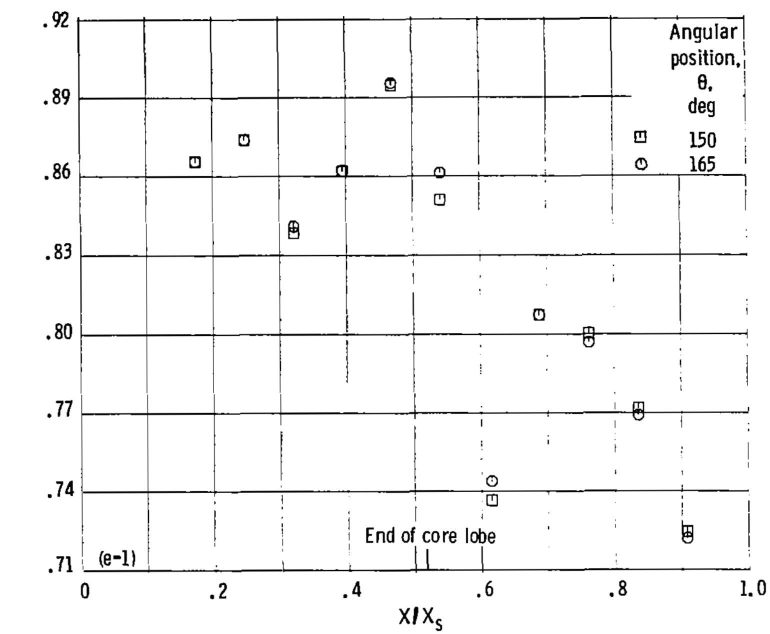
.92
.89
.86
.83
.80
.77
.74
.71
Angular position, θ, deg
150
165
(e-1)
End of core lobe
0
.2
.4
.6
.8
1.0
X/X_S

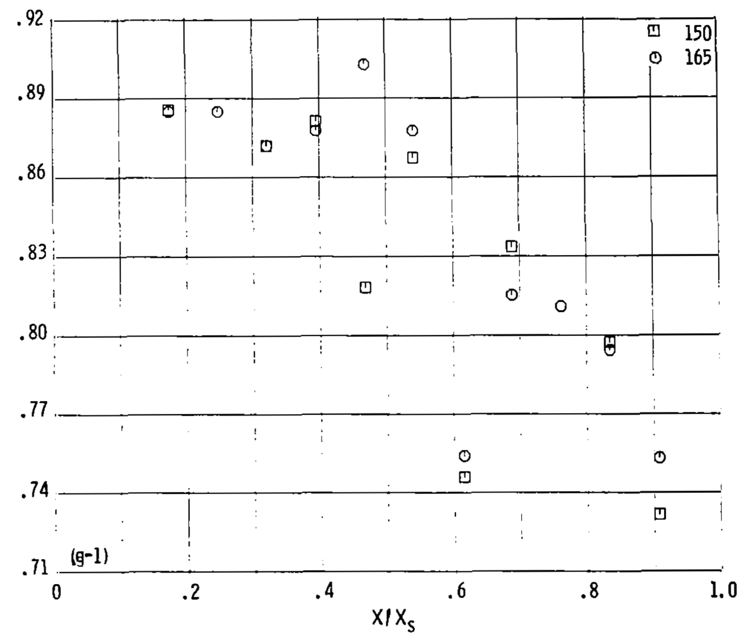
.92
.89
.86
.83
.80
.77
.74
.71
150
165
(g-1)
0
.2
.4
.6
.8
1.0
X/X_S

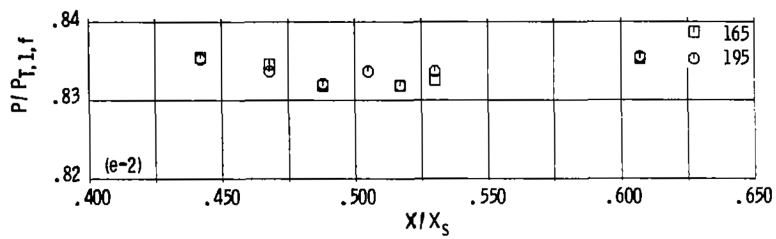
P/P_T,1,f
.84
.83
.82
165
195
(e-2)
.400
.450
.500
.550
.600
.650
X/X_S

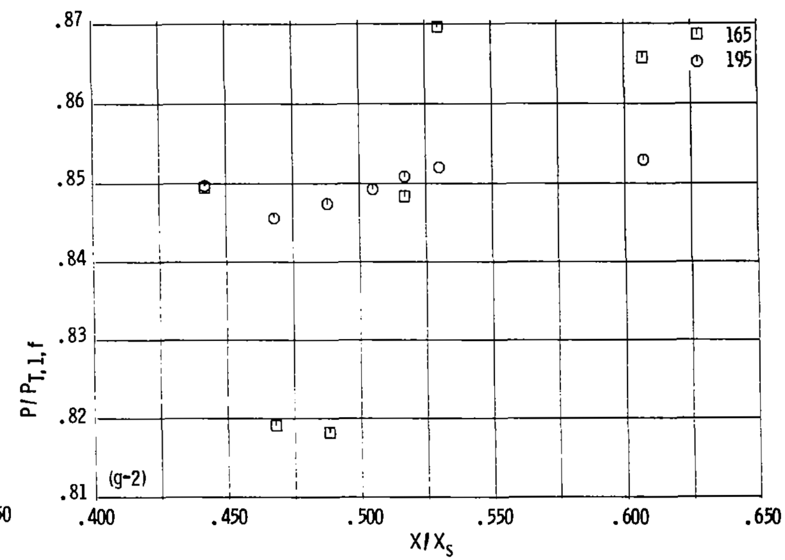
P/P_T,1,f
.87
.86
.85
.84
.83
.82
.81
165
195
(g-2)
.400
.450
.500
.550
.600
.650
X/X_S

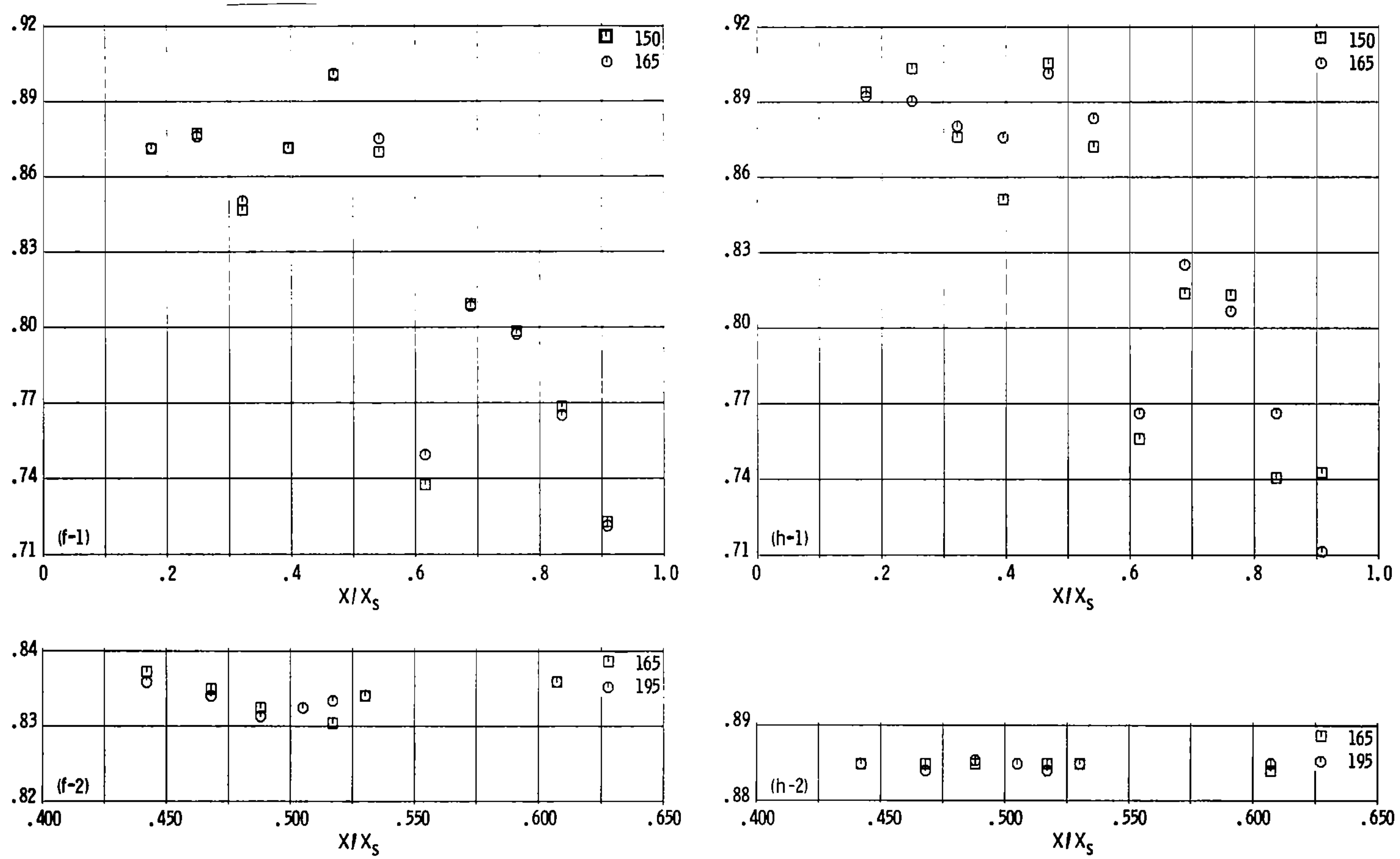


(e-1) Shroud statics. (e-2) Plug statics.
(e) 12B/2AC mixer configuration.
(f-1) Shroud statics. (f-2) Plug statics.
(f) 12B/2AC-S mixer configuration.
(g-1) Shroud statics. (g-2) Plug statics.
(g) 12A/REF mixer configuration.
(h-1) Shroud statics. (h-2) Plug statics.
(h) 12A/2AC mixer configuration.

Figure 15. – Continued.

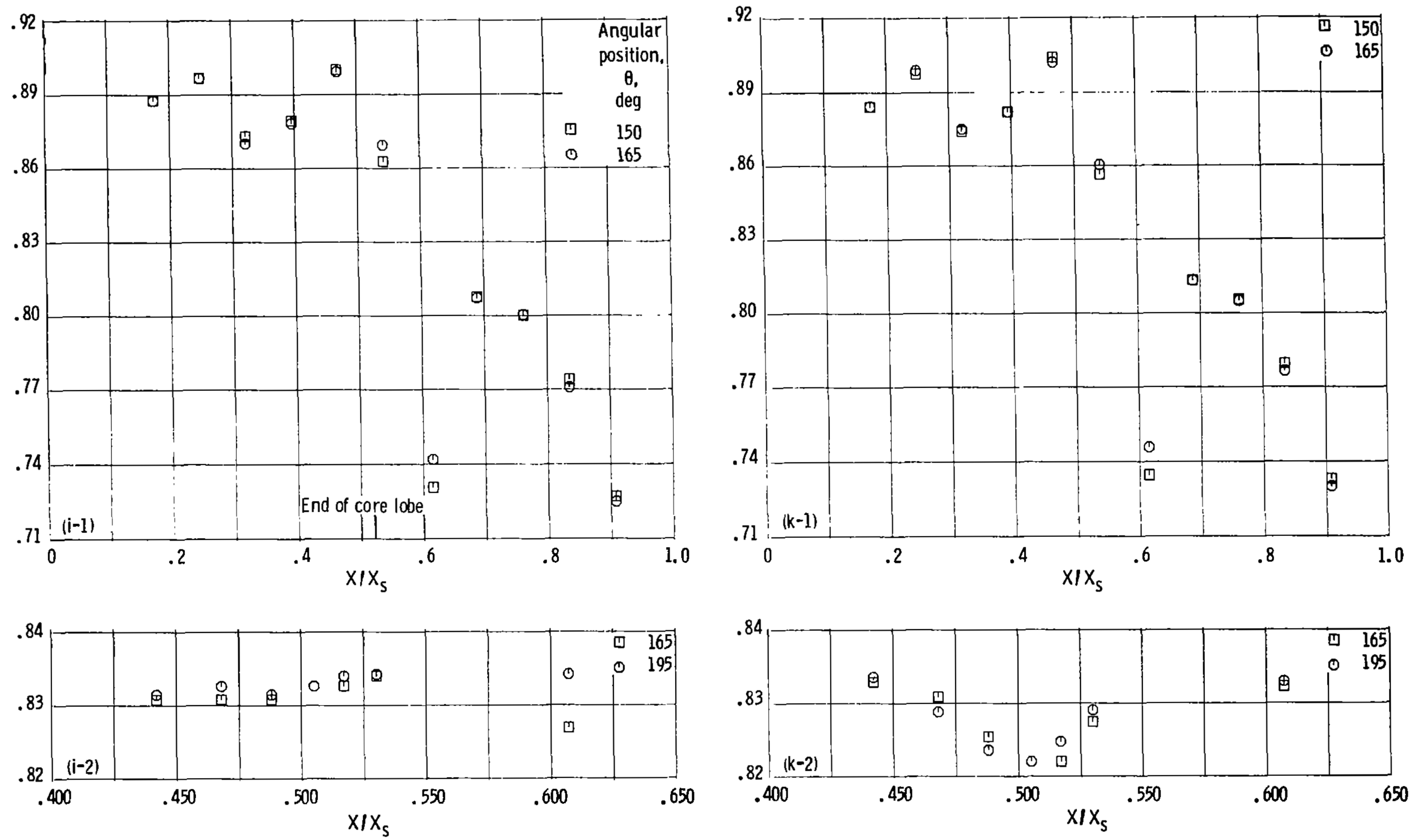
Angular position, θ, deg
150
165
End of core lobe
(i-1)
(k-1)
X/X_s
165
195
(i-2)
(k-2)
X/X_s
.92
.89
.86
.83
.80
.77
.74
.71
0
.2
.4
.6
.8
1.0
.84
.83
.82
.400
.450
.500
.550
.600
.650

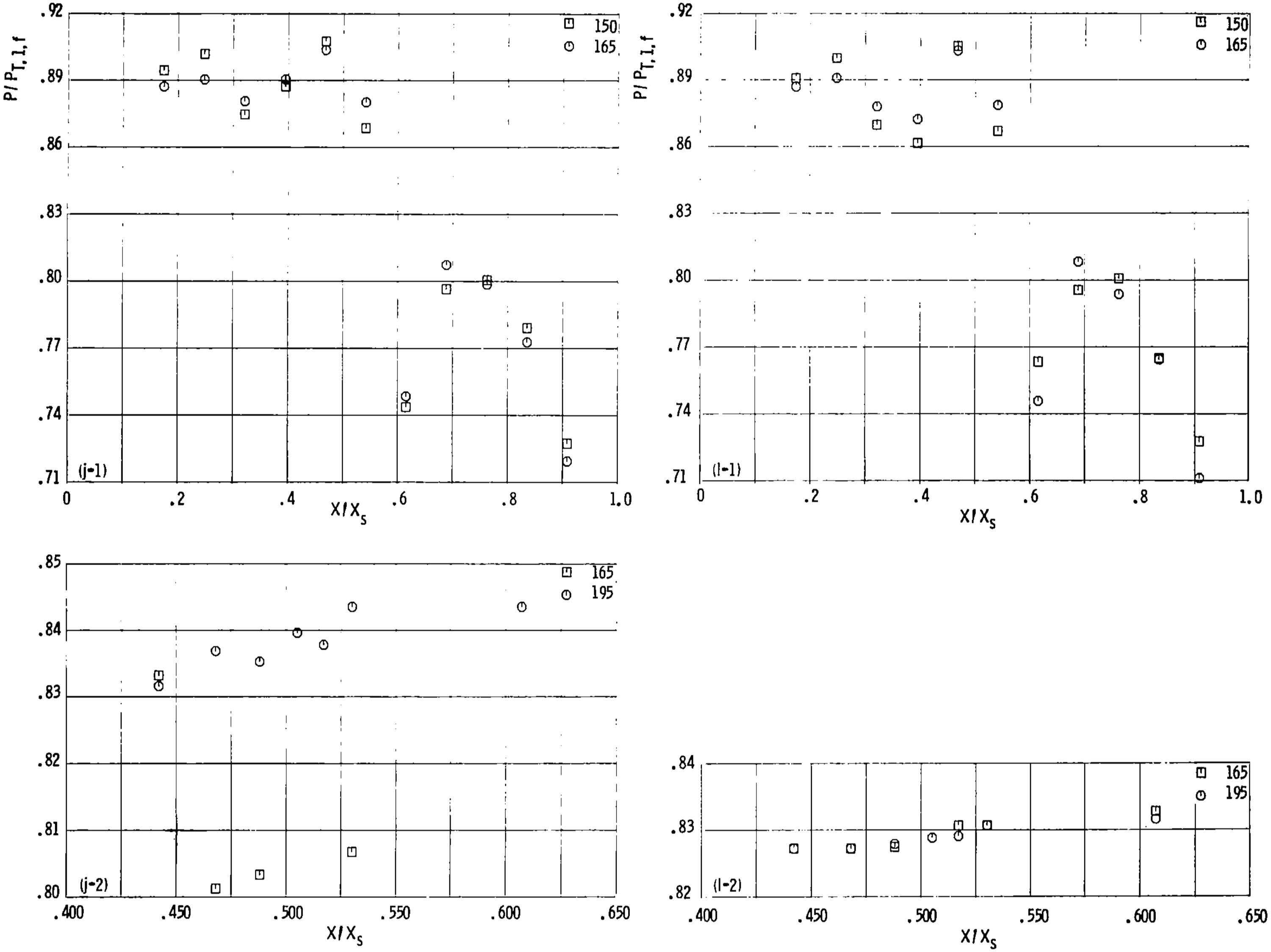


(i-1) Shroud statics. (i-2) Plug statics.
(i) 12C/REF mixer configuration.
(j-1) Shroud statics. (j-2) Plug statics.
(j) 12C/REF-S mixer configuration.
(k-1) Shroud statics. (k-2) Plug statics.
(k) 12C/2AC mixer configuration.
(l-1) Shroud statics. (l-2) Plug statics.
(l) 12C/2AC-S mixer configuration.

Figure 15. – Continued.

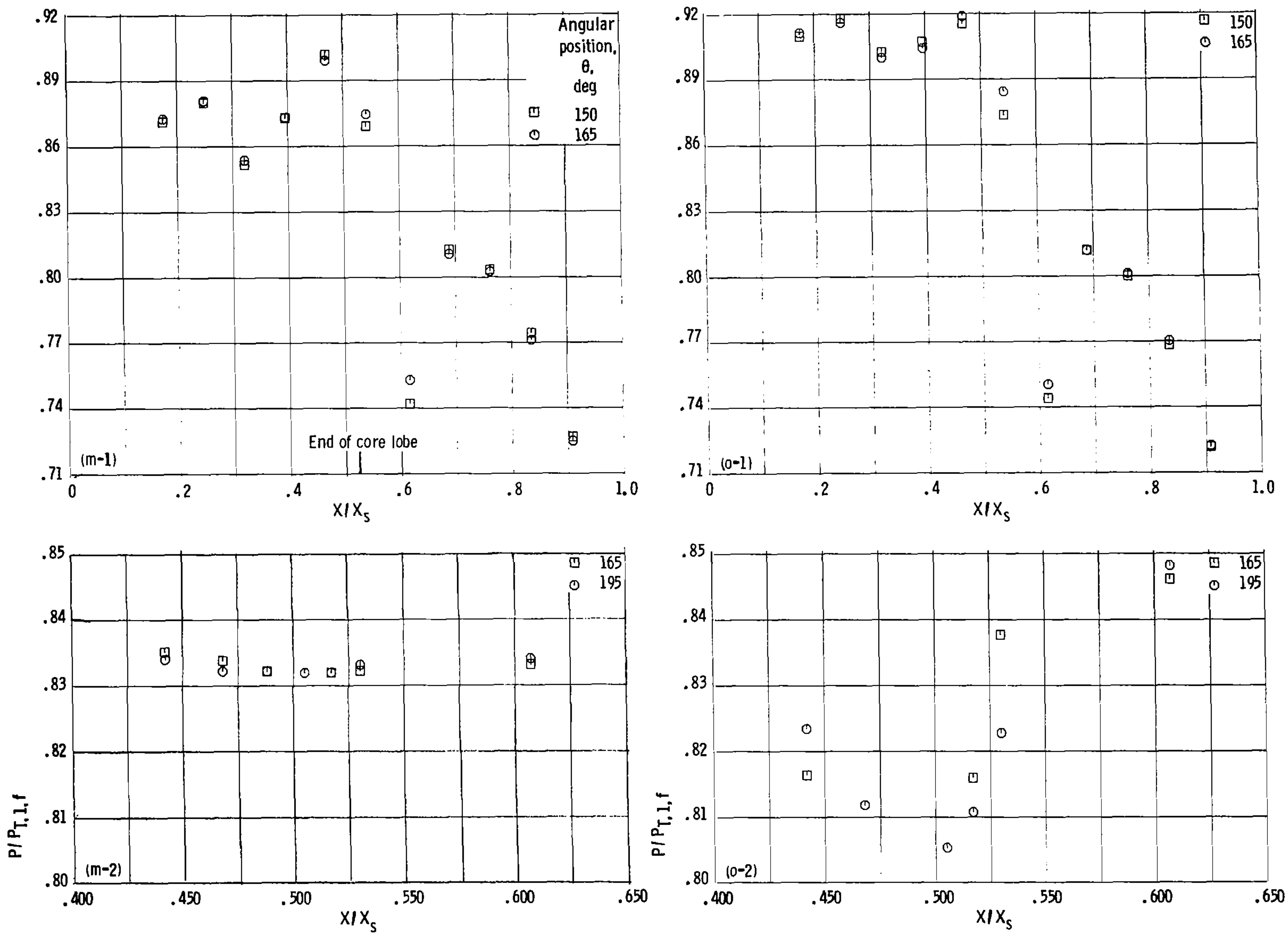
Angular position, θ, deg
150
165
End of core lobe
(m-1)
(o-1)
X/X_s
(m-2)
(o-2)
195
P/P_T,1,f
X/X_s

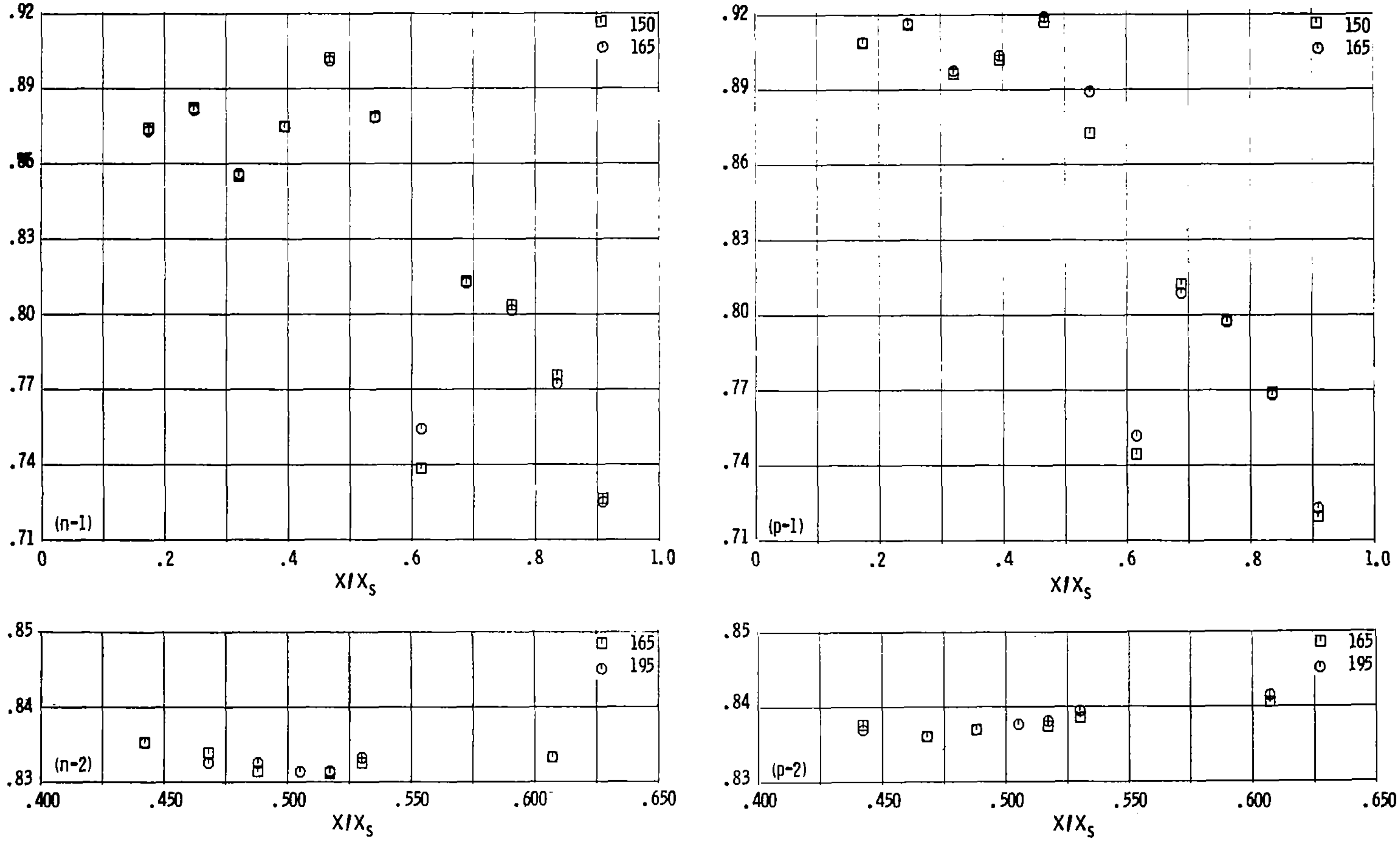


(m-1) Shroud statics. (m-2) Plug statics.
(m) 1E/2AC mixer configuration.
(n-1) Shroud statics. (n-2) Plug statics.
(n) 1E/2AC-S mixer configuration.
(o-1) Shroud statics. (o-2) Plug statics.
(o) 2E/REF mixer configuration.
(p-1) Shroud statics. (p-2) Plug statics.
(p) 2E/REF-CB mixer configuration.

Figure 15. – Continued.

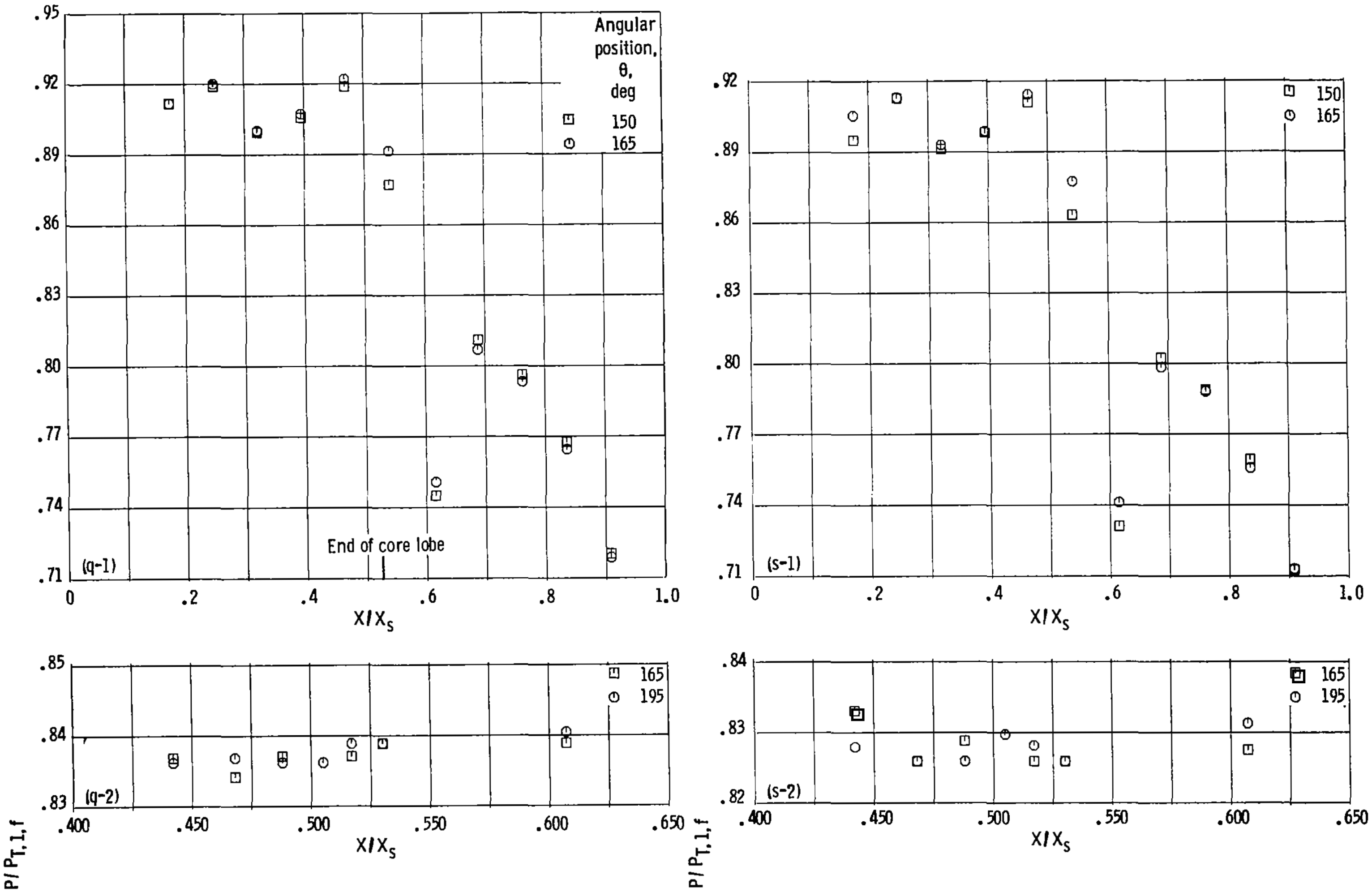
Angular position, θ, deg
150
165
(q-1)
End of core lobe
X/X_S
(s-1)
(q-2)
(s-2)
195
P/P_T,1,f
.95
.92
.89
.86
.83
.80
.77
.74
.71
0
.2
.4
.6
.8
1.0
.85
.84
.83
.82
.400
.450
.500
.550
.600
.650

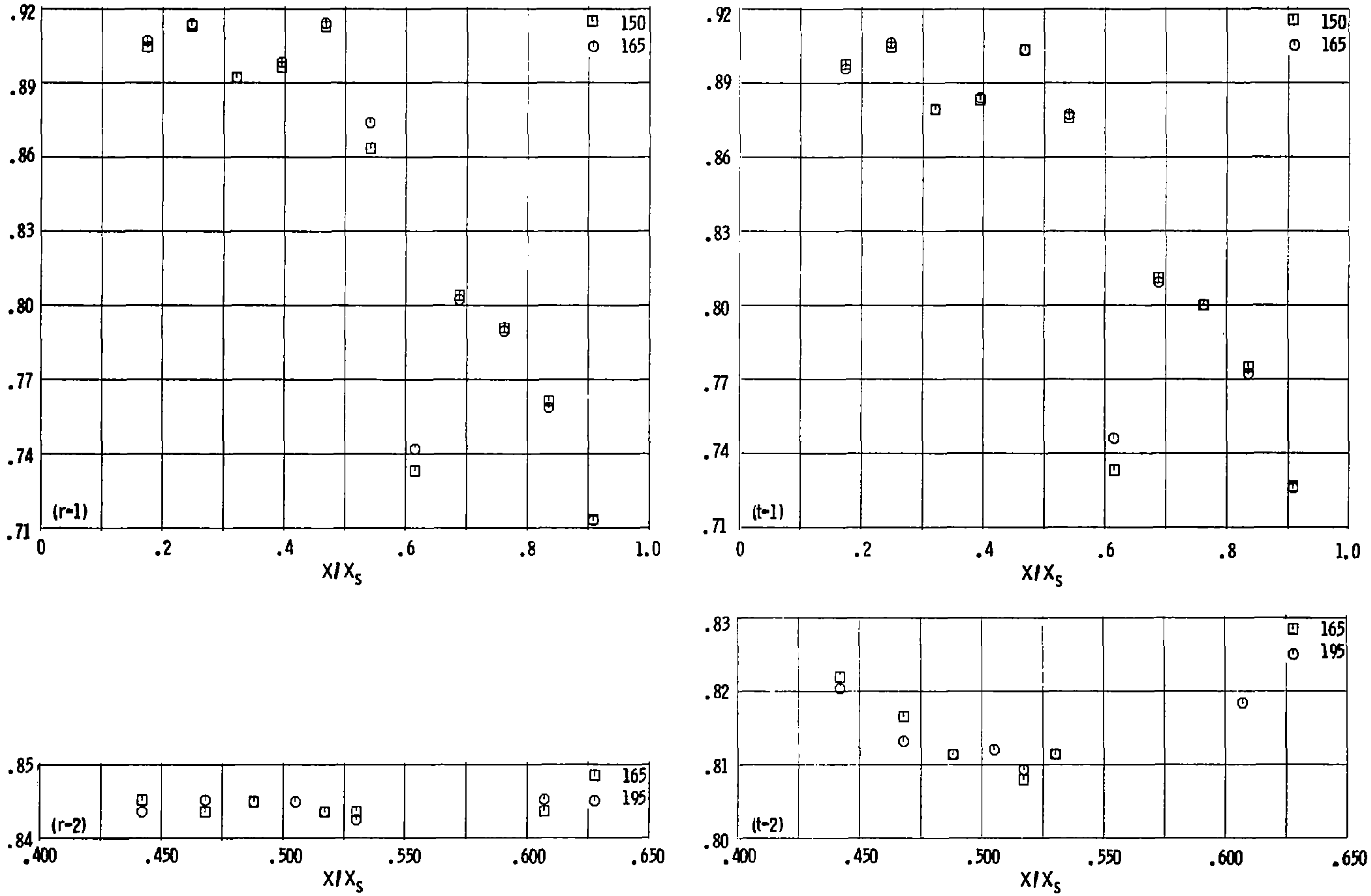


(q-1) Shroud statics. (q-2) Plug statics.
(q) 2E/REF–CB–S mixer configuration.
(r-1) Shroud statics. (r-2) Plug statics.
(r) 2E/3B–CB mixer configuration.
(s-1) Shroud statics. (s-2) Plug statics.
(s) 2E/3B–CB–S mixer configuration.
(t-1) Shroud statics. (t-2) Plug statics.
(t) 3E/2AC mixer configuration.

Figure 15. – Concluded.

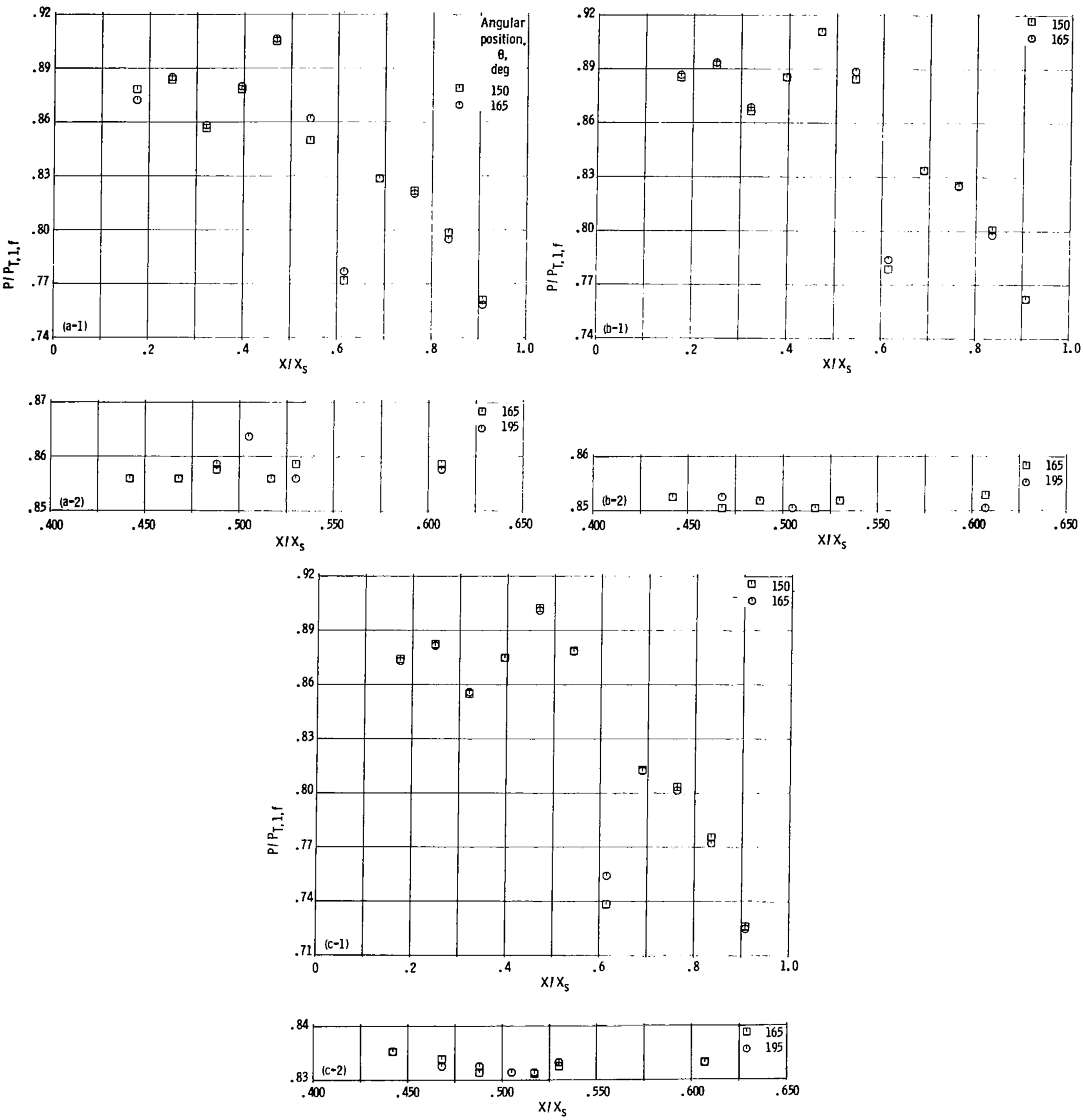


(a-1) Shroud statics. (a-2) Plug statics.
(a) 12B/3B mixer configuration.
(b-1) Shroud statics. (b-2) Plug statics.
(b) 1E/2AC mixer configuration.
(c-1) Shroud statics. (c-2) Plug statics.
(c) 1E/2AC-S mixer configuration.

Figure 16. – Static pressure distribution for nozzle shroud and centerbody. Nozzle pressure ratio, 2.5 (takeoff condition).

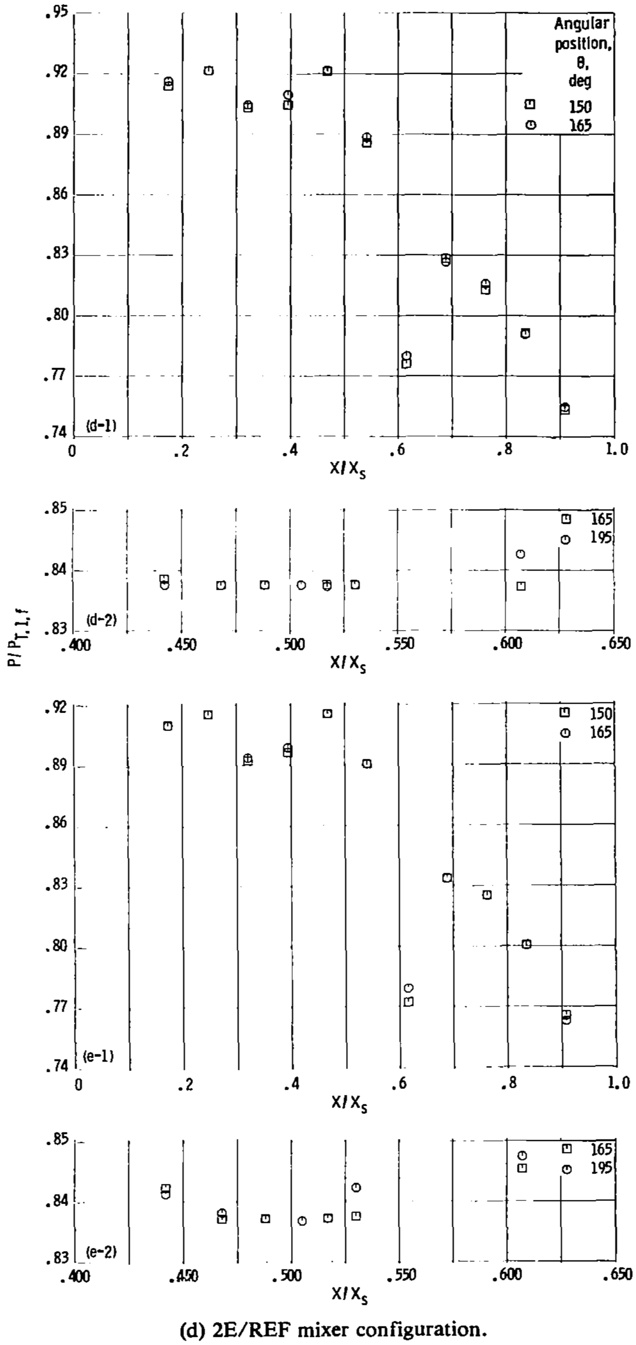


(d) 2E/REF mixer configuration.
(e) 3E/2AC mixer configuration.

Figure 16. – Concluded.

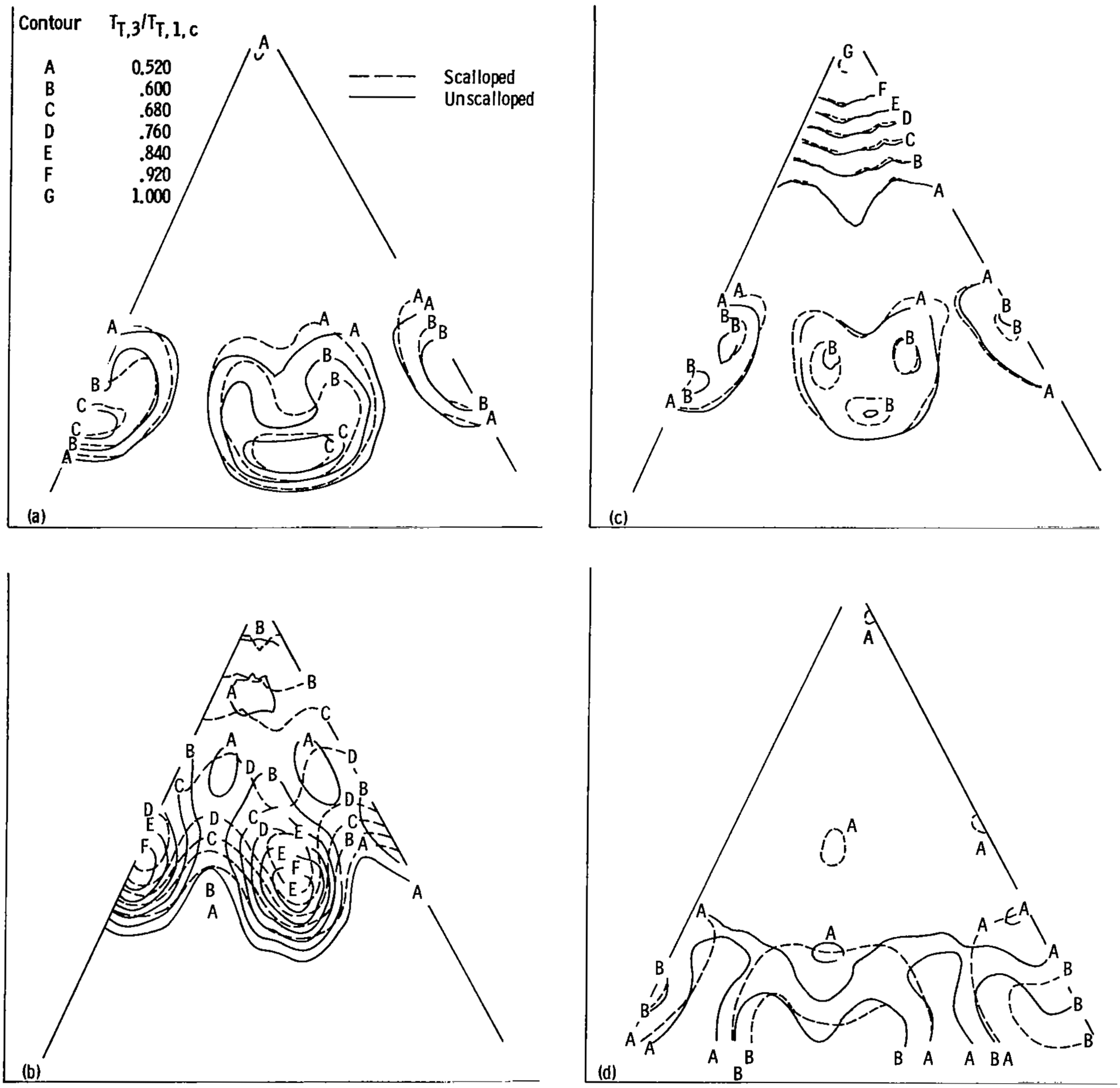


(a) 12B/3B mixer configuration.
(b) 12C/REF mixer configuration.
(c) 1E/2AC mixer configuration.
(d) 2E/3B-CB mixer configuration.

Figure 17. – Effect of lobe scalloping on mixer exit temperature ratio contours.

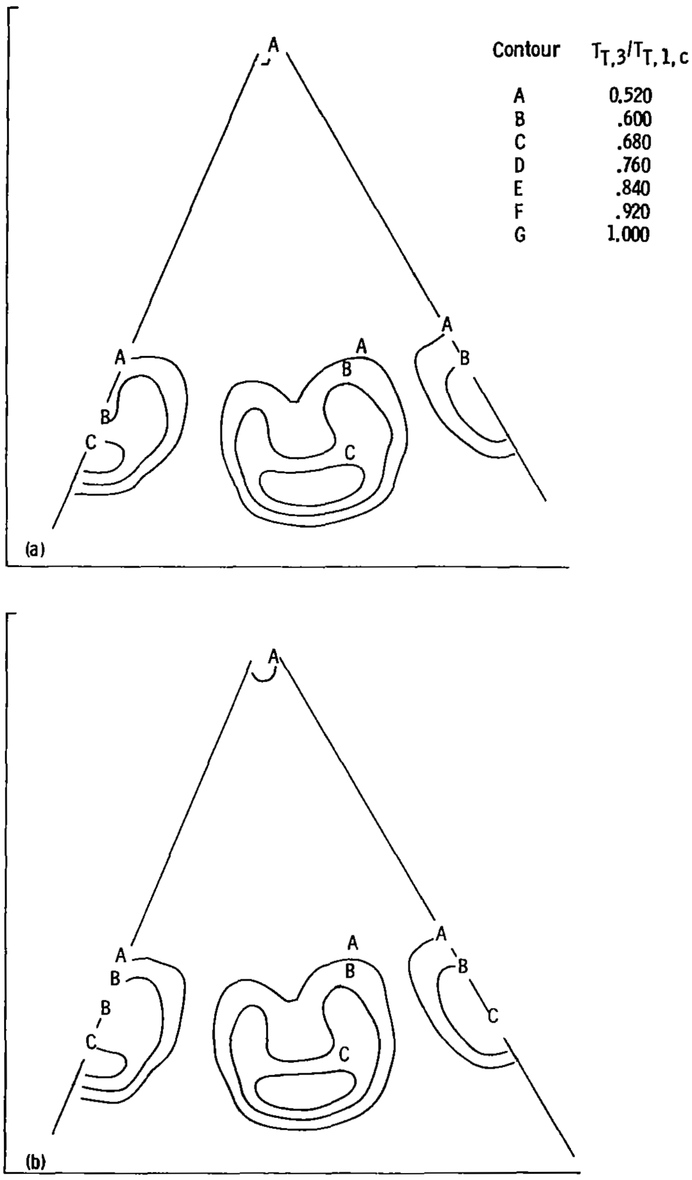


(a) Nozzle pressure ratio, 2.4.
(b) Nozzle pressure ratio, 1.6.

Figure 18. – Effect of pressure ratio on mixer exit temperature ratio contours. Mixer temperature ratio, 2.5; 12B/3B nozzle configuration.

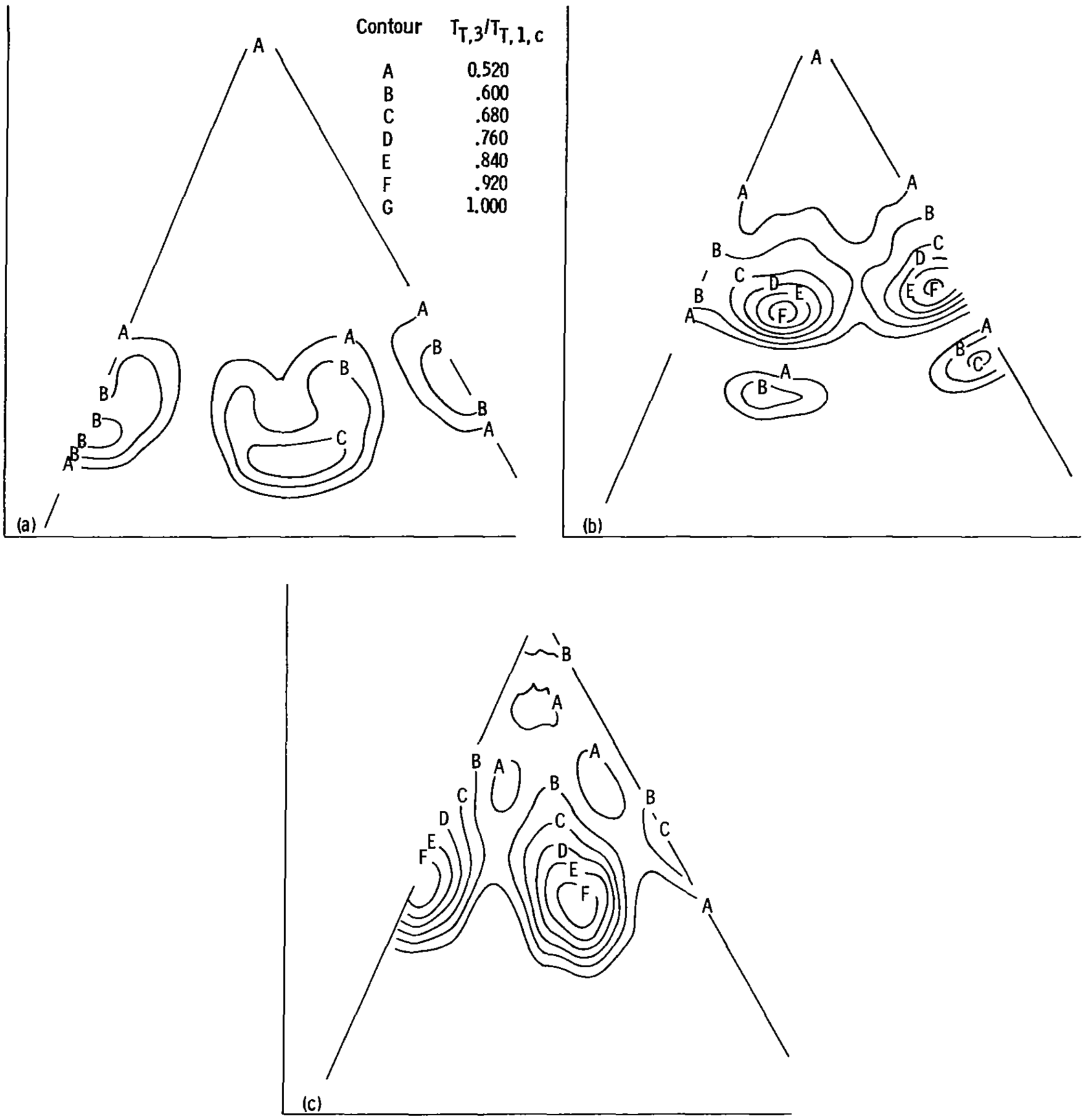


(a) 12B mixer configuration; penetration, 0.822.
(b) 12A mixer configuration; penetration, 0.776.
(c) 12C mixer configuration; penetration, 0.721.

Figure 19. – Effect of mixer lobe penetration on mixer exit temperature ratio distribution for three 12-lobe geometries.

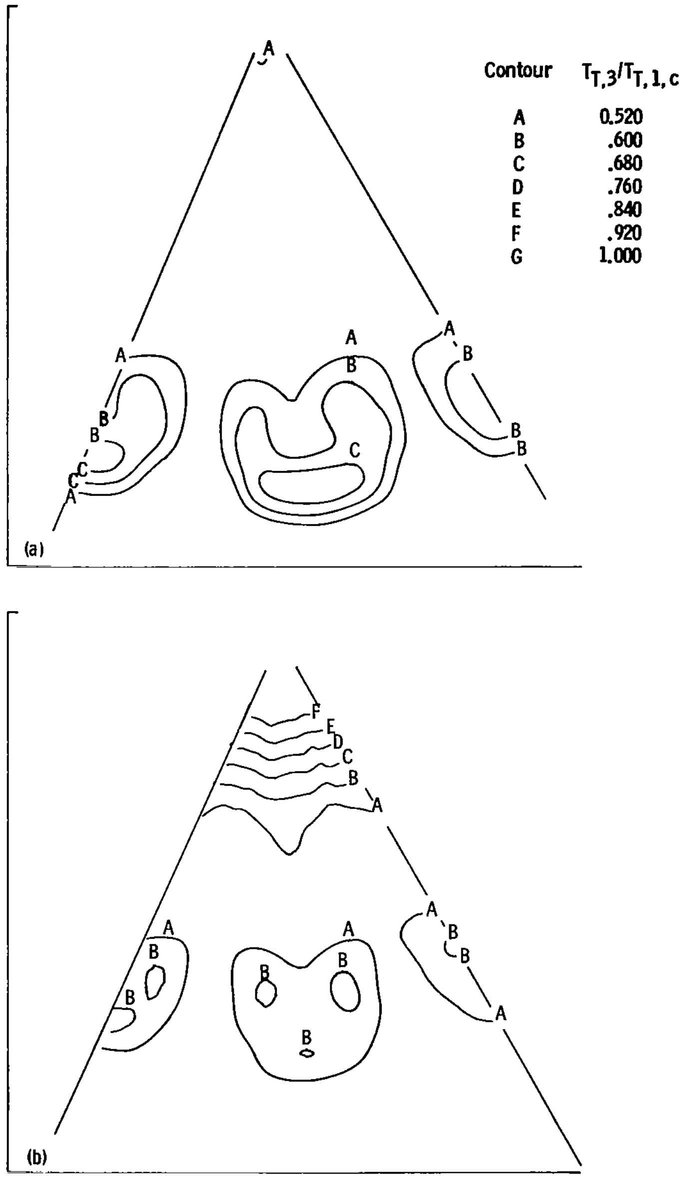


(a) 12B mixer configuration.
(b) 12C mixer configuration.

Figure 20. – Effect of gap height on mixer exit temperature ratio distribution.

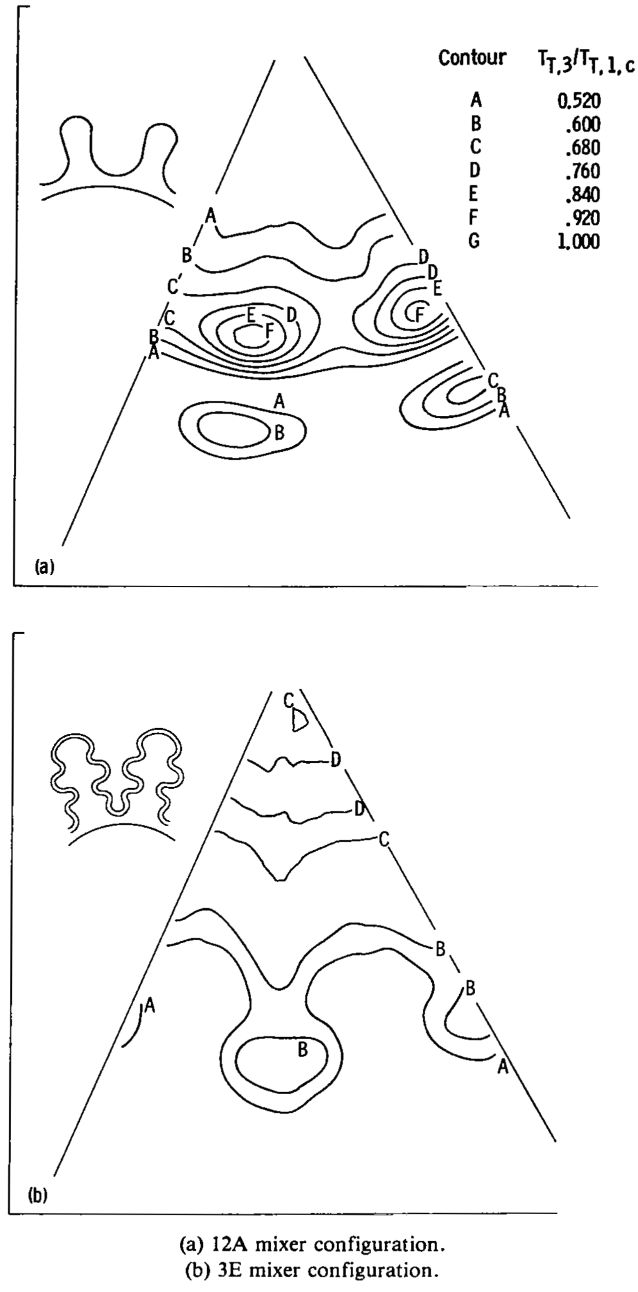


(a) 12A mixer configuration.
(b) 3E mixer configuration.

Figure 21. – Effect of radial wall convolutions on mixer exit temperature ratio distribution.

| 1. Report No. | 2. Government Accession No. | 3. Recipient's Catalog No. |
|---|---|---|
| NASA TP-2268 | | |

| 4. Title and Subtitle | |
|---|---|
| Hot-Flow Tests of a Series of 10-Percent-Scale Turbofan Forced Mixing Nozzles | 5. Report Date<br>January 1984 |
| | 6. Performing Organization Code<br>505-40-02 |
| 7. Author(s)<br>Verlon L. Head, Louis A. Povinelli, and William H. Gerstenmaier | 8. Performing Organization Report No.<br>E-1746 |
| | 10. Work Unit No. |
| 9. Performing Organization Name and Address<br>National Aeronautics and Space Administration<br>Lewis Research Center<br>Cleveland, Ohio 44135 | 11. Contract or Grant No. |
| | 13. Type of Report and Period Covered<br>Technical Paper |
| 12. Sponsoring Agency Name and Address<br>National Aeronautics and Space Administration<br>Washington, D.C. 20546 | 14. Sponsoring Agency Code |

15. Supplementary Notes

16. Abstract

An approximately 1/10-scale model of a mixed-flow exhaust system was tested in a static facility with fully simulated hot-flow cruise and takeoff conditions. Nine mixer geometries with 12 to 24 lobes were tested. The areas of the core and fan stream were held constant to maintain a bypass ratio of approximately 5. The research results presented in this report were obtained as part of a program directed toward developing an improved mixer design methodology by using a combined analytical and experimental approach. The effects of lobe spacing, lobe penetration, lobe-to-centerbody gap, lobe contour, and scalloping of the radial side walls were investigated. Test measurements included total pressure and temperature surveys, flow angularity surveys, and wall and centerbody surface static pressure measurements. Contour plots at various stations in the mixing region are presented to show the mixing effectiveness for the various lobe geometries.

| 17. Key Words (Suggested by Author(s)) | 18. Distribution Statement |
|---|---|
| Mixer<br>Turbofan forced mixers<br>Mixing<br>Exhaust systems | Unclassified - unlimited<br>STAR Category 34 |

| 19. Security Classif. (of this report) | 20. Security Classif. (of this page) | 21. No. of pages | 22. Price* |
|---|---|---|---|
| Unclassified | Unclassified | 96 | A05 |

*For sale by the National Technical Information Service, Springfield, Virginia 22161

NASA-Langley, 1984